

Biological soil crust and climate effects on soil stabilization, erosion, and nutrient dynamics across the Chilean Coastal Range

Dissertation
der Mathematisch-Naturwissenschaftlichen Fakultät
der Eberhard Karls Universität Tübingen
zur Erlangung des Grades eines
Doktors der Naturwissenschaften
(Dr. rer. nat.)

vorgelegt von
M.Sc. Nicolás Riveras Muñoz
aus Puente Alto

Tübingen
2025

Gedruckt mit Genehmigung der Mathematisch-Naturwissenschaftlichen Fakultät der
Eberhard Karls Universität Tübingen.

Tag der mündlichen Qualifikation: XX.XX.2025

Dekan: Prof. Dr. Thilo Stehle

1. Berichterstatter: Prof. Dr. Thomas Scholten

2. Berichterstatter:

Abstract

Biological soil crusts (biocrusts) and climate effects profoundly shape soil stabilization, erosion, and nutrient dynamics, especially across diverse environmental gradients like the Chilean Coastal Range (arid to humid). This research explored these intricate interactions by integrating field observations, rainfall simulations, laboratory experiments, and advanced analytical techniques. The focus was on the interplay between biocrusts, microbial communities, plant roots, and fundamental soil properties.

Key findings reveal that biocrusts significantly enhance soil aggregate stability, particularly in drier regions, thereby reducing surface runoff and erosion. Their stabilizing influence, however, lessens in humid climates where dense vegetation becomes the dominant factor. Biocrusts modify hydrological pathways, typically decreasing surface flow while sometimes increasing percolation. They also modulate carbon (C) and nitrogen (N) fluxes in climate-dependent ways, influencing both sediment-bound and dissolved nutrient transport.

The critical role of microbial communities in soil aggregation and development was confirmed, with their activity and resilience strongly linked to climate legacy and moisture patterns (e.g., wetting-drying cycles). Plant roots emerged as powerful drivers of macroaggregation, exerting distinct influences during their living (rhizosphere) and decaying (detritusphere) phases, which in turn affects microbial succession and organic matter protection. Overall, this work highlights the interconnected, context-dependent nature of these biotic and abiotic factors in governing soil structure and function.

Kurzfassung

Biologische Bodenkrusten (Biokrusten) und Klimaeffekte prägen maßgeblich die Bodenstabilisierung, Erosion und Nährstoffdynamik, insbesondere entlang diverser Umweltgradienten wie der chilenischen Küstenkordillere (arid bis humid). Diese Forschung untersuchte diese komplexen Wechselwirkungen durch die Integration von Feldbeobachtungen, Regensimulationen, Laborexperimenten und fortschrittlichen Analysetechniken. Der Fokus lag auf dem Zusammenspiel zwischen Biokrusten, mikrobiellen Gemeinschaften, Pflanzenwurzeln und grundlegenden Bodeneigenschaften.

Wichtige Ergebnisse zeigen, dass Biokrusten die Aggregatstabilität des Bodens signifikant erhöhen, besonders in trockeneren Regionen, wodurch Oberflächenabfluss und Erosion reduziert werden. Ihr stabilisierender Einfluss nimmt jedoch in humiden Klimazonen ab, wo dichte Vegetation zum dominierenden Faktor wird. Biokrusten modifizieren hydrologische Pfade, indem sie typischerweise den Oberflächenabfluss verringern, während sie manchmal die Perkolation erhöhen. Sie modulieren auch Kohlenstoff- (C) und Stickstoff- (N) Flüsse auf klimaabhängige Weise und beeinflussen sowohl den sedimentgebundenen als auch den gelösten Nährstofftransport.

Die entscheidende Rolle mikrobieller Gemeinschaften bei der Bodenaggregation und -entwicklung wurde bestätigt, wobei ihre Aktivität und Resilienz stark mit Klima-Legacy-Effekten und Feuchtemustern (z.B. Benetzungs-Trocknungs-Zyklen) verknüpft sind. Pflanzenwurzeln erwiesen sich als starke Treiber der Makroaggregation, die während ihrer lebenden (Rhizosphäre) und zerfallenden (Detritussphäre) Phasen unterschiedliche Einflüsse ausüben, was wiederum die mikrobielle Sukzession und den Schutz organischer Substanz beeinflusst. Insgesamt hebt diese Arbeit die vernetzte, kontextabhängige Natur dieser biotischen und abiotischen Faktoren bei der Steuerung von Bodenstruktur und -funktion hervor.

Contents

1	Introduction	1
1.1	Biological soil crusts and soil aggregate stability along a climatic gradient	1
1.2	Microbial communities as drivers of aggregate structure	2
1.3	Climate as a driver of soil and microbial dynamics	3
1.4	Influence of plant roots and interactions with biocrusts along the climate gradient	4
1.5	Biocrusts, hydrological processes, and nutrient fluxes influencing soil erosion	5
1.6	Understanding biocrusts across a climatic gradient	6
1.7	Objectives and hypothesis	7
2	Methodology	9
2.1	Study sites and experimental setting	9
2.2	Field methods	13
2.2.1	Biocrust sampling and characterization	13
2.2.2	Soil sampling	14
2.2.3	Rainfall simulations	15
2.3	Laboratory methods	17
2.3.1	Baseline soil characterization	17
2.3.2	Aggregate stability	17
2.3.3	Incubation experiments	20
2.3.4	Molecular analyses	20
2.3.5	Organic matter and microbial biomarker characterization	21
2.4	Statistical analyses	22
3	Results and discussion	25
3.1	Effect of biocrust on soil aggregate stability (manuscript 1)	25
3.1.1	Climate-induced changes in soil properties	25
3.1.2	Biocrust-induced changes in soil properties	27
3.1.3	Biocrust and climate interactions on aggregate stability	29
3.2	Effect of biocrust on water flow, erosion and nutrient flow (manuscript 2)	30
3.2.1	Biocrust influence on water flow and sediment transport	30
3.2.2	Biocrust modulation of carbon and nitrogen fluxes	34

Contents

3.3 Microbial, plant and moisture controls on soil structure and functionality (Manuscripts 3, 4 and 5)	35
4 Conclusion & Outlook	41
Bibliography	45
Appendix	59
A Biocrust-linked changes in soil aggregate stability along a climatic gradient in the Chilean Coastal Range	61
A.1 Introduction	62
A.2 Materials and methods	64
A.2.1 Study sites and experimental settings	64
A.2.2 Biocrust sampling and classification	65
A.2.3 Soil sampling and analyses	68
A.2.4 Statistical analyses	70
A.3 Results	70
A.3.1 Soil properties	70
A.3.2 Soil aggregate stability	72
A.4 Discussion	76
A.4.1 Aggregate stability and soil properties along the climatic gradient	76
A.4.2 Biocrusts altering soil properties along the climatic gradient .	77
A.5 Conclusions	78
B Biocrusts as climate-dependent regulators of erosion, water and nutrient cycling	83
B.1 Introduction	84
B.2 Materials and methods	87
B.2.1 Study sites	87
B.2.2 Rainfall simulation experiment	87
B.2.3 Statistical analysis	88
B.3 Results	89
B.3.1 Surface runoff, percolating water fluxes, and their interrelation with biocrust cover along different climatic conditions	89

List of Tables

2.1	Taxonomical composition of mosses and lichens in the biological soil crust for the study sites along the climatic gradient.	14
3.1	Surface runoff fluxes on the study sites (SG: Santa Gracia, QdT: Quebrada de Talca, LC: La Campana, NA: Nahuelbuta) with (+) and without (-) biocrust (BSC) cover. Values correspond to mean \pm standard deviation (SD) of five field replicates. Different letters indicate statistically significant different values based on Šidák correction post-hoc test results.	32
3.2	Percolating water fluxes on the study sites (SG: Santa Gracia, QdT: Quebrada de Talca, LC: La Campana, NA: Nahuelbuta) with (+) and without (-) biocrust (BSC) cover. Values correspond to mean \pm standard deviation (SD) of five field replicates. Different letters indicate statistically significant different values based on Šidák correction post-hoc test results.	33
A.1	Taxonomical composition of mosses and lichens in the biological soil crust for the study sites along the climatic gradient.	68
A.2	Appendix A. Significant factors for response variables based on generalized linear models. Models with significant interaction also include the predictors as simple parameters based on marginality principle. ($p\text{-value} \leq 0$: "****"; $p\text{-value} \leq 0.001$: "***"; $p\text{-value} \leq 0.01$: **)	80
B.1	Surface runoff fluxes on the study sites (SG: Santa Gracia, QdT: Quebrada de Talca, LC: La Campana, NA: Nahuelbuta) with (+) and without (-) biocrust (BSC) cover. Values correspond to mean \pm standard deviation (SD) of five field replicates. A letter-based display of Šidák correction accompanies surface runoff parameters, and the significance of the studied factors is shown as a p-value and list of covariates (C _T , N _T : total carbon and nitrogen content). Different letters indicate statistically significant different values based on our data, ns: non-significant.	90

- B.2 Percolating water fluxes on the study sites (SG: Santa Gracia, QdT: Quebrada de Talca, LC: La Campana, NA: Nahuelbuta) with (+) and without (-) biocrust (BSC) cover. Values correspond to mean \pm standard deviation (SD) of five field replicates. A letter-based display of Šidák correction accompanies surface runoff parameters, and the significance of the studied factor is shown as a p-value and list of covariates (C_T , N_T : total carbon and nitrogen content). Different letters indicate statistically significant different values based on our data, ns: non-significant. 91

List of Figures

2.1	Location of study sites relative to South America. From north to south: Pan de Azúcar (PdA), Santa Gracia (SG), Quebrada de Talca (QdT), La Campana (LC), and Nahuelbuta (NA).	10
2.2	General view (a, c, d, g, and i) and sampled biocrust (b, d, f, h, and j) of PdA, SG, QdT, LC, and NA.	12
2.3	Construction diagram of the soil erosion flux box used in the experiment (a), general view of a plot with the presence of biocrust prior to sampling (b). (c, d) shows an installed cutting frame and the cleared and prepared soil. (e) demonstrates the setting for rainfall simulations at the Nahuelbuta (NA) study site.	16
3.1	Soil physical and chemical properties across the four study sites (PdA: Pan de Azúcar, SG: Santa Gracia, LC: La Campana, and NA: Nahuelbuta). Letter-based display accompanying soil properties with significant effect for site. Different letters indicate statistically significant differences ($p < 0.05$, Šidák correction).	26
3.2	Biocrust (a) and interaction (b) effects on soil properties. Soil physical and chemical properties across for biocrust (BSC+ vs. BSC-) and the interaction with the site (PdA: Pan de Azúcar, SG: Santa Gracia, LC: La Campana, and NA: Nahuelbuta). Letter-based display accompanying soil properties with significant effect for site or site*biocrust. Different letters indicate statistically significant differences ($p < 0.05$, Šidák correction).	28
3.3	Aggregate stability indexes for Pan de Azúcar (PdA), Santa Gracia (SG), La Campana (LC), and Nahuelbuta (NA) for biocrust (BSC+) and non-biocrust (BSC-) treatments displayes as mean and standard error. Δ MWD: difference in mean weight diameter, Δ GMD: difference in geometric mean diameter, WSAR: water stability aggregate ratio, $R_{<2\text{mm}}$: ratio of aggregates less than 2 mm.	30

3.4 Representation of total carbon in sediments and DOC in water fluxes for the four study sites. The diagrams at the right side with slightly green surface represents the BSC+ treatments and the one at the left the BSC-. Grey-filled arrows correspond to C fluxes, and yellowish arrows to N. At the same time, arrows with solid borders correspond to the flow attached to the sediments, and dashed arrows dissolved in water. Each type of arrow is proportional inside each group in width to the concentration of nutrients and in length to the mass of it.	35
3.5 Principal Component Analyses of soil properties in native soils (squares) and sterilized soils (circles) including significant soil properties. A) arid, B) semi-arid, C) mediterranean and D) humid site. Microbial influence is indicated by sample separation along the x-axis.	37
3.6 Relative abundance of top 15 bacterial phyla for Pan de Azúcar and Santa Gracia and the different time points. Time is represented as T0 (original), T1 (2 weeks), T2 (12 weeks) and T3 (16 weeks). Each bubble is the mean of the different treatments (in situ, BSCs and plants) and technical triplicates.	38
A.1 Sampled biological soil crust for PA (a), SG (b), LC (c), and NA (d). . .	67
A.2 Mean and standard error of soil properties for Pan de Azúcar (PA), Santa Gracia (SG), La Campana (LC) and Nahuelbuta (NA), without (BSC-) and with biocrust cover (BSC+), and the interaction of both factors. (EC = electrical conductivity, BD = bulk density, C _t = total carbon, SOC = soil organic carbon, SIC = soil inorganic carbon, N _t = total nitrogen, C/N = carbon to nitrogen ratio). Significant factors include Tukey's Post-hoc-Test indicated by letters on the top of the bars. Different letters represent significant differences at $p < 0.05$	71
A.3 Mean value and standard error of aggregate proportion for dry (a) and wet (b) sieved fractions for Pan de Azúcar (PA), Santa Gracia (SG), La Campana (LC), and Nahuelbuta (NA) for biocrust (BSC+) and non-biocrust (BSC-) treatments. Significant factors and corresponding models for response variables are included in Appendix A.2.	74
A.4 Mean and standard deviation of aggregate size distribution changes between dry and wet sieving for the sites Pan de Azúcar (PA), Santa Gracia (SG), La Campana (LC), and Nahuelbuta (NA) for biocrust (BSC+) and non-biocrust (BSC-) treatments. Error bars were, in some cases, truncated for better visualization.	74

List of publications

1. **Riveras-Muñoz, N.**; Seitz, S.; Witzgall, K.; Rodríguez, V.; Kühn, P.; Mueller, C. W.; Oses, R.; Seguel, O.; Wagner, D.; and Scholten, T. (2022): Biocrust-linked changes in soil aggregate stability along a climatic gradient in the Chilean Coastal Range. *SOIL*, 8, 717–731. DOI: 10.5194/soil-8-717-2022.
2. **Riveras-Muñoz, N.**; Seitz, S.; Gall, C.; Rodríguez, V.; Witzgall, K.; Kühn, P.; Mueller, C.W.; Oses, R.; Seguel, O.; Wagner, D.; Scholten, T. (submitted): Biocrusts as climate-dependent regulators of erosion, water and nutrient cycling. *Geoderma*.
3. Rodríguez, V.; Bartholomäus, A.; Witzgall, K.; **Riveras-Muñoz, N.**; Oses, R.; Liebner, S.; Kallmeyer, J.; Rach, O.; Mueller, C.W.; Seguel, O.; Scholten, T. and Wagner. D. (2024): Microbial impact on initial soil formation in arid and semi-arid environments under simulated climate change. *Frontiers in Microbiology*, 15:1319997. DOI: 10.3389/fmicb.2024.1319997.
4. Mitzscherling, J.; Oses, R.; **Riveras-Muñoz, N.**; Mueller, C. W.; Seguel, O. and Kühn, P.; Scholten, T. and Wagner, D. (2024): Microbially Induced Soil Aggregate Turnover Across Different Climates and Moisture Regimes. SSRN: DOI: 10.2139/ssrn.4740477.
5. Witzgall, K.; Steiner, F.A.; Hesse, B.D.; **Riveras-Muñoz, N.**; Rodríguez, V.; Teixeira, P.P.C.; Li, M.; Oses, R.; Seguel, O.; Seitz, S.; Wagner, D.; Scholten, T.; Buegger, F.; Angst, G.; Mueller, C.W. (2024): Living and decaying roots as regulators of soil aggregation and organic matter formation—from the rhizosphere to the detritusphere. *Soil Biology and Biochemistry*, 197, 109503. ISSN 0038-0717. DOI: 10.1016/j.soilbio.2024.109503.

Chapter 1

Introduction

1.1 Biological soil crusts and soil aggregate stability along a climatic gradient

Life has deeply shaped the surface of Earth over billions of years, actively modifying its environment within the Critical Zone—Earth’s living skin—which forms the dynamic interface between the lithosphere, atmosphere, hydrosphere, and biosphere (Amundson et al., 2007; Brantley et al., 2017; Dietrich and Perron, 2006). The soil, a central component of this zone, mediates essential biogeochemical processes and supports terrestrial ecosystems. Although soil is subject to constant reshaping by erosion, weathering, and tectonic activity (Scholten et al., 2017), organisms, particularly biological soil crusts (biocrusts), significantly influence its structural integrity and stabilization.

Biocrusts are formed from complex interactions among diverse organisms, including photoautotrophs such as cyanobacteria, algae, lichens, and bryophytes, and heterotrophs such as bacteria, fungi, and archaea, which intertwine with soil particles through their own filamentous structures and polysaccharide-based adhesives (Belnap et al., 2016; Gao et al., 2017; Weber et al., 2022; Xiao et al., 2022). This intricate biological network establishes a cohesive, mesh-like layer that firmly binds the uppermost soil surface, functioning as a protective, living skin on Earth’s surface. Biocrust enhance soil aggregate stability by physically protecting soil aggregates, sheltering organic matter, and facilitating microbial colonization.

The stabilizing role of biocrusts is especially crucial in arid environments, where their drought tolerance and low water requirements make them the predominant biological cover (Chen et al., 2020; Oliver et al., 2005). This resilience comes from their ability to remain dormant during extended dry periods, reviving rapidly upon rewetting, even after complete desiccation, a capability attributed to the lack of specialized desiccation control structures like stomata or impermeable cuticles (Mägdefrau and Wutz, 1951; Proctor et al., 2007; Thielen et al., 2021). Consequently, biocrust water content directly reflects the humidity of the surrounding environment, making them uniquely adapted to arid and semi-arid regions (Colesie et al., 2016; Grote et al., 2010). Under these conditions, biocrust-induced soil stability achieves its maximum impact, significantly

reducing erosion susceptibility and facilitating soil formation processes.

However, as climate humidity increases along a gradient towards more temperate conditions, vegetation competes more effectively and biocrusts are often relegated to resource-limited niches (Büdel et al., 2016). In temperate regions, biocrusts establish on bare soils or soils with minimal plant development, where conditions such as high salinity, low nutrient availability, and limited water availability mirror the limiting conditions of arid landscapes (Corbin and Thiet, 2020). Thus, the interplay between biocrusts, microbial communities, and plant roots shifts along this climatic gradient, diminishing, but not eliminating, the protagonism of biocrusts on soil stability, structure and size distribution of soil aggregates.

1.2 Microbial communities as drivers of aggregate structure

Soil, far from being an inert substrate, is a dynamic and living entity teeming with a vast, often underappreciated, majority: microbial communities. These microscopic organisms, including bacteria, archaea, fungi, and protists, are the main drivers of soil development and functioning, influencing almost every aspect of terrestrial ecosystems (Bardgett and van der Putten, 2014). Their ubiquity and sheer abundance, with cell counts often reaching billions per gram of soil, underscore their significance in biogeochemical processes (Nunan et al., 2001). Microorganisms mediate complex nutrient cycles that involve carbon, nitrogen, and phosphorus, transforming organic matter and making essential elements accessible for plant uptake (Schimel and Schaeffer, 2012). Furthermore, they actively participate in the weathering of minerals, contributing to soil development and releasing nutrients into the environment (Barkay and Schaefer, 2001; Burford et al., 2003). Their metabolic activities influence soil pH, redox conditions, and the overall chemical environment, thus creating diverse microhabitats that sustain a wide variety of life forms (Brehm et al., 2005).

The resilience and adaptability of microbial communities is perhaps most strikingly demonstrated in extreme environments. Arid climates, characterized by drastic temperature fluctuations, minimal precipitation, and limited nutrient availability, provide compelling examples of how microbial life thrives under harsh conditions. Research in these arid ecosystems has revealed unexpectedly high abundances of diverse microorganisms, even in extremely dry desert environments (Bernhard et al., 2018; Newsham et al., 2016). This ability to withstand environmental stress makes desert soils particularly valuable for understanding the potential effects of climate change on microbial communities (Pearce et al., 2012). Studying these environments offers valuable insights into the limits of life and the adaptive strategies microorganisms employ when confronted with adversity. Such knowledge is invaluable for understanding the potential

responses of microbial communities to ongoing and future environmental changes.

The connection between microbes and the development of soil structure is profound. Microorganisms colonize raw mineral substrates such as saprolite or newly formed desert soils, initiating a complex successional process that transforms bare rock into fertile soil (?Stradling et al., 2002). They contribute to mineral weathering through the production of organic acids and other metabolites that dissolve rock surfaces (Bajerski and Wagner, 2013; Mavris et al., 2010; Štyriaková et al., 2012). Along the Chilean Coastal Range, climate distinctly shapes microbial community composition, driving shifts in microbial functions, including their capability to stabilize soil aggregates (Bernhard et al., 2018). Microbes decompose organic matter derived from plant and animal residues, releasing nutrients and contributing to the formation of soil organic matter, a critical component of soil structure and fertility Oades (1993). Furthermore, microbial communities actively participate in the formation of soil aggregates by exuding substances like polysaccharides, which act as a glue, binding soil particles together and creating a stable soil structure (Martens and Frankenberger, 1992; Schlecht-Pietsch et al., 1994). Consequently, climatic-driven microbial succession directly influences soil aggregation, which is essential for maintaining soil stability, enhancing water infiltration, reducing soil erodibility, and ultimately fostering ecosystem development.

1.3 Climate as a driver of soil and microbial dynamics

Climate stands as a primary architect of soil, profoundly influencing its formation, structure, and function (Jenny, 1941). Temperature and precipitation regimes, along with evapotranspiration rates, dictate the weathering of parent material, the accumulation and decomposition of organic matter, and the development of distinct soil horizons (Scholten et al., 2017). These climatic factors also exert a strong influence on the soil water balance, which in turn affects nutrient availability and the overall biogeochemical cycling within the soil ecosystem Eldridge et al. (2020); Thielen et al. (2021).

The influence of climate extends beyond the purely abiotic realm, shaping the composition and activity of microbial communities that inhabit the soil (Nemergut et al., 2005). Different climatic conditions select for distinct microbial populations, influencing their functional capabilities and the biogeochemical processes they mediate (Newsham et al., 2016). For instance, arid environments, characterized by low precipitation and high temperatures, harbor specialized microbial communities adapted to these extreme conditions (Pearce et al., 2012). These microbial communities play a vital role in initial soil formation and nutrient cycling, even in the face of resource scarcity Bernhard et al. (2018). Our own studies in the Chilean Coastal Range revealed distinct patterns in soil properties and microbial communities along a climate gradient (Bernhard et al., 2018). Interestingly, these trends often followed specific, rather than homogeneous, patterns, indicating the presence of threshold processes and buffering mechanisms in soil ecosys-

tems Bernhard et al. (2018).

The development and distribution of biological soil crusts (BSCs) are also intricately linked to climate. Water availability, driven by precipitation and evapotranspiration, is a major determinant of biocrust cover and composition (Bowker et al., 2016). Arid regions tend to favor biocrust dominance due to the scarcity of vascular plant cover (Colesie et al., 2016; Grote et al., 2010), while more humid climates support greater plant diversity, leading to a mosaic of biocrusts interspersed with plants (Issa et al., 1999). The protective effects of BSCs against erosion and their influence on soil hydrology also vary depending on climate, with potential trade-offs between runoff reduction and water infiltration (Thielen et al., 2021). These findings demonstrate the importance of considering climate not only as a driver of soil properties but also as a key factor shaping microbial communities and the distribution and functionality of biocrusts. The Chilean Coastal Range, with its dramatic gradient from arid to humid conditions, provides a natural laboratory for investigating these complex interactions. This gradient allows us to explore how the interplay of climate, soil, microbes, and biocrusts shapes the Earth's surface across varying environmental conditions. Furthermore, understanding how climate influences these components individually and in combination is crucial for predicting how soil ecosystems will respond to future environmental changes. The non-linear nature of some of these climate-driven changes, coupled with the potential existence of thresholds in soil processes across environmental gradients, highlights the need for comprehensive research in diverse climatic settings Bernhard et al. (2018).

1.4 Influence of plant roots and interactions with biocrusts along the climate gradient

Soil, far from being a simple mixture of minerals and organic matter, is a dynamic and intricate web of interactions between diverse biotic and abiotic components. Central to this web are plant roots, which exert a profound influence on the surrounding soil environment, driving structural changes, altering nutrient availability, and shaping microbial communities (Hinsinger et al., 2009). These complex interactions among roots, microbes, and soil particles constitute a fundamental axis supporting soil development and ecosystem functioning.

Roots physically restructure the soil matrix through growth and penetration, creating channels and pores, thereby enhancing aeration and water infiltration (Bruand et al., 1996). This process of bioturbation is particularly relevant in developed soils, where root systems establish intricate networks of interactions with the surrounding environment. Moreover, roots release a variety of compounds, known as rhizodeposits, including sugars, amino acids, and organic acids, which serve as primary substrates for soil microorganisms (Hinsinger et al., 2009; Rasse et al., 2005). This concentrated release

of labile carbon in the rhizosphere fuels microbial activity, creating a "hotspot" of biological processes (Hinsinger et al., 2009).

The impact of roots, however, extends beyond the immediate vicinity of the living root. As roots senesce and decompose, they enter the detritusphere, a zone characterized by the breakdown of plant-derived organic matter (Vidal et al., 2018). In this zone, the legacy of roots persists as decomposed root material contributes to soil organic matter formation and influences the structure and stability of soil aggregates Six et al. (2004). The transition from rhizosphere to detritusphere marks a shift in the microbial community, as the readily available carbon from rhizodeposits is replaced by more complex organic compounds derived from decaying root tissues (Vidal et al., 2018). This shift in resource availability triggers microbial succession, favoring microorganisms capable of degrading these more recalcitrant substances.

Importantly, the interactions between biocrusts and vascular plants form a dynamic feedback loop in soil ecosystems. Biocrusts, as early colonizers of bare ground, contribute to the initial stabilization of the soil surface, creating microhabitats that facilitate subsequent plant establishment (?Bowker et al., 2006). As plants colonize and their root systems develop, they further enhance soil structure formation, promoting the accumulation of organic matter, and creating conditions for diverse microbial communities to thrive (Schweizer et al., 2018; Six et al., 2004). This positive feedback loop between biocrusts and plants drives the development from initial, unstable soil environments towards more mature and resilient soil ecosystems. Thus, along environmental gradients, plant roots progressively become primary agents of aggregate stability, influenced indirectly but significantly by earlier biocrust colonization and microbial activity.

1.5 Biocrusts, hydrological processes, and nutrient fluxes influencing soil erosion

Climatic conditions strongly shape biocrust composition, morphological characteristics, and ecological functions, thus influencing hydrological processes, nutrient cycling, and susceptibility to soil erosion (Belnap, 2003; Concostrina-Zubiri et al., 2014). In arid environments, biocrusts dominated by cyanobacteria and lichens typically form smooth, compact surfaces enriched with microbial biomass and extracellular polysaccharides (EPS), profoundly affecting surface hydrology (Rodríguez-Caballero et al., 2018; Weber et al., 2022). Such biocrust structures frequently lead to surface pore clogging, potentially increasing runoff initiation but simultaneously reducing sediment loss by enhancing aggregate stability and protecting soil organic matter (Kidron et al., 2021). Conversely, in humid climates, biocrusts with higher proportions of bryophytes and fungi possess rougher surfaces that promote water retention, facilitate infiltration, and reduce runoff, thereby strongly influencing sediment transport and nutrient dynamics

(?Seitz et al., 2017).

These functional differences across climate conditions emphasize the critical role biocrusts play in regulating carbon (C) and nitrogen (N) fluxes, erosion dynamics, and soil fertility. Biocrusts act as initial stabilizers of soil organic matter, even preceding plant colonization, thus shaping early nutrient cycling pathways (Belnap et al., 2007; Young et al., 2022). Furthermore, by physically absorbing raindrop energy, trapping sediment, and promoting microbial-driven aggregate formation, biocrusts provide a protective barrier against erosion, influencing water and sediment fluxes Costa et al. (2018); Xiao et al. (2022).

However, the way in which biocrust-mediated hydrological processes, nutrient cycling, and erosion control shift across gradients of temperature and humidity remains uncertain. These functional patterns are complex and nonlinear, reflecting intricate interactions between biocrust structure, microbial activity, vegetation competition, and climatic variability rather than a simple linear climatic transition (Bernhard et al., 2018; ?).

1.6 Understanding biocrusts across a climatic gradient

Soil represents an intricate web of interactions among diverse organisms, where biocrusts play a pivotal climate-dependent role in stabilizing aggregates, regulating erosion, and controlling water and nutrient fluxes. This biocrust-mediated stabilization effect is most pronounced in arid regions due to minimal vegetation, decreasing in relative importance but persisting as climates become more humid. Along the Chilean Coastal Range, this dynamic illustrates how biocrusts, microbial communities, and plant roots co-evolve, shaping soil structure, erosion resistance, and nutrient cycling.

Addressing these complex interactions and feedbacks is crucial for predicting how soils and associated ecosystems will respond to ongoing climate changes, especially considering the non-linear and threshold-driven nature of soil processes across environmental gradients Bernhard et al. (2018); Wang et al. (2014). Future research should deepen understanding of these interactions, exploring quantitative relationships to inform conservation strategies and enhance ecosystem resilience in a rapidly changing world.

Understanding how biocrust functions shift across climatic gradients is critical for predicting soil ecosystem responses to environmental changes. The interactions among biocrusts, microbial communities, and plant roots along these gradients exemplify the inherent complexity and nonlinearity of soil processes (Wang et al., 2014). Biocrusts exert differing influences on soil aggregate stability, soil erodibility, water and nutrient flows, reflecting adaptive responses to variations in moisture availability, temperature, and vegetation cover (Belnap, 2003; Weber et al., 2022). In arid climates, biocrusts typically dominate soil surfaces, forming protective layers that significantly modulate

hydrological processes, sediment transport, and microbial activity, thereby strongly influencing soil structure and organic matter dynamics (Kidron et al., 2021; Rodríguez-Caballero et al., 2018). However, as climatic humidity increases, the interplay between biocrusts and plant roots becomes more intricate, with intensified competition from vegetation altering microbial community composition and reshaping nutrient pathways (?Seitz et al., 2017). Rather than transitioning gradually, these interactions likely exhibit thresholds and complex feedback loops Wang et al. (2014), implying that even subtle climatic shifts can substantially modify ecosystem functions (Bernhard et al., 2018). Recognizing these nonlinear responses is critical for predicting how soils—and the ecosystems they sustain—will adapt to current and future climatic changes. Addressing these knowledge gaps through quantitative assessments of biocrust-driven processes is therefore essential for developing effective conservation strategies, promoting soil health, and enhancing ecosystem resilience (?Weber et al., 2022).

1.7 Objectives and hypothesis

This research forms part of the DFG Priority Program: EarthShape: Earth Surface Shaping by Biota (DFG-SPP 1803), specifically within the subproject Microbial Engineers - Drivers of Earth Surface Development and Stabilization. The subproject aims to understand microbial processes that shape Earth's surface, focusing on the roles microorganisms play and providing a quantitative understanding of the mechanisms and microbial taxa involved under various climate conditions. It addresses these questions by: (i) experimentally investigating how microorganisms alone control the formation and transition of initial soils into resilient ecosystems; and (ii) analyzing the combined influence of microorganisms, biocrusts, and plant roots on soil surface stability and erosion under natural and controlled conditions along climatic gradients.

It is hypothesized that biocrusts enhance soil aggregate stability by physically protecting the soil surface, sheltering organic matter, altering microbial community structures, and modifying water infiltration patterns (Manuscripts 1 and 2). This stabilizing effect is expected to be most pronounced in arid climates, where biocrusts represent the primary soil cover due to minimal vegetation and limited organic matter inputs. With increasing humidity, however, the influence of biocrusts on soil stabilization is predicted to diminish, though it will not disappear entirely, due to greater water availability and competition from vegetation (Manuscript 1).

Furthermore, soil microbial communities are hypothesized to accelerate soil formation processes in arid environments when moisture and temperature conditions are favorable. Responses to simulated climate change are expected to be mediated by soil legacy effects, shaping microbial community structure and interactions over time. Bacterial diversity and adaptation processes likely reflect climatic shifts, providing insight into long-term soil developmental dynamics (Manuscript 3). Microbial communities are

also expected to be crucial for soil aggregation by influencing soil structure and stability across different climates and stages of soil development. Specific microbial taxa may differentially influence aggregation processes, with their contributions being modulated by biotic and abiotic factors, including wetting-drying cycles and moisture fluctuations (Manuscript 4).

Roots are hypothesized to promote water-stable macroaggregate formation in topsoil and subsoil, with legacy effects persisting after plant death within the detritusphere (Manuscript 5). Microbial abundance near roots is expected to increase due to labile carbon availability, especially in carbon-poor subsoils. The transition from rhizosphere to detritusphere likely triggers microbial succession, favoring gram-positive bacteria as readily available carbon compounds are replaced by more complex materials. Root-derived organic matter, including rhizodeposits and litter, is presumed to significantly influence organic matter dynamics by facilitating the formation of particulate and mineral-associated organic matter, thereby shaping aggregate formation and biogeochemical processes (Manuscript 5).

Lastly, biocrusts are hypothesized to regulate hydrological processes such as runoff, sediment discharge, and percolation flows, along with associated carbon and nitrogen fluxes, thereby reducing soil erosion irrespective of climatic conditions. However, climate-specific feedbacks among these hydrological processes likely mediate carbon and nitrogen transport within biocrust-dominated ecosystems (Manuscript 2). To test these hypotheses, the objectives of this thesis were to:

- Evaluate the role of biocrusts in soil aggregate stabilization and their regulation of erosion, water, and nutrient fluxes across a climatic gradient in the Chilean Coastal Range, examining how variations in biocrust properties correlate with changes in climate and vegetation cover (Manuscripts 1 and 2).
- Examine how soil microbial communities influence aggregate formation and stability under different climatic and moisture regimes, as well as their responses to simulated climate-change scenarios (Manuscripts 3 and 4).
- Determine the influence of plant roots on soil structure development, microbial succession, and organic matter dynamics during transitions from rhizosphere to detritusphere, emphasizing their role in soil aggregate formation (Manuscript 5).

Chapter 2

Methodology

2.1 Study sites and experimental setting

In order to assess the climatic effect on soil and its interactions with biocrusts, five study sites distributed between latitudes from 26°6' S to 37°48' S and over 1315 km were established in the Chilean Coastal Range (Figure 2.1): Pan de Azúcar National Park (PdA), Santa Gracia Natural Reserve (SG), Quebrada de Talca Private Reserve (QdT), La Campana National Park (LC) and Nahuelbuta National Park (NA), corresponding to arid, coastal semi-arid, inland semi-arid, Mediterranean and humid climates, respectively (Bernhard et al., 2018).

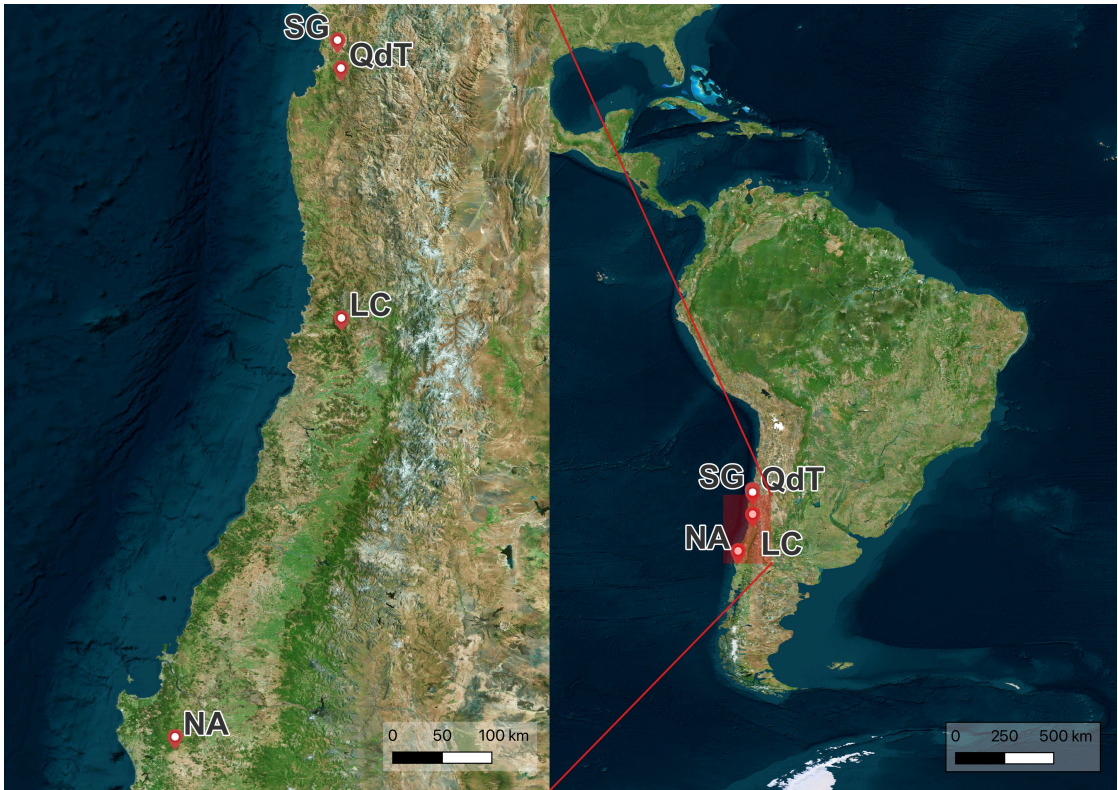


Figure 2.1: Location of study sites relative to South America. From north to south: Pan de Azúcar (PdA), Santa Gracia (SG), Quebrada de Talca (QdT), La Campana (LC), and Nahuelbuta (NA).

The study sites are comparable in geology, geomorphology, land use, and influence of glaciers and volcanoes (Bernhard et al., 2018). The parent material in all the study sites is granitoid (Bernhard et al., 2018). The dominant topography is generally fluvial valleys, and the sites had no glacial influence during the last glaciation (Hulton et al., 2002). The sites are located within nature protection areas, with limited anthropogenic influence compared to the surrounding areas. Despite this, cattle occasionally enter these locations, and goats, mules, and donkeys have been reported to SG (Armesto and Arroyo, 2007).

The mean annual temperature (MAT) decreases from north to south (PdA: 16.8 °C, SG: 13.7 °C, QdT: 14.3 °C, LC: 14.1 °C, NA: 6.6 °C). The mean annual precipitation (MAP) in the study sites increases from north to south (PdA: 12 mm yr⁻¹, SG: 66 mm yr⁻¹, QdT: 109 mm yr⁻¹, LC: 367 mm yr⁻¹, NA: 1469 mm yr⁻¹) with similar rainfall distribution mostly concentrated in winter months (May to August) (Bernhard et al., 2018; Santibáñez Quezada, 2017). The elevation of the sites increases from north to south (PdA: 329 m to 351 m, SG: 642 m to 720 m, QdT: 565 m to 611 m, LC: 708 m to 732 m, NA: 1200 m to 1270 m). Paleoclimate modeling studies (Mutz et al., 2018) indicate that these climate patterns have been persistent since the late Pliocene; thus, the

2.1 Study sites and experimental setting

study sites represent the long-term impact of climate on the soil (Ewing et al., 2006). Bernhard et al. (2018) classified soils in the study sites as Regosols in PdA, Cambisols for SG and LC, and Umbrisols in NA. In general, pedogenic properties such as soil depth, clay content, organic matter accumulation, porosity, and activity ratio are positively correlated with site humidity (Bernhard et al., 2018).

For each of the 5 study sites (Figure 2.2), 5 plots of 1 m × 1 m were set up as replicates (P1 to P5). Each plot was assigned in the top-slope position with a south-facing exposition, considering a high presence of site-typical biocrust communities, similar slope and aspect, lack of anthropogenic disturbance, and a maximum distance of 30 m between each plot. Within each plot, patches with the highest available biocrust cover were included as treatment BSC+, and nearby bare soil without biocrust cover was defined as control (BSC-).

Chapter 2 Methodology

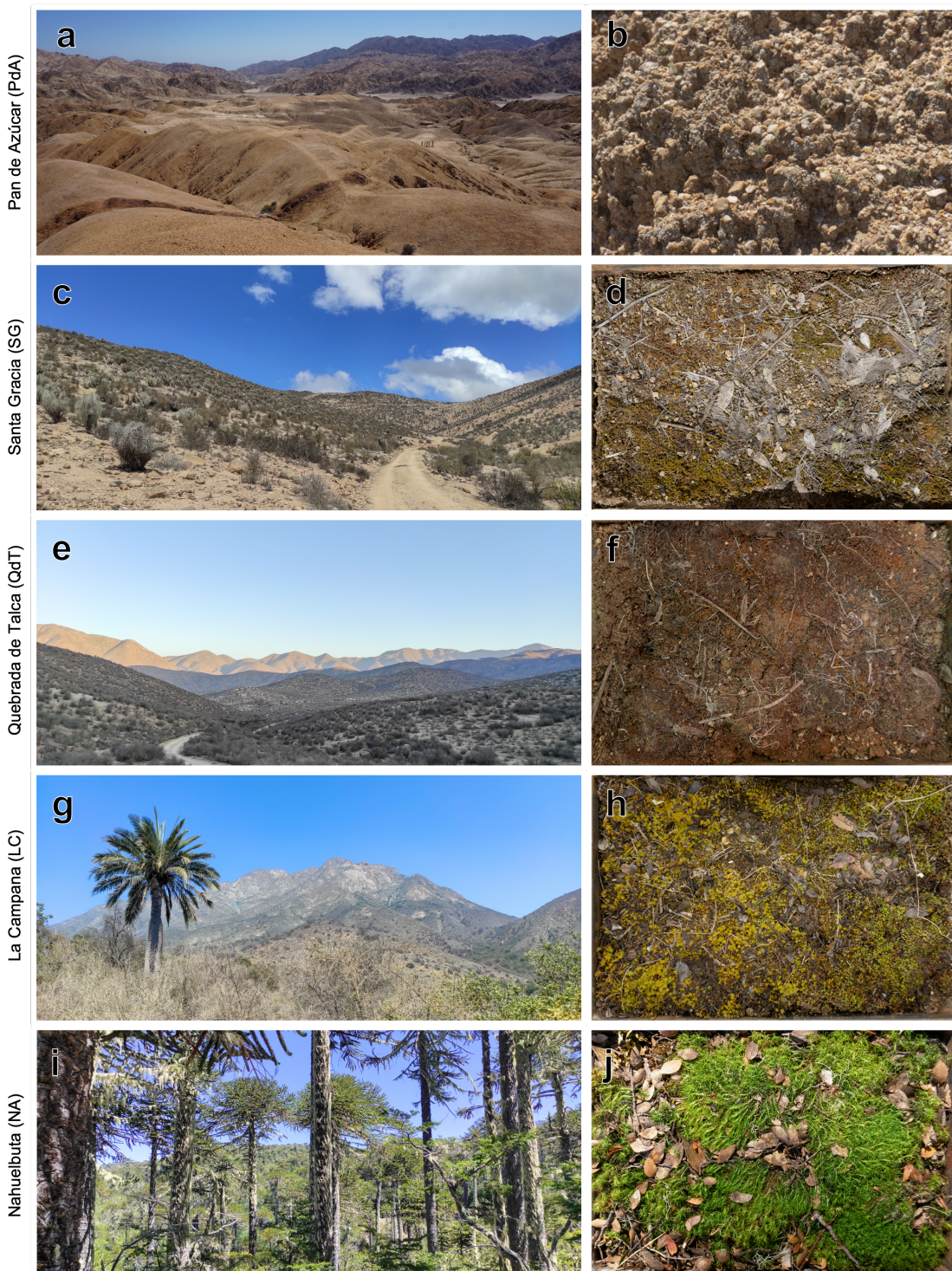


Figure 2.2: General view (a, c, d, g, and i) and sampled biocrust (b, d, f, h, and j) of PdA, SG, QdT, LC, and NA.

2.2 Field methods

2.2.1 Biocrust sampling and characterization

In a first field campaign during March 2019, biocrust patches of approximately 100 cm² were collected in PdA, SG, LC and NA and identified according to Lange and Belnap (2016). The patches were collected in the field by carefully detaching the biocrust layer, removing the loose soil, and storing it in paper envelopes after air-drying for every research plot. Samolov et al. (2020) describes a biocrusts dominance in PdA with cover of up to 40%. The other study sites are dominated by higher vegetation that limits the cover of biocrust up to 15% in SG and 5% in LC and NA. Sampled communities showed all typical biocrust classes from cyanobacteria, algae, fungi, lichens, liverworts, and mosses. The species composition further showed a graduating change from lichen-dominating biocrusts in the northernmost site to bryophyte-dominating biocrusts in the southernmost site. Biocrusts in NA were specifically found in zones of forest soil disturbance. Bryophyte-dominated biocrusts were sampled with rhizoids down to 5 mm depth; all other communities were down to 2 mm. Dominant macroscopic biocrust species were determined for each of the four sites to the genus level by morphological characteristics using a stereomicroscope (Leitz TS, Wetzlar, Germany), a transmitted-light microscope (Leitz Laborlux S, Wetzlar, Germany), and ultraviolet light. Species groups were separated into bryophytes (Ardiles and Fariña, 2014; Bednarek-Ochyra, 2001; Cuvertino et al., 2012; He, 1998; Lightowers, 2013) and lichens (Galloway, 2007) and assigned to the different regions (Table A.1). Bernhard et al. (2018), based on morphological identification of enrichment cultures, reported that the biocrusts of the four studied sites were composed of 18 to 15 species of algae and cyanobacteria; where the richness of green algae increased, while the richness of cyanobacteria decreased with increasing humidity and decreasing mean annual temperature. While Samolov et al. (2020), based on morphological and molecular traits, reported 18 species in PdA, 26 species in SG, 40 species in LC, and 27 species in NA.

Chapter 2 Methodology

Table 2.1: Taxonomical composition of mosses and lichens in the biological soil crust for the study sites along the climatic gradient.

Site / Division	Family	Genus	No. species
PdA			
Lichens	Cladoniaceae	<i>Cladonia</i> sp.	2
	Verrucariaceae	<i>Placidium</i> sp.	2
	Lecanoraceae	<i>Lecidella</i> sp.	1
	Rhizocarpaceae	<i>Rhizocarpon</i> sp.	1
SG			
Mosses	Pottiaceae	<i>Syntrichia</i> sp.	2
	Pottiaceae	<i>Tortella</i> sp.	2
Unidentified lichens			2
LC			
Mosses	Bartramiaceae	<i>Philonotis</i> sp.	1
	Bryaceae	<i>Bryum</i> sp.	1
	Pottiaceae	<i>Syntrichia</i> sp.	2
	Pottiaceae	<i>Tortella</i> sp.	2
Unidentified mosses and lichens			2 + 1
NA			
Mosses	Amblystegiaceae	<i>Acrocladium</i> sp.	1
	Amblystegiaceae	<i>Amblystegium</i> sp.	1
	Bartramiaceae	<i>Bartramia</i> sp.	1
	Bryaceae	<i>Bryum</i> sp.	1
	Dicranaceae	<i>Campylopus</i> sp.	2
	Pterigynandraceae	<i>Myurella</i> sp.	1
Unidentified liverworts, lichens, fungi			2 + 2 + 1

2.2.2 Soil sampling

Soil sampling campaigns were primarily conducted during the austral dry season (typically January-April) to capture baseline soil conditions prior to the onset of winter precipitation. Specific sampling approaches were adapted based on the objectives of individual studies. For investigations concerning aggregate stability, moisture regime effects, and general baseline characterization across the full gradient (PdA, SG, LC, NA), bulk topsoil samples (0 cm to 5 cm depth) were collected from each plot on mid-slope, south-facing locations using metal-core augers or by sampling from shallow soil pits (Manuscripts 1 and 4). These samples were processed in the field by sieving (<2 mm), another batch of samples was sieved and sterilized with ethanol, before being homogenized per site or kept discrete per plot depending on the experimental design and subsequently stored at 4 °C pending laboratory analysis. For studies focusing on initial soil formation and rhizosphere/detritusphere dynamics (PdA, SG), distinct soil horizons (A horizon: 0 cm to 2 cm/0 cm to 3 cm; B horizon: 2 cm to 3 cm/25 cm to 40 cm) where

sampled from excavated soil pits (Manuscripts 3 and 5). Processing involved similar steps: sieving (<2 mm), homogenization per horizon and site, and storage at 4 °C.

2.2.3 Rainfall simulations

Following observations of limited soil stabilization at PdA, further rainfall simulation experiments were conducted during subsequent expeditions in 2020 and 2022 at SG, Quebrada de Talca (QdT), LC, and NA. Five 1 m × 1 m plots were established as replicates at each of the four sites, consistently located on south-facing top slopes. Plot selection considered the presence of representative biocrust communities, similar slope and aspect, minimal anthropogenic disturbance, and a maximum inter-plot distance of 30 m. Within each plot, runoff plots (ROPs) were established in areas with maximum biocrust cover for biocrust-present (BSC+) treatments, and adjacent biocrust-free (BSC-) locations served as controls. The experimental design was a factorial completely randomized design, incorporating four sites (SG, QdT, LC, and NA) (Figure 2.2), two biocrust conditions (BSC+ and BSC-), five replicate plots (P1-P5), and three technical replicate ROPs (R1-R3) per plot. This resulted in a total of eight treatments (site × biocrust) with 15 samples per treatment (plot × technical replicate), yielding a total sample size of n = 60.

Undisturbed soil samples for rainfall simulation were collected (Figures 2.3b and 2.3c), using piercing frames (20 m × 30 m × 7 m) (Figure 2.3a) and carefully installed into infiltration boxes to minimize surface and subsurface disturbance (Figure 2.3d). These steel boxes, designed with a triangular surface runoff gutter and a bottom outlet, captured both runoff and percolated water. Soil water content was measured using a TDR probe (Delta-T Devices Ltd. Cambridge, UK), averaging three measurements adjacent to each ROP. Biocrust cover in BSC+ ROPs was assessed using perpendicular photographs taken with a digital camera (Sony ILCE-6000, SELP1650 lens; Tokyo, Japan). Photographs were analyzed using the grid-quadrat method with a 100-subdivision grid, and biocrusts were identified visually (Belnap et al., 2001).

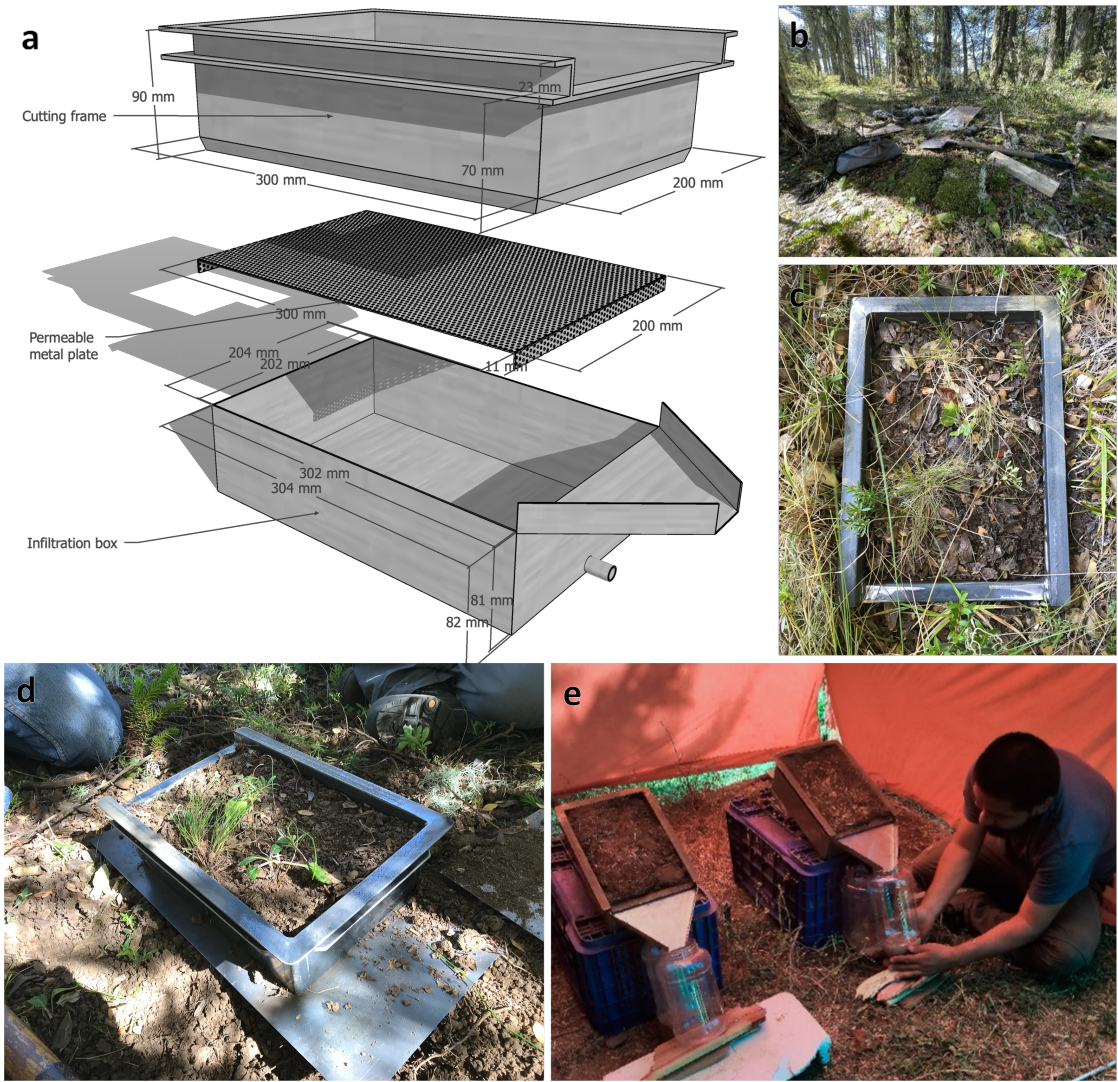


Figure 2.3: Construction diagram of the soil erosion flux box used in the experiment (a), general view of a plot with the presence of biocrust prior to sampling (b). (c, d) shows an installed cutting frame and the cleared and prepared soil. (e) demonstrates the setting for rainfall simulations at the Nahuelbuta (NA) study site.

Rainfall simulations were conducted near the sampling locations using the Tübingen rainfall simulator (Iserloh et al., 2013; Seitz, 2015) equipped with a Lechler 460.788.30 nozzle and set to a falling height of 3.5 m. Infiltration boxes were placed inside the simulator on a 10° slope (Figure 2.3e). A rainfall event was simulated using an intensity of 45 mm h^{-1} sustained over a 30-minute period. According to regional intensity-duration-frequency analyses for central Chile (Pizarro-Tapia et al., 2020), such an intensity falls within the extreme rainfall category, well above the heavy precipitation threshold even

for relatively wet climates. This extreme intensity was selected to exceed the soil infiltration capacities and reliably generate surface runoff at all study sites. The time to initial runoff and percolation was recorded. Runoff and sediment-laden water samples were collected separately. Runoff volume was measured using a graduated beaker. Samples were allowed to settle by gravity for 12 hours, after which a water sample was extracted from the supernatant via siphoning, frozen at -4°C and transported to the University of Tübingen for DOC and DON analysis. The remaining sediment was oven-dried at 105°C for 48 hours after all visible moisture was removed, then weighed. Sediment load was determined by dividing the dry sediment weight by the corresponding runoff volume and transported to the University of Tübingen for total C and N analyses.

2.3 Laboratory methods

2.3.1 Baseline soil characterization

Before commencing experimental manipulations, a suite of baseline soil properties was determined on the sieved ($<2\text{ mm}$), air-dried field samples. Physical properties measured included bulk density (BD), determined gravimetrically, and particle size distribution (PSD). PSD was analyzed following the method of ?, which combines sieving for fractions larger than $20\text{ }\mu\text{m}$ with pipetting for fractions smaller than $20\text{ }\mu\text{m}$ (Manuscript 1). Soil texture classes were subsequently interpreted based on World Reference Base (WRB) guidelines (Jahn et al., 2006). Chemical properties assessed included soil pH and electrical conductivity (EC), measured in soil:water suspensions (1:2.5 or 1:5 ratios) using calibrated meters (Manuscripts 1, 3 and 5). Total carbon (C_T) and total nitrogen (N_T) contents were quantified via oxidative heat combustion at high temperatures (1150°C) using an elemental analyzer (Vario EL III, Euro EA) (Manuscripts 1, 3, 4 and 5). Soil organic carbon (SOC) was typically calculated by subtracting the inorganic carbon (SIC) content from the C_T content. SIC was measured using a calcimeter (Scheibler method) or determined through acid digestion, particularly for soils with pH values exceeding 6.7–7.0 (Manuscripts 1, 3 and 4). Additionally, concentrations of various inorganic ions (Cl^- , NO_3^- , PO_4^{3-} , SO_4^{2-} , Na^+ , Ca^{2+}) were measured in soil leachates prepared from the samples, utilizing ion chromatography (IC) (Manuscript 3).

2.3.2 Aggregate stability

Various methods were utilized to evaluate soil aggregate stability and to physically separate soil into different fractions based on aggregate size or density, tailored to the specific research objectives of each study. To assess overall aggregate stability across the climate gradient (Manuscript 1), a large-sample (200 g, homogenized $<30\text{ mm}$) two-stage siev-

ing method based on Horn (2009) and Six et al. (2000) was employed. Samples underwent initial dry sieving through a nested stack of sieves (ranging from 19.0 mm down to 2.0 mm), followed by a repetition of the sieving process underwater. Water-stable aggregates ($WSA_{2.0\text{ mm}}$) were determined, and several stability indices were calculated from the dry and wet sieving results. The difference in mean weight diameter (MWD), representing the average size of aggregates weighted by their mass proportion, was calculated as:

- Difference in mean weight diameter (ΔMWD)

$$\Delta MWD = \frac{\sum_{i=1}^n X_i * W_i}{\sum_{i=1}^n W_i}$$

were:

- X_i : The mean diameter of the stable aggregate fraction i .
- W_i : The corrected mass proportion of the stable aggregate fraction i within the total considered range (e.g., 2-30 mm).
- n : The total number of aggregate size fractions being analyzed.

- Difference in geometric mean diameter (ΔGMD):

$$\Delta GMD = \exp \left[\frac{\sum_{i=1}^n X_i \lg W_i}{\sum_{i=1}^n W_i} \right]$$

were:

- X_i : The mean diameter of the stable aggregate fraction i .
- W_i : The corrected mass proportion of the stable aggregate fraction i within the total considered range (e.g., 2-30 mm).
- n : The total number of aggregate size fractions being analyzed.

- Water stability aggregate ratio (WSAR):

$$WSAR = \frac{WSA}{A} * 100$$

were:

- WSA : The content (mass or weight) of water-stable aggregates larger than 2 mm after a stability test.
- A : The content (mass or weight) of dry aggregates larger than 2 mm before the stability test.

- Proportion of soil macroaggregate of a diameter less than 2 mm ($R_{<2mm}$)

$$R_{<2mm} = \frac{W_{r>2}}{W_T} * 100 = \left(1 - \frac{W_{r<2}}{W_T} \right)$$

were:

- $W_{r>2}$: The content (mass or weight) of water-stable aggregates larger than 2 mm after a stability test.
- W_T : The content (mass or weight) of dry aggregates larger than 2 mm before the stability test.
- $W_{r<2}$: The weight of microaggregates and primary particles with a diameter less than 2 mm.

For other investigations focusing on aggregate turnover dynamics and the association of microbial communities or organic matter with specific aggregate sizes (Manuscripts 3, 4 and 5), wet sieving techniques were applied to smaller soil samples (5 g to 10 g). One approach utilized a modified Casagrande apparatus, shaking 5 g of soil on stacked sieves (250 µm to 53 µm) through 1000 cycles at 2 Hz. This yielded fractions defined as macroaggregates (>250 µm), large microaggregates (250–53 µm), and a combined fraction of small microaggregates and primary particles (<53 µm) (Manuscript 3). Another frequently used method, adapted from Elliott (1986), involved pre-wetting 10 g of soil, followed by manual immersion sieving. This typically involved moving a stack of sieves (>500 µm, 500 µm–250 µm, 250–53 µm, 53–20 µm) gently up and down in water for a set number of repetitions (30 strokes over 5 minutes), with the finest fraction (<20 µm) captured on a filter paper (Manuscript 4). Following separation by either method, the recovered aggregate fractions were carefully oven-dried (at 40 °C or 105 °C) and weighed. The MWD was often calculated from the resulting mass distribution across the obtained size classes.

To isolate soil organic matter (SOM) pools based on their physical protection and association with minerals (Manuscript 5), density fractionation was performed. This procedure typically used sodium polytungstate (SPT) solution at an adjusted density of 1.8 g cm⁻³. Bulk soil or pre-defined aggregate fractions were suspended in the SPT solution, allowing the lighter, free particulate OM (fPOM) to float and be separated. Subsequently, ultrasonic dispersion (using an energy input of 440 J mL⁻¹) was applied to break apart remaining aggregates and release occluded POM (oPOM). This oPOM was then further separated by wet sieving into 3 different size classes (>63 µm, 63–20 µm, <20 µm). The dense mineral material remaining after these separation steps constituted the mineral-associated OM (MAOM). All physically separated SOM fractions were thoroughly rinsed to remove the SPT, dried, and weighed. The SOC, C_T and N_T contents of these individual aggregate size or density fractions were then determined using elemental analysis, providing crucial information on carbon and nitrogen storage

and distribution within the soil's physical structure (Manuscripts 3, 4 and 5). In addition, stable isotope analysis ($\delta^{13}\text{C}$, $\delta^{15}\text{N}$) was conducted on density fractions to elucidate the sources and transformation pathways of the organic matter (Manuscript 5).

2.3.3 Incubation experiments

Controlled laboratory incubations were central to simulating specific environmental scenarios or distinct stages of soil succession. To mimic a climate change scenario involving a shift to more humid conditions for arid and semi-arid soils (Manuscript 3), soil microcosms were established using sterilized PVC columns filled with 130 g of sieved soil. These were incubated under controlled diurnal temperature fluctuations, a 14/10 h day/night photoperiod, and a defined moisture regime involving rewetting to 65% water-filled pore space (WFPS) three times per week, reflecting conditions of the humid Nahuelbuta (NA) site. Experimental treatments encompassed sterile controls, native soil containing indigenous microorganisms (*in situ*), native soil where biocrusts were allowed to develop (BSC), and native soil cultivated with a pioneer plant species (*Helenium aromaticum*). Destructive sampling of microcosms occurred at baseline (T0) and after 2, 12, and 16 weeks of incubation. To specifically assess the impact of differing moisture regimes on soil properties and microbial communities (Manuscript 4), native and sterilized soils (60 g) were incubated in Tübingen cups (T-cups) for a total of six weeks. Treatments included repeated wetting-drying (WD) cycles and a constant moisture (CM) condition. WD cycles involved saturating the soil to field capacity (pF 1.8), allowing it to air-dry (25 °C, 1-2 days), and then re-saturating it by placing the T-cup on a sterile sand bed. CM samples remained continuously saturated on the sand bed. Sampling points included the initial state (R0) and after one, three, and six WD cycles (R1, R3, R6), as well as after six weeks under constant moisture (CM). For studying the transition from a living root system to a decomposing one (Manuscript 5), an experiment focusing on rhizosphere and detritusphere dynamics was conducted. Semi-arid topsoil and subsoil were incubated in pots, either with or without the pioneer plant *Helenium aromaticum*, under greenhouse conditions for 70 days (representing the rhizosphere phase). Following this, the aboveground plant biomass was clipped at the soil surface, and the pots were moved to darkness at room temperature for an additional 100 days, allowing the roots and shoots to decompose *in situ* (representing the detritusphere phase). Soil samples were collected at the conclusion of both the rhizosphere and detritusphere phases, carefully separating root-adhering soil from bulk rhizosphere/detritusphere soil where feasible.

2.3.4 Molecular analyses

The abundance and composition of microbial communities were investigated using quantitative PCR (qPCR) and high-throughput amplicon sequencing. Total genomic

DNA was extracted from soil samples (typically 0.25–0.5 g per extraction), often in duplicate or triplicate, using commercially available kits like the DNeasy PowerSoil Kit (Qiagen), adhering to the manufacturer's protocols (Manuscripts 3 and 4). The abundance of major microbial groups – bacteria, archaea, and fungi – was quantified by qPCR targeting specific ribosomal RNA gene fragments. Commonly used primer pairs included Eub341F/Eub534R for bacterial 16S rRNA genes, 340F/1000R for archaeal 16S rRNA genes, and NL1F/LS2R for fungal 28S rRNA genes or ITS region primers. qPCR assays were performed using SYBR Green-based detection on real-time PCR platforms (Bio-Rad CFX96). Quantification relied on standard curves generated from serial dilutions of plasmids containing known copy numbers of the target gene. Rigorous quality control included monitoring reaction efficiencies and analyzing melt curves to ensure amplification specificity (Manuscripts 3 and 4). For detailed community composition analysis, the V4 hypervariable region of the 16S rRNA gene was typically amplified using universal primers (515F/806R) tagged with unique barcodes for sample multiplexing. Sequencing was performed using the Illumina MiSeq platform, generating paired-end reads (2x300bp) (Manuscripts 3 and 4). The resulting raw sequence data underwent a standardized bioinformatics pipeline. This involved demultiplexing reads based on barcodes (using cutadapt), performing quality filtering and trimming, merging paired-end reads (where applicable), identifying and removing chimeric sequences, and generating Amplicon Sequence Variants (ASVs) using algorithms like DADA2. Taxonomic classification of ASVs was achieved by comparison against established reference databases, primarily SILVA. Sequences identified as originating from chloroplasts, mitochondria, or represented by only a single read (singletons) were typically removed from the final dataset (Manuscripts 3 and 4). In some cases, potential ecological functions of the identified prokaryotic taxa were inferred using predictive tools such as FAPROTAX (Manuscript 4).

2.3.5 Organic matter and microbial biomarker characterization

To gain deeper insights into the composition of soil organic matter (SOM) and the structure of microbial communities, advanced analytical techniques were employed. The chemical composition of bulk plant material and specific SOM pools isolated via density fractionation (POM fractions) was characterized using solid-state ^{13}C Cross-Polarization Magic Angle Spinning (CP-MAS) Nuclear Magnetic Resonance (NMR) spectroscopy. The resulting spectra were quantified based on established chemical shift regions corresponding to major biochemical classes, including alkyl C, O-alkyl C, aromatic C, and carbonyl C. Diagnostic indices, such as the alkyl C/O-alkyl C ratio, were calculated to infer OM composition and degradation state. Additionally, a Molecular Mixing Model (MMM) was sometimes applied to estimate the relative contributions of broader biochemical categories like carbohydrates, proteins, lipids, and lignin to the overall OM (Manuscript 5).

The composition of lignin within plant and root biomass was specifically investigated through cupric oxide (CuO) oxidation. This method breaks down the lignin polymer into characteristic phenolic monomers (vanillyl (V), syringyl (S), and cinnamyl (C) units), which were then quantified using Gas Chromatography-Mass Spectrometry (GC-MS). Total lignin content was estimated based on the sum of these units (VSC), and diagnostic ratios, such as S/V, C/V, and acid-to-aldehyde ratios within each phenol group (e.g., $(\text{Ac}/\text{Al})_V$), were calculated to assess lignin source and degradation stage (Manuscript 5).

Phospholipid Fatty Acid (PLFA) analysis was used to characterize the structure and biomass of the active microbial community. Lipids were extracted from soil using methods like a modified Bligh & Dyer extraction, and PLFAs were separated from neutral and glycolipids, often via solid-phase extraction. The purified PLFAs were then converted into Fatty Acid Methyl Esters (FAMEs) through transesterification and subsequently analyzed using Gas Chromatography coupled with Flame Ionization Detection (GC-FID). Specific FAMEs served as biomarkers for different microbial groups: e.g., 18:2 ω 6,9 for fungi; iso- and anteiso-branched fatty acids for gram-positive bacteria; and monounsaturated or cyclic fatty acids for gram-negative bacteria. These data allowed for the calculation of total microbial biomass and structural indices such as the fungi:bacteria ratio and the gram⁺:gram⁻ ratio (Manuscript 5).

2.4 Statistical analyses

The statistical analyses across manuscripts 1 to 5 employed a range of methods to investigate the relationships between biocrusts, microbial communities, plant roots, and soil properties. Generalized linear models (GLMs) were commonly used to assess the influence of factors like climate, biocrust presence, and treatments on soil properties and aggregate stability (Manuscripts 1, 2 and 3). Model selection was based on the Akaike Information Criterion (AIC) and data characteristics, utilizing appropriate link functions (Gaussian, Gamma, inverse Gaussian, Tweedie) to account for non-normal distributions (Dunn, 2017; Team, 2018; Wickham, 2016). Tukey's post-hoc test was used for pairwise comparisons ($p < 0.05$).

Analysis of variance (ANOVA) and analysis of covariance (ANCOVA) were also employed, particularly to assess differences in measured properties between treatments and across sites or horizons. Where applicable, soil baseline variables were used as covariates in ANCOVA (Manuscripts 2 and 5). Non-parametric tests, such as the Kruskal-Wallis test followed by Mann-Whitney post-hoc tests, were used when normality or homoscedasticity assumptions were violated (Manuscript 3). Data transformations were applied when necessary, using the *bestNormalize* package (?Peterson, 2021). The Dunn-Šidák correction was implemented for multiple comparisons (Hothorn et al., 2008).

Microbial community data were analyzed using various multivariate techniques. Non-

2.4 Statistical analyses

metric multidimensional scaling (NMDS) was used to visualize community structure and beta diversity (Oksanen et al., 2013). Permutational multivariate analysis of variance (PERMANOVA) assessed the significance of differences between groups (e.g., sites, horizons, time points), often followed by pairwise PERMANOVA for detailed comparisons (Martinez Arbizu, 2020) (Manuscripts 3 and 4). Distance-based redundancy analysis (dbRDA) identified environmental factors influencing community composition (Manuscript 4). Indicator species analysis revealed taxa associated with specific sites or horizons using the *indval* function (Dufrêne and Legendre, 1997; Roberts and Roberts, 2016) (Manuscript 4).

Co-occurrence networks explored the complex relationships within microbial communities. Network properties, including modularity, connectance, and hub species, were calculated using the *igraph* package (Csardi and Nepusz, 2006), and correlations between ASVs were assessed using Pearson correlation (Harrell Jr and Harrell Jr, 2019) (Manuscript 4). Weighted gene co-expression network analysis (WGCNA) grouped highly correlated ASVs into modules to explore their relationships with physicochemical properties (Langfelder and Horvath, 2008) (Manuscript 4).

Molecular mixing models were used to quantify the relative contributions of different organic matter components (carbohydrates, proteins, lignin, lipids) based on ^{13}C NMR spectroscopy data (Nelson and Baldock, 2005; Prater et al., 2020) (Manuscript 5).

Chapter 3

Results and discussion

3.1 Effect of biocrust on soil aggregate stability (manuscript 1)

This study investigated the influence of biological soil crusts (biocrusts) on soil aggregate stability and their interplay with soil properties along a climatic gradient in the Chilean Coastal Range, spanning arid (PdA), semi-arid (SG), Mediterranean (LC), and humid (NA) conditions.

3.1.1 Climate-induced changes in soil properties

Soil properties varied significantly ($p < 0.05$) along the climate gradient (Figure 3.1), reflecting the influence of increasing precipitation and decreasing temperature from north to south on weathering and soil development. Bulk density generally decreased from the drier northern sites (PdA: 1.5 g cm^{-3} , SG: 1.6 g cm^{-3}) to the humid south (NA: 0.6 g cm^{-3}). Conversely, soil organic carbon (SOC) content increased significantly along the gradient, from approximately 0.3 % in PdA to 12.5 % in NA, emphasizing the role of climate in organic matter accumulation. Total nitrogen (N_T) followed a similar pattern, increasing from 0.04 % in PdA to 0.51 % in NA. However, the C/N ratio was highest at the climatic extremes (PdA: 33.9, NA: 24.5), potentially indicating nitrogen limitation in both the most arid and most humid environments, as suggested by Brust (2019). Soil pH decreased consistently and significantly along the gradient, from alkaline conditions in PdA (mean pH 7.7) to acidic conditions in NA (mean pH 4.4), likely due to increased leaching of base cations and higher biological acid production in wetter climates. Clay content also increased significantly from north (PdA: 9.6 %) to south (NA: 24.6 %).

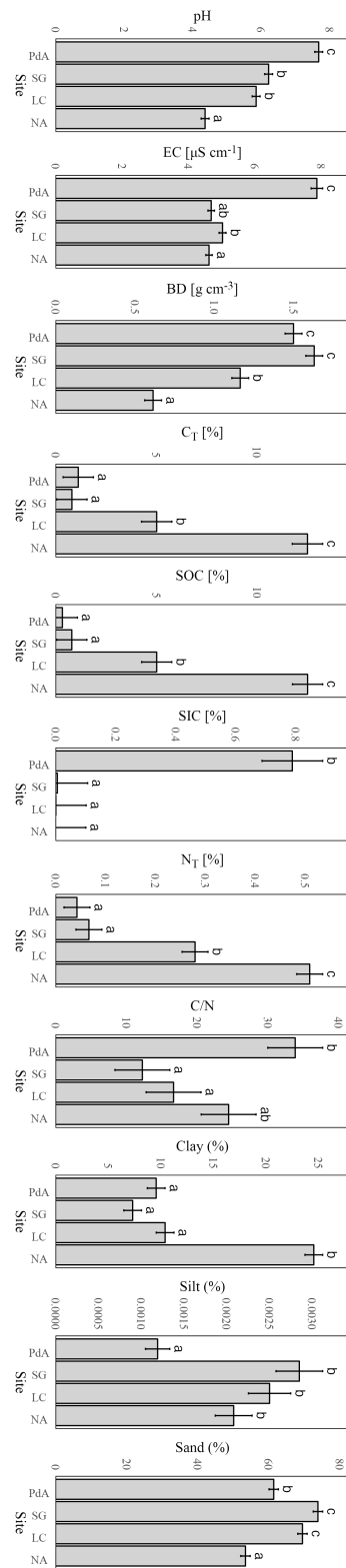


Figure 3.1: Soil physical and chemical properties across the four study sites (PdA: Pan de Azúcar, SG: Santa Gracia, LC: La Campana, and NA: Nahuelbuta). Letter-based display accompanying soil properties with significant effect for site. Different letters indicate statistically significant differences ($p < 0.05$, Šidák correction).

3.1.2 Biocrust-induced changes in soil properties

Biocrust presence significantly ($p < 0.05$) influenced several soil properties (Figure 3.2a), often interacting with the climatic site (Figure 3.2b). A significant site \times biocrust interaction was observed for bulk density, with biocrusts associated with a decrease in BD in arid PdA but an increase in Mediterranean LC. Biocrust presence significantly affected soil texture overall, associated with a slight decrease in clay and an increase in silt content when averaged across sites. However, the site \times biocrust interaction was significant for clay, showing a notable increase under biocrusts specifically in PdA. Across all sites, biocrust presence led to a small but statistically significant decrease in soil pH, potentially reflecting localized acidification due to respiration (Bachar et al., 2010). C_T and SOC contents were significantly lower under biocrusts when averaged across all sites. A significant site \times biocrust interaction affected N_T, showing significantly lower values under biocrusts only in the humid LC and NA sites. The C/N ratio was significantly lower under biocrusts overall, driven partly by changes in PdA. Electrical conductivity (EC) was extremely high in PdA compared to other sites, and the site \times biocrust interaction showed a significant reduction in EC under biocrusts only in PdA.

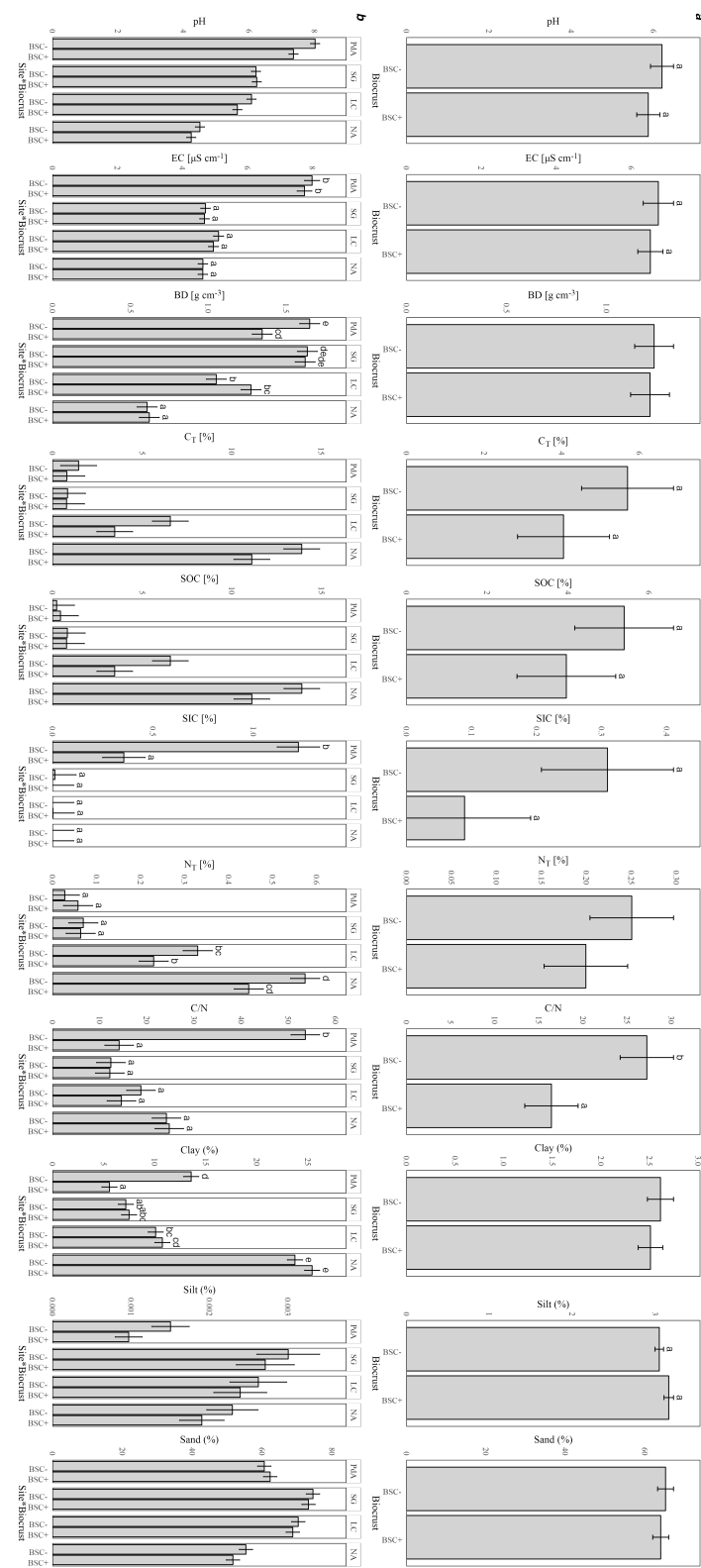


Figure 3.2: Biocrust (a) and interaction (b) effects on soil properties. Soil physical and chemical properties across for biocrust (BSC+ vs. BSC-) and the interaction with the site (PdA: Pan de Azúcar, SG: Santa Gracia, LC: La Campana, and NA: Nahuelbuta). Letter-based display accompanying soil properties with significant effect for site or site*biocrust. Different letters indicate statistically significant differences ($p < 0.05$, Šidák correction).

3.1.3 Biocrust and climate interactions on aggregate stability

Soil aggregate stability showed clear responses to both the climatic gradient and biocrust cover, particularly when assessed under wet conditions. Overall aggregate stability, indicated by the difference in geometric mean diameter (ΔGMD), significantly increased (lower ΔGMD indicates higher stability) along the climatic gradient from PdA (mean ΔGMD 1.86 mm) to NA (mean ΔGMD 0.83 mm), although SG showed higher stability (mean ΔGMD 1.2 mm) than LC (mean ΔGMD 1.4 mm). The water stability aggregate ratio (WSAR) confirmed this trend, with NA (mean WSAR 81.1%) being significantly more stable than the other sites (mean WSAR 57.7% - 73.4%).

Biocrusts exerted a significant stabilizing effect, particularly on larger aggregates under wet sieving conditions. The presence of biocrusts significantly increased the proportion of water-stable aggregates >2 mm overall. Specifically, the interaction between site and biocrust was significant for wet aggregates in the 9.5–30.0 mm range, showing a stabilizing effect (increase in proportion) in PdA, SG, and LC, but not in the humid NA site. This suggests a threshold effect, where the stabilizing role of biocrusts diminishes as vascular vegetation and associated stabilizing agents become more dominant under humid conditions. Correspondingly, biocrust presence significantly decreased the proportion of water-stable aggregates <2 mm ($R_{<2\text{ mm}}$) overall (from mean 63.7% without biocrusts to 57.5% with biocrusts) (Figure 3.3).

These findings highlight that biocrusts contribute to soil structure by binding particles and microaggregates, likely through mechanisms involving fungal hyphae, cyanobacterial filaments, and the production of extracellular polymeric substances (Six et al., 2004; Totsche et al., 2018). While biocrusts influenced bulk C and N contents, the lack of a direct correlation between these bulk changes and stability across all sites suggests that the specific composition and micro-spatial arrangement of organic binding agents within aggregates, rather than just total C or N, are critical for stability (Wagner et al., 2007). The results emphasize the crucial role of biocrusts as primary stabilizing agents in arid and semi-arid ecosystems (Belnap and Büdel, 2016), with their influence gradually yielding to vascular plants and associated soil organic matter dynamics in more humid environments.

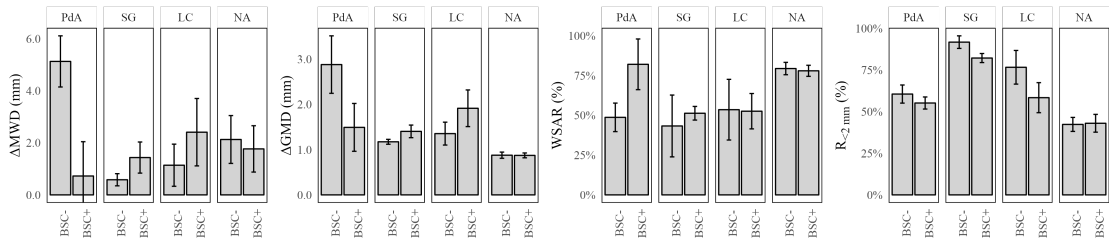


Figure 3.3: Aggregate stability indexes for Pan de Azúcar (PdA), Santa Gracia (SG), La Campana (LC), and Nahuelbuta (NA) for biocrust (BSC+) and non-biocrust (BSC-) treatments displays as mean and standard error. ΔMWD : difference in mean weight diameter, ΔGMD : difference in geometric mean diameter, WSAR: water stability aggregate ratio, $R_{<2\text{ mm}}$: ratio of aggregates less than 2 mm.

3.2 Effect of biocrust on water flow, erosion and nutrient flow (manuscript 2)

This study investigated the role of biological soil crusts (biocrusts) as climate-dependent regulators of erosion, water, and nutrient cycling using rainfall simulation experiments across a 910 km climate gradient in the Coastal Mountain Range of Chile. Four study sites represented coastal semi-arid (SG), inland semi-arid (QdT), Mediterranean (LC), and humid (NA) climates. These sites, characterized by comparable topography and granitic parent material, allowed for assessing biocrust influence under varying climatic conditions by comparing undisturbed soil monoliths with (+) and without (-) biocrust cover. We analyzed surface runoff, percolation flow, sediment transport, and associated carbon (C) and nitrogen (N) fluxes.

Soil properties varied across the climate gradient, reflecting differing weathering intensities and soil development stages relevant to hydrological and erosion responses. Notably, the inland semi-arid site (QdT) exhibited high biocrust cover despite lower water availability compared to the coastal SG site, likely due to protection from disturbance within a fenced area since 2011, fostering biocrust development (Büdel et al., 2016). Soil texture across sites was predominantly sandy loam, with clay content increasing southward, influencing water retention and infiltration pathways.

3.2.1 Biocrust influence on water flow and sediment transport

Biocrusts significantly modulated water flow and erosion dynamics, though their effects varied with climate and the specific pathway (runoff vs. percolation). Regarding runoff dynamics (Table B.1), biocrusts delayed runoff initiation across all sites, with a mean delay of 97.7%. This effect was particularly noticeable at the humid NA site, where dense bryophyte cover increased surface roughness and water storage (Kidron et al., 2022). Overall, biocrusts reduced total runoff volume by an average of 28.0%, although

3.2 Effect of biocrust on water flow, erosion and nutrient flow (manuscript 2)

this was site-specific, ranging from a 72.4% reduction in NA to an unexpected 36.4% increase in LC. Despite these impacts on surface flow, biocrusts did not measurably affect the time required for percolation to commence (Table B.2). The reduction in runoff volume (Table B.1) coupled with unchanged percolation timing (Table B.2) indicated enhanced cumulative infiltration and saturated hydraulic conductivity in the presence of biocrusts compared to bare soil. In terms of erosion and sediment flux, biocrusts proved highly effective at reducing soil erosion via surface runoff, decreasing total sediment transport by an average of 69.9% and sediment concentration in runoff by 60.9% (Table B.1). The most significant reduction occurred at the inland semi-arid QdT site, highlighting the protective role of biocrusts (Rodríguez-Caballero et al., 2018). Conversely, sediment mobilization via percolation increased by 28.3%, and sediment concentration in percolation rose by 58.3% when biocrusts were present. This demonstrates a clear shift in sediment transport dynamics, moving from predominantly surface erosion on bare soil to increased subsurface transport under biocrust cover.

Table 3.1: Surface runoff fluxes on the study sites (SG: Santa Gracia, QdT: Quebrada de Talca, LC: La Campana, NA: Nahuelbuta) with (+) and without (-) biocrust (BSC) cover. Values correspond to mean \pm standard deviation (SD) of five field replicates. Different letters indicate statistically significant different values based on Šidák correction post-hoc test results.

Factor		Time to start runoff ^a [s]	Runoff ^a [L h ⁻¹]	Sediment in runoff ^a [g m ⁻² h ⁻¹]	Sediment load of runoff ^a [gL ⁻¹ m ⁻²]
Mean \pm SD	SG	65.1 \pm 20.7 (a)	49 \pm 18 (b)	617 \pm 473 (c)	12.1 \pm 7.9 (a)
	QdT	78.7 \pm 30.4 (a)	40 \pm 16 (a)	398 \pm 459 (b)	9.6 \pm 9.6 (a)
	LC	83.5 \pm 56.0 (a)	39 \pm 22 (a)	241 \pm 293 (b)	7.3 \pm 8.8 (a)
	NA	236.7 \pm 273.0 (b)	44 \pm 43 (a)	28 \pm 44 (a)	3.0 \pm 14.0 (a)
Biocrust	BSC+	154.0 \pm 211.5 (b)	36 \pm 21 (a)	149 \pm 222 (a)	4.5 \pm 10.4 (a)
	BSC-	77.9 \pm 33.8 (a)	50 \pm 31 (b)	495 \pm 492 (b)	11.5 \pm 10.0 (b)
Site*Biocrust	SG BSC+	62.7 \pm 21.2 (ab)	44 \pm 16 (ab)	340 \pm 340 (bc)	7.5 \pm 5.7 (abc)
	SG BSC-	67.5 \pm 20.6 (ab)	54 \pm 18 (ab)	873 \pm 456 (d)	16.7 \pm 7.1 (de)
	QdT BSC+	87.3 \pm 37.5 (ab)	38 \pm 15 (ab)	131 \pm 96 (ab)	3.3 \pm 2.0 (abd)
	QdT BSC-	70.1 \pm 18.7 (ab)	42 \pm 18 (ab)	665 \pm 524 (cd)	15.8 \pm 10.2 (ce)
	LC BSC+	85.8 \pm 67.1 (ab)	45 \pm 20 (ab)	87 \pm 94 (a)	2.1 \pm 1.9 (a)
	LC BSC-	81.2 \pm 44.6 (ab)	33 \pm 23 (ab)	395 \pm 344 (bc)	12.6 \pm 9.9 (bcde)
	NA BSC+	380.4 \pm 329.5 (b)	19 \pm 23 (a)	16 \pm 49 (a)	5.2 \pm 19.9 (abcde)
	NA BSC-	93.0 \pm 40.2 (a)	69 \pm 45 (b)	40 \pm 36 (a)	0.9 \pm 1.2 (abcde)

^a Letter-based display accompanying surface runoff parameters. Different letters within a column section (Mean, Biocrust, or Site*Biocrust interaction) indicate statistically significant differences ($p < 0.05$, Šidák correction).

Table 3.2: Percolating water fluxes on the study sites (SG: Santa Gracia, QdT: Quebrada de Talca, LC: La Campana, NA: Nahuelbuta) with (+) and without (-) biocrust (BSC) cover. Values correspond to mean \pm standard deviation (SD) of five field replicates. Different letters indicate statistically significant different values based on Šídák correction post-hoc test results.

Factor	Time to start percolation flow [s]		Percolation ^a [L h ⁻¹]	Sediments in percolation flow ^a [g m ⁻² h ⁻¹]		Sediment load in percolation [gL ⁻¹ m ⁻²]
	Mean \pm SD			(a)	19 \pm 34	
Mean \pm SD	SG	223 \pm 190	18.0 \pm 14.0	(a)	19 \pm 34	4.2 \pm 19.7
	QdT	175.0 \pm 94.5	22.8 \pm 15.0	(a)	7 \pm 10	0.2 \pm 0.3
	LC	234 \pm 183	22.4 \pm 13.0	(a)	13 \pm 15	0.5 \pm 0.5
	NA	145 \pm 169	65.0 \pm 39.0	(b)	23 \pm 25	0.4 \pm 0.4
Biocrust	BSC+	171 \pm 133	42.6 \pm 34.0	(b)	19 \pm 22	(b)
	BSC-	218 \pm 190	21.5 \pm 21.0	(a)	12 \pm 24	(a)
Site*Biocrust	SG BSC+	202 \pm 103	24.8 \pm 15.0	(ab)	19 \pm 18	0.7 \pm 0.5
	SG BSC-	244 \pm 251	11.1 \pm 10.0	(a)	18 \pm 46	7.5 \pm 27.5
	QdT BSC+	148.0 \pm 63.9	30.5 \pm 13.0	(b)	9 \pm 13	0.3 \pm 0.3
	QdT BSC-	202 \pm 113	15.1 \pm 13.0	(ab)	5 \pm 6	0.2 \pm 0.2
	LC BSC+	226 \pm 223	23.5 \pm 14.0	(ab)	17 \pm 19	0.6 \pm 0.5
	LC BSC-	241 \pm 139	21.3 \pm 14.0	(ab)	9 \pm 9	0.4 \pm 0.3
	NA BSC+	107.0 \pm 35.6	91.5 \pm 28.0	(c)	30 \pm 32	0.4 \pm 0.4
	NA BSC-	183 \pm 234	38.5 \pm 30.0	(b)	16 \pm 15	0.4 \pm 0.3

^a Letter-based displaying accompanying parameters where shown. Different letters within a column section (Mean, Biocrust, or Site*Biocrust interaction) indicate statistically significant differences ($p < 0.05$, Šídák correction).

3.2.2 Biocrust modulation of carbon and nitrogen fluxes

Biocrusts significantly altered the transport pathways and amounts of C and N in both sediment-bound and dissolved forms, with effects dependent on climate and site conditions (Figure 3.4). For carbon fluxes, sediment-associated C loss via runoff generally increased with climatic humidity. Biocrusts significantly reduced this sediment C loss, by up to a factor of four compared to bare soil. In percolation flow, biocrusts also reduced the C content in mobilized sediments, an effect most pronounced in drier climates where reductions reached 20-40%. Furthermore, biocrusts consistently increased dissolved organic carbon (DOC) concentrations in runoff across all sites, suggesting an alteration of C cycling pathways towards leaching rather than just physical erosion (Baumert et al., 2021). Similar patterns, though moderated by site*biocrust interactions, were observed for DOC transported via percolation. Regarding nitrogen fluxes, sediment-associated N loss via runoff also increased with humidity. The biocrust effect on this sediment N was strongly site-specific, causing an increase in SG but a decrease in NA, and explaining 48.8% of the observed variability. Dissolved organic nitrogen (DON) fluxes in runoff showed trends analogous to DOC, generally increasing with biocrust presence, especially in northern sites like SG (increasing from 1.3 ± 1.0 ppm in BSC- to 2.2 ± 2.0 ppm in BSC+). However, a contrasting effect was observed at the humid NA site, where biocrusts decreased DON in runoff (from 0.6 ± 0.7 ppm in BSC- to 0.3 ± 0.8 ppm in BSC+), potentially indicating enhanced N immobilization or uptake in this N-richer ecosystem. DON fluxes transported via percolation followed similar site-dependent trends influenced by biocrust interactions.

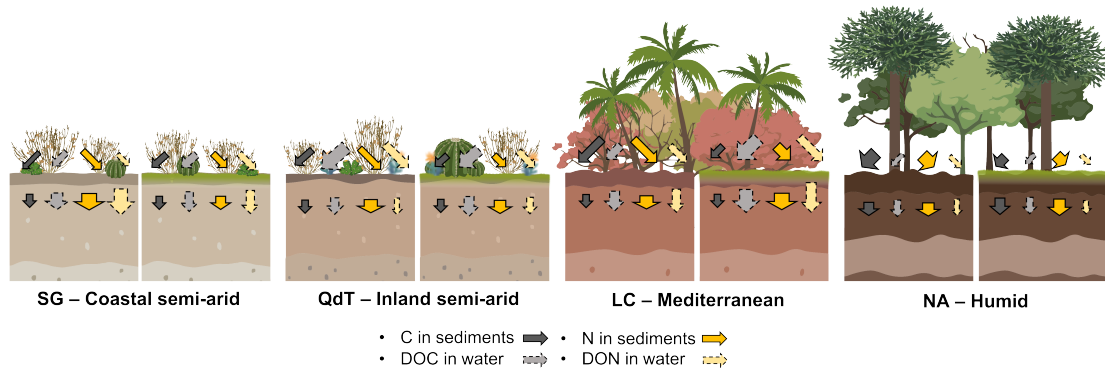


Figure 3.4: Representation of total carbon in sediments and DOC in water fluxes for the four study sites. The diagrams at the right side with slightly green surface represents the BSC+ treatments and the one at the left the BSC-. Grey-filled arrows correspond to C fluxes, and yellowish arrows to N. At the same time, arrows with solid borders correspond to the flow attached to the sediments, and dashed arrows dissolved in water. Each type of arrow is proportional inside each group in width to the concentration of nutrients and in length to the mass of it.

Overall, biocrusts play a crucial, climate-dependent role in regulating water flow, significantly reducing surface runoff erosion, but potentially increasing subsurface sediment transport. They profoundly influence C and N cycling, generally reducing C losses via runoff while altering dissolved nutrient pathways, with specific effects on N mobilization varying strongly between arid and humid environments.

3.3 Microbial, plant and moisture controls on soil structure and functionality (Manuscripts 3, 4 and 5)

Beyond the direct impacts of biological soil crusts (BSCs) and the broad climatic gradient, further investigations using subsets of the study sites (primarily arid Pan de Azúcar (PdA) and semi-arid Santa Gracia (SG), but also including mediterranean La Campana (LC) and humid Nahuelbuta (NA) in Manuscript 4) provided deeper insights into the roles of the indigenous microbial community, plant roots, and moisture dynamics in shaping soil aggregation, organic matter turnover, and nutrient cycling. These studies employed controlled laboratory incubations simulating specific scenarios: a shift to humid conditions for arid/semi-arid soils (Manuscript 3), repeated wetting-drying (W-D) versus constant moisture (CM) regimes across the climate gradient (Manuscript 4), and the natural transition from a living rhizosphere to a decomposing detritusphere in semi-arid soil (Manuscript 5).

A central finding emerging from these experiments is that the impact of microbial

activity on soil aggregation and related properties is highly dependent on the origin of the soil and the prevailing environmental conditions. This was clearly demonstrated in the moisture regime experiment (Manuscript 4), where the responses of native, microbially active soils to repeated wetting-drying (W-D) cycles were compared against sterilized controls across the climate gradient. Principal Component Analysis visually distinguished the trajectories of native versus sterile soils under W-D stress, directly highlighting the significant contribution of microbial activity to changes in soil edaphic properties (Figure 3.5). Crucially, the nature of this microbial influence differed markedly between climate zones. In arid soils, the microbially-influenced samples were primarily characterized by changes in aggregate C/N ratios, suggesting accelerated turnover of labile organic matter (OM) fueled by the Birch effect (Figure 3.5A). In contrast, microbially-influenced semi-arid and mediterranean soils under W-D were distinguished from controls mainly by shifts in aggregate size distribution, particularly an increase in microaggregates (MIC) relative to macroaggregates (MAC) (Figure 3.5B-C). This direct comparison underscores that while microbes actively mediate soil structural changes during moisture fluctuations, the specific mechanisms and outcomes (OM turnover vs. aggregate reorganization) are strongly dictated by the climate legacy imprinted on the soil and its microbial community.

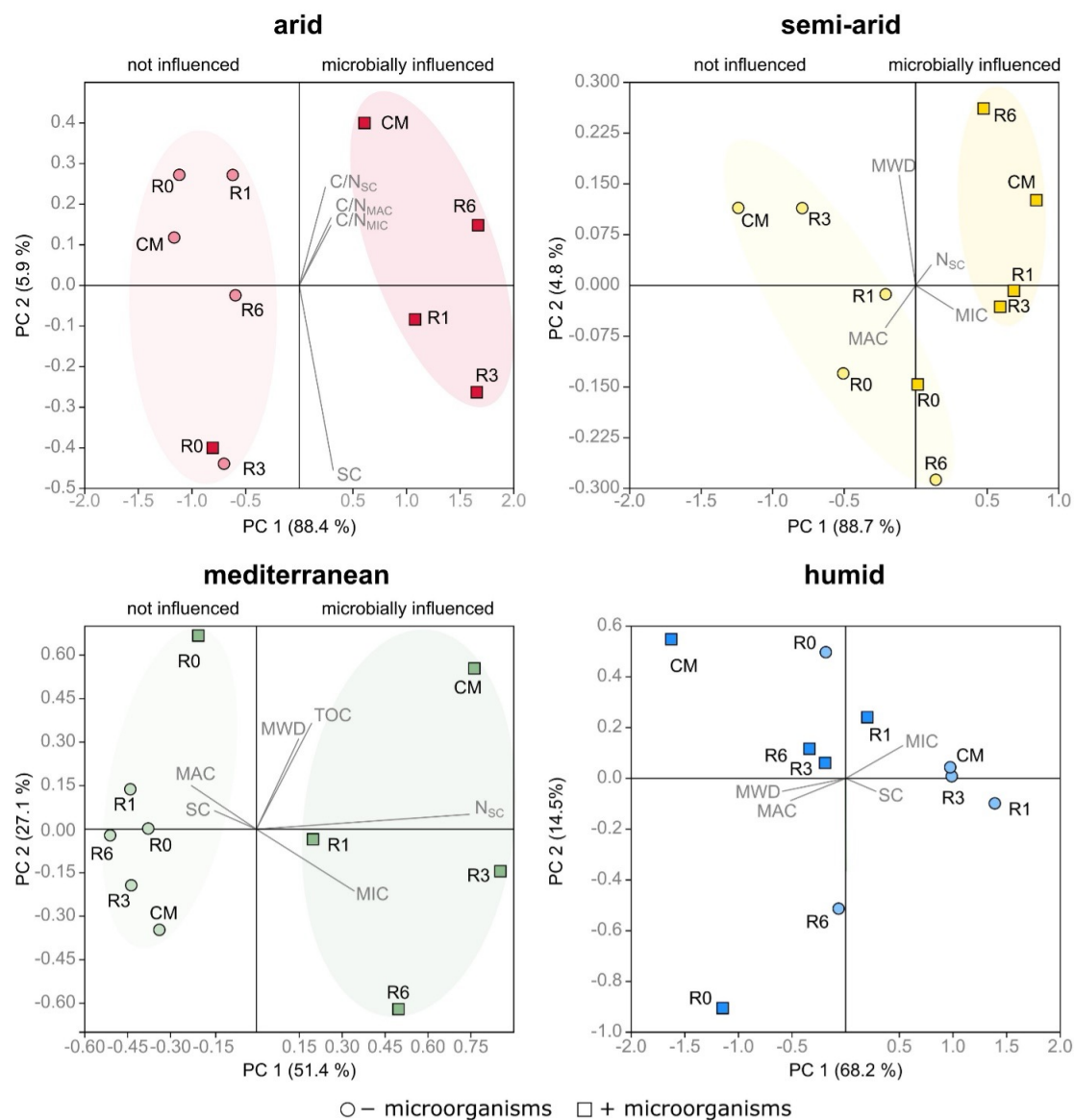


Figure 3.5: Principal Component Analyses of soil properties in native soils (squares) and sterilized soils (circles) including significant soil properties. A) arid, B) semi-arid, C) mediterranean and D) humid site. Microbial influence is indicated by sample separation along the x-axis.

Further results support this picture of context-dependent microbial influence and climate legacy effects. The observed increase in aggregate C/N ratios in microbially active arid soils (Figure 3.6A) aligns with findings of stimulated microbial abundance under W-D but also a net breakdown of MAC and only a slight decrease in overall aggregate stability (MWD) (Manuscript 4), consistent with rapid consumption of labile OM released from decomposing larger aggregates. The microaggregate formation observed in

microbially influenced semi-arid and mediterranean soils (Figure 3.5B-C) corresponds with outcomes where overall stability either slightly decreased (semi-arid) or increased (mediterranean) (Manuscript 4), suggesting different stabilization pathways potentially involving OM redistribution or transformation.

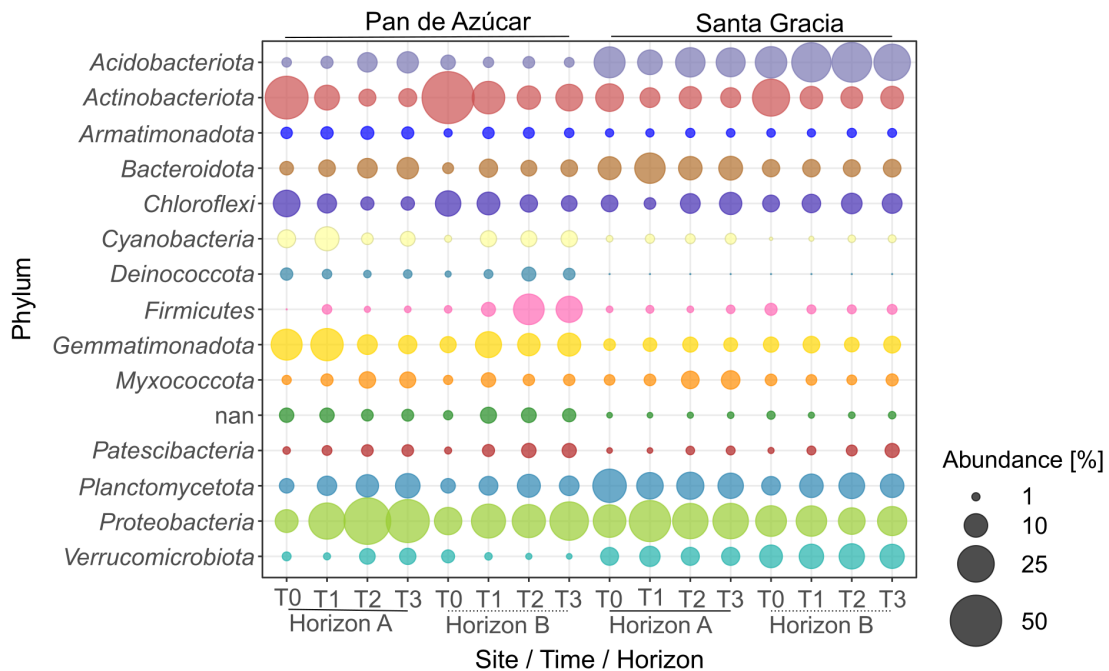


Figure 3.6: Relative abundance of top 15 bacterial phyla for Pan de Azúcar and Santa Gracia and the different time points. Time is represented as T0 (original), T1 (2 weeks), T2 (12 weeks) and T3 (16 weeks). Each bubble is the mean of the different treatments (in situ, BSCs and plants) and technical triplicates.

The importance of climate legacy was also evident in the differential resilience of microbial communities themselves. The arid PdA community, adapted to stable hyperaridity, showed significant structural changes and diversity loss under simulated humid conditions (Manuscript 3), while the semi-arid SG community, from a more variable climate, demonstrated greater stability (Figure 3.6), mirroring the patterns observed in the PCA analysis (Figure 3.5).

Beyond the intrinsic microbial community and moisture effects, the powerful role of plants was confirmed (Manuscript 5). Living roots acted as potent drivers of macroaggregation in both topsoil and subsoil of semi-arid origin. However, a distinct root legacy effect was apparent, as this enhanced aggregation only persisted after plant death in the topsoil, indicating a requirement for continuous C input or greater inherent stability factors in the subsoil. This transition from rhizosphere to detritusphere also drove a microbial succession from fungal to Gram-positive bacterial dominance and altered OM

3.3 Microbial, plant and moisture controls on soil structure and functionality (Manuscripts 3, 4 and 5)

protection mechanisms, notably increasing occluded POM in the topsoil detritusphere.

Chapter 4

Conclusion & Outlook

This research investigated the multifaceted role of biological soil crusts (biocrusts) and microbial communities in shaping soil development, stability, and nutrient cycling across a climate gradient in the Chilean Coastal Range. By combining field observations, laboratory experiments, and advanced analytical techniques, this work provides valuable insights into the complex interactions between biota, climate, and soil processes.

A key focus of this research was to understand the influence of biocrusts on soil aggregate stability and their interplay with soil properties along a climate gradient. Four sites representing arid, semi-arid, Mediterranean, and humid conditions were selected, allowing for a comparative analysis of biocrust effects under contrasting environmental conditions. The results revealed significant variations in soil properties along the gradient, with bulk density decreasing and soil organic carbon (SOC), total nitrogen (N_T), and clay content increasing with humidity. These variations reflect the influence of climate on weathering processes, organic matter accumulation, and soil development Jenny (1941). Biocrust cover significantly influenced soil properties, particularly in arid and semi-arid sites, where it increased SOC and N_T content and altered soil texture, indicating its role in trapping organic matter and modifying soil structure (Belnap, 2003; Bowker et al., 2006). Aggregate stability, a key indicator of soil resilience to erosion, was enhanced by the presence of biocrusts across all climates, with the most pronounced effect observed in the arid site. This finding underscores the crucial role of biocrusts in protecting vulnerable soils in dryland environments (Chamizo et al., 2012). The difference in geometric mean diameter of aggregates further emphasized the stabilizing effect of biocrusts, particularly in the arid site, where they significantly increased aggregate size.

Extending the investigation of biocrusts beyond their impact on soil structure, this research also explored their role as climate-dependent regulators of erosion, water, and nutrient cycling. Utilizing rainfall simulation experiments across the same climate gradient, the study assessed the effects of biocrusts on surface runoff, percolation flow, and sediment and nutrient fluxes. Biocrusts significantly delayed the initiation of runoff and reduced overall runoff volume in all climates, highlighting their capacity to retain

water and mitigate erosion (Kidron et al., 2022). The influence of biocrusts on sediment discharge was equally pronounced, with significant reductions observed across all sites, particularly in the inland semi-arid environment. Furthermore, biocrusts influenced both sediment-bound and dissolved carbon and nitrogen dynamics, with contrasting effects observed across the climate gradient. While biocrusts increased carbon content in sediments mobilized by runoff at drier sites, they also enhanced dissolved organic carbon (DOC) concentrations, indicating alterations in carbon cycling pathways. Similarly, biocrusts influenced nitrogen fluxes, increasing dissolved organic nitrogen (DON) concentrations, but with varying effects across the climatic gradient. These findings underscore the complex and context-dependent role of biocrusts in regulating both hydrological and biogeochemical processes in soil ecosystems.

Complementing the field and rainfall simulation studies, laboratory experiments explored the microbial drivers of soil aggregate turnover across different climates and moisture regimes. By subjecting soils from the same climate gradient sites to controlled wetting-drying (W-D) cycles, this research aimed to dissect the relative contributions of abiotic and biotic factors in shaping soil structure. The results revealed distinct patterns in aggregate size distribution and stability across climates and in response to W-D cycles. Sterilization significantly altered aggregate dynamics, highlighting the crucial role of microbial communities in soil structure formation and stabilization (Six et al., 2004). Microbial abundance, diversity, and community composition also exhibited climate-specific responses to W-D cycles, reflecting the adaptive strategies of soil microorganisms to fluctuating moisture conditions. W-D cycles also impacted predicted microbial functions, influencing the decomposition of organic matter and nutrient cycling processes.

Building upon the findings related to microbial influence on soil aggregate dynamics, the research further explored the role of microbial communities in initial soil formation under simulated climate change scenarios. Using soil samples from arid and semi-arid sites, the study simulated increased humidity conditions, reflecting potential climate change projections for these regions. The results revealed significant shifts in microbial community structure and function in response to the simulated climate change, with certain microbial groups, notably *Sphingomonas*, exhibiting increased abundance and potential for nitrogen fixation. These findings underscore the importance of soil legacy effects and the potential for microbial communities to adapt and mediate soil processes under changing environmental conditions.

Lastly, the research delved into the specific role of roots in regulating soil aggregation and organic matter dynamics, focusing on the transition from rhizosphere to detritusphere. Microcosm experiments with living and decaying cereal roots revealed significant differences in soil aggregate formation, microbial community composition, and organic matter characteristics. Living roots promoted the development of macroaggregates, particularly in the subsoil, while decaying roots stimulated microbial activity and

altered organic matter decomposition pathways. These findings emphasize the dynamic interplay between living and decaying roots and their influence on soil structure, microbial communities, and organic matter cycling. The transition from rhizosphere to detritusphere represents a shift from root-driven soil formation to decomposition-dominated processes, highlighting the interconnectedness of plant and microbial contributions to soil ecosystem functioning.

In summary, this body of research demonstrates the complex and interconnected roles of biocrusts, microbial communities, and plant roots in shaping soil development, stability, and nutrient cycling across a climate gradient. Biocrusts act as key regulators of surface processes, enhancing soil aggregate stability, reducing erosion, and modulating water and nutrient fluxes. Microbial communities, as the engines of biogeochemical processes, drive soil aggregation, organic matter decomposition, and respond dynamically to changes in moisture availability and climate conditions. Plant roots, both living and decaying, influence soil structure formation, microbial communities, and organic matter dynamics, with distinct effects observed in rhizosphere and detritusphere environments.

Future research should focus on further disentangling the complex interactions between biocrusts, microbial communities, and plants. This includes investigating the specific mechanisms driving biocrust formation and their influence on different soil types, exploring the functional diversity of microbial communities involved in soil aggregate formation, and examining the long-term legacy effects of plant-soil interactions on soil carbon sequestration. Moreover, considering the projected impacts of climate change, future studies should assess the resilience of biocrusts and microbial communities to altered precipitation patterns, temperature regimes, and increased atmospheric CO_2 concentrations. By deepening our understanding of these complex interactions, we can develop more effective strategies for soil conservation, ecosystem management, and promoting the sustainable use of soil resources in the face of global environmental change.

Bibliography

- Abed, R. M. M., Tamm, A., Hassenrück, C., Al-Rawahi, A. N., Rodríguez-Caballero, E., Fiedler, S., Maier, S., and Weber, B. (2019). Habitat-dependent composition of bacterial and fungal communities in biological soil crusts from oman. *Scientific Reports*, 9(1):6468.
- Allison, L. E. and Richards, L. A. (1954). *Diagnosis and Improvement of Saline and Alkali Soils*. Number 60. Soil and Water Conservative Research Branch, Agricultural Research Service, U.S. Department of Agriculture. Last accessed: 30 November 2022.
- Amundson, R., Richter, D. D., Humphreys, G. S., Jobbagy, E. G., and Gaillardet, J. (2007). Coupling between biota and earth materials in the critical zone. *Elements*, 3(5):327–332.
- Ardiles, V. and Fariña, M. (2014). Flora no vascular de la Región de Arica y Parinacota, Chile: nuevos registros y consideraciones biogeográficas. *Boletín Museo Nacional de Historia Natural*, 63:213–223.
- Armesto, J. J. and Arroyo, M. T. K. (2007). The mediterranean environment of central Chile.
- Bachar, A., Al-Ashhab, A., Soares, M. I., Sklarz, M. Y., Angel, R., Ungar, E. D., and Gillor, O. (2010). Soil microbial abundance and diversity along a low precipitation gradient. *Microb Ecol*, 60(2):453–61.
- Bajerski, F. and Wagner, D. (2013). Bacterial succession in Antarctic soils of two glacier forefields on Larsemann Hills, East Antarctica. *FEMS Microbiol Ecol*, 85(1):128–42.
- Bardgett, R. D. and van der Putten, W. H. (2014). Belowground biodiversity and ecosystem functioning. *Nature*, 515(7528):505–11.
- Barger, N. N., Weber, B., Garcia-Pichel, F., Zaady, E., and Belnap, J. (2016). *Patterns and Controls on Nitrogen Cycling of Biological Soil Crusts*, pages 257–285. Springer International Publishing, Cham.
- Barkay, T. and Schaefer, J. (2001). Metal and radionuclide bioremediation: issues, considerations and potentials. *Curr Opin Microbiol*, 4(3):318–23.

Bibliography

- Baumann, K., Jung, P., Samolov, E., Lehnert, L. W., Büdel, B., Karsten, U., Bendix, J., Achilles, S., Schermer, M., Matus, F., Osse, R., Osses, P., Morshedizad, M., Oehlschläger, C., Hu, Y., Klysubun, W., and Leinweber, P. (2018). Biological soil crusts along a climatic gradient in chile: Richness and imprints of phototrophic microorganisms in phosphorus biogeochemical cycling. *Soil Biology and Biochemistry*, 127:286–300.
- Baumert, V. L., Forstner, S. J., Zethof, J. H. T., Vogel, C., Heitkötter, J., Schulz, S., Kögel-Knabner, I., and Mueller, C. W. (2021). Root-induced fungal growth triggers macroaggregation in forest subsoils. *Soil Biology and Biochemistry*, 157:108244.
- Bavel, C. H. M. v. (1950). Mean weight-diameter of soil aggregates as a statistical index of aggregation.
- Bednarek-Ochyra, H. (2001). A note on the moss genus codriophorus p. beauv. *Cryptogamie Bryologie*, 22(2):105–111.
- Belnap, J. (2003). The world at your feet: desert biological soil crusts. *Frontiers in Ecology and the Environment*, 1(4):181–189.
- Belnap, J. and Büdel, B. (2016). Biological soil crusts as soil stabilizers. *Biological soil crusts: an organizing principle in drylands*, pages 305–320.
- Belnap, J., Kaltenecker, J. H., Rosentreter, R., Williams, J., Leonard, S., and Eldridge, D. (2001). Biological soil crusts: Ecology and management. *US Department of the Interior, Bureau of Land Management, National Science and Technology Center. Denver, Colorado*, 110.
- Belnap, J., Phillips, S. L., Flint, S., Money, J., and Caldwell, M. (2007). Global change and biological soil crusts: effects of ultraviolet augmentation under altered precipitation regimes and nitrogen additions. *Global Change Biology*, 14(3):670–686.
- Belnap, J., Weber, B., and Büdel, B. (2016). *Biological soil crusts as an organizing principle in drylands*. Springer.
- Bernhard, N., Moskwa, L.-M., Schmidt, K., Oeser, R. A., Aburto, F., Bader, M. Y., Baumann, K., von Blanckenburg, F., Boy, J., van den Brink, L., Brucker, E., Büdel, B., Canessa, R., Dippold, M. A., Ehlers, T. A., Fuentes, J. P., Godoy, R., Jung, P., Karsten, U., Köster, M., Kuzyakov, Y., Leinweber, P., Neidhardt, H., Matus, F., Mueller, C. W., Oelmann, Y., Osse, R., Osses, P., Paulino, L., Samolov, E., Schaller, M., Schmid, M., Spielvogel, S., Spohn, M., Stock, S., Stroncik, N., Tielbörger, K., Übernickel, K., Scholten, T., Seguel, O., Wagner, D., and Kühn, P. (2018). Pedogenic and microbial interrelations to regional climate and local topography: New insights from a climate gradient (arid to humid) along the Coastal Cordillera of Chile. *Catena*, 170:335–355.

- Bowker, M. A., Belnap, J., Büdel, B., Sannier, C., Pietrasik, N., Eldridge, D. J., and Rivera-Aguilar, V. (2016). Controls on distribution patterns of biological soil crusts at micro-to global scales. *Biological soil crusts: an organizing principle in drylands*, pages 173–197.
- Bowker, M. A., Belnap, J., and Miller, M. E. (2006). Spatial modeling of biological soil crusts to support rangeland assessment and monitoring. *Rangeland Ecology Management*, 59(5):519–529.
- Bowker, M. A., Maestre, F. T., Eldridge, D., Belnap, J., Castillo-Monroy, A., Escolar, C., and Soliveres, S. (2014). Biological soil crusts (biocrusts) as a model system in community, landscape and ecosystem ecology. *Biodiversity and Conservation*, 23(7):1619–1637.
- Brantley, S. L., Eissenstat, D. M., Marshall, J. A., Godsey, S. E., Balogh-Brunstad, Z., Karwan, D. L., Papuga, S. A., Roering, J., Dawson, T. E., Evaristo, J., Chadwick, O., McDonnell, J. J., and Weathers, K. C. (2017). Reviews and syntheses: on the roles trees play in building and plumbing the critical zone. *Biogeosciences*, 14(22):5115–5142.
- Brehm, U., Gorbushina, A., and Mottershead, D. (2005). *The role of microorganisms and biofilms in the breakdown and dissolution of quartz and glass*, pages 117–129. Elsevier, Amsterdam.
- Bruand, A., Cousin, I., Nicoullaud, B., Duval, O., and Begon, J. C. (1996). Backscattered electron scanning images of soil porosity for analyzing soil compaction around roots. *Soil Science Society of America Journal*, 60(3):895–901.
- Brust, G. E. (2019). *Management strategies for organic vegetable fertility*, pages 193–212. Elsevier.
- Burford, E., Fomina, M., and Gadd, G. (2003). Fungal involvement in bioweathering and biotransformation of rocks and minerals. *Mineralogical Magazine*, 67(6):1127–1155.
- Büdel, B., Dulić, T., Darienko, T., Rybalka, N., and Friedl, T. (2016). *Cyanobacteria and Algae of Biological Soil Crusts*, book section Chapter 4, pages 55–80. Ecological Studies. Springer International Publishing, Cham.
- Chamizo, S., Cantón, Y., Lázaro, R., Solé-Benet, A., and Domingo, F. (2012). Crust composition and disturbance drive infiltration through biological soil crusts in semi-arid ecosystems. *Ecosystems*, 15:148–161.

Bibliography

- Chamizo, S., Cantón, Y., Rodríguez-Caballero, E., and Domingo, F. (2016). Biocrusts positively affect the soil water balance in semiarid ecosystems. *Ecohydrology*, 9(7):1208–1221.
- Chen, J., Blume, H.-P., and Beyer, L. (2000). Weathering of rocks induced by lichen colonization — a review. *CATENA*, 39(2):121–146.
- Chen, N., Wang, X., Zhang, Y., Yu, K., and Zhao, C. (2018). Ecohydrological effects of biological soil crust on the vegetation dynamics of restoration in a dryland ecosystem. *Journal of Hydrology*, 563:1068–1077.
- Chen, N., Yu, K., Jia, R., Teng, J., and Zhao, C. (2020). Biocrust as one of multiple stable states in global drylands. *Science Advances*, 6(39):eaay3763.
- Colesie, C., Felde, V. J. M. N. L., and Büdel, B. (2016). *Composition and macrostructure of biological soil crusts*, book section 9, pages 159–172.
- Colesie, C., Green, T. G. A., Haferkamp, I., and Büdel, B. (2014). Habitat stress initiates changes in composition, CO_2 gas exchange and C-allocation as life traits in biological soil crusts. *The ISME Journal*, 8(10):2104–2115.
- Concostrina-Zubiri, L., Pescador, D. S., Martínez, I., and Escudero, A. (2014). Climate and small scale factors determine functional diversity shifts of biological soil crusts in iberian drylands. *Biodiversity and conservation*, 23:1757–1770.
- Corbin, J. D. and Thiet, R. K. (2020). Temperate biocrusts: mesic counterparts to their better-known dryland cousins. *Frontiers in Ecology and the Environment*, 18(8):456–464.
- Corwin, D. L. (2021). Climate change impacts on soil salinity in agricultural areas. *European Journal of Soil Science*, 72(2):842–862.
- Costa, O. Y. A., Raaijmakers, J. M., and Kuramae, E. E. (2018). Microbial extracellular polymeric substances: Ecological function and impact on soil aggregation. *Front Microbiol*, 9:1636.
- Cox, D. R. (1992). Causality: Some statistical aspects. *Journal of the Royal Statistical Society. Series A (Statistics in Society)*, 155:291–301.
- Csardi, G. and Nepusz, T. (2006). igraph: Network analysis and visualization. *R package version*, 1695:1–9.
- Cuvertino, J., Ardiles, V., Osorio, F., and Romero, X. (2012). New records and additions to the Chilean bryophyte flora. *Ciencia e investigación agraria: revista latinoamericana de ciencias de la agricultura*, 39(2):245–254.

- Dietrich, W. E. and Perron, J. T. (2006). The search for a topographic signature of life. *Nature*, 439(7075):411–8.
- Drahorad, S. L., Steckenmesser, D., Felix-Henningsen, P., Lichner, , and Rodný, M. (2013). Ongoing succession of biological soil crusts increases water repellency — a case study on arenosols in sekule, slovakia. *Biologia*, 68(6):1089–1093.
- Dufrêne, M. and Legendre, P. (1997). Species assemblages and indicator species: the need for a flexible asymmetrical approach. *Ecological monographs*, 67(3):345–366.
- Dunn, P. K. (2017). Tweedie: Evaluation of tweedie exponential family models. *R package version*. Last access: 30 November 2022.
- Elbert, W., Weber, B., Burrows, S., Steinkamp, J., Büdel, B., Andreae, M. O., and Pöschl, U. (2012). Contribution of cryptogamic covers to the global cycles of carbon and nitrogen. *Nature Geoscience*, 5(7):459–462.
- Eldridge, D. J., Reed, S., Travers, S. K., Bowker, M. A., Maestre, F. T., Ding, J., Havrilla, C., Rodriguez-Caballero, E., Barger, N., Weber, B., Antoninka, A., Belnap, J., Chaudhary, B., Faist, A., Ferrenberg, S., Huber-Sannwald, E., Malam Issa, O., and Zhao, Y. (2020). The pervasive and multifaceted influence of biocrusts on water in the world's drylands. *Glob Chang Biol*, 26(10):6003–6014.
- Elliott, E. T. (1986). Aggregate structure and carbon, nitrogen, and phosphorus in native and cultivated soils. *Soil Science Society of America Journal*, 50(3):627–633.
- Ewing, S. A., Sutter, B., Owen, J., Nishiizumi, K., Sharp, W., Cliff, S. S., Perry, K., Dietrich, W., McKay, C. P., and Amundson, R. (2006). A threshold in soil formation at Earth's arid–hyperarid transition. *Geochimica et Cosmochimica Acta*, 70(21):5293–5322.
- Fariña, V. and Ardiles, M. (2014). Flora no vascular de la región de arica y parinacota, chile: nuevos registros y consideraciones biogeográficas. *Boletín del Museo Nacional de Historia Natural, Chile*, 63:213–223.
- Fischer, T., Yair, A., and Veste, M. (2012). Microstructure and hydraulic properties of biological soil crusts on sand dunes: a comparison between arid and temperate climates. *Biogeosciences Discussions*, 9:12711–12734.
- Fischer, T., Yair, A., Veste, M., and Geppert, H. (2013). Hydraulic properties of biological soil crusts on sand dunes studied by ^{13}C -cp/mas-nmr: A comparison between an arid and a temperate site. *CATENA*, 110:155–160.
- Galloway, D. (2007). *Flora of New Zealand: Lichens, including lichen-forming and lichenicolous fungi, Vol 1 and 2*.

Bibliography

- Galloway, D. J. and Quilhot, W. (2009). Checklist of chilean lichen-forming and lichenicolous fungi. *Gayana Botánica*, 55:111–185.
- Gao, L., Bowker, M. A., Xu, M., Sun, H., Tuo, D., and Zhao, Y. (2017). Biological soil crusts decrease erodibility by modifying inherent soil properties on the Loess Plateau, China. *Soil Biology and Biochemistry*, 105:49–58.
- Garcia-Pichel, F., Felde, V. J. M. N. L., Drahorad, S. L., and Weber, B. (2016). *Microstructure and Weathering Processes Within Biological Soil Crusts*, book section Chapter 13, pages 237–255. Ecological Studies. Springer International Publishing, Cham.
- Gardner, W. R. (1956). Representation of Soil Aggregate-Size Distribution by a Logarithmic-Normal Distribution. *Soil Science Society of America Journal*, 20(2):151–153.
- Goebes, P., Seitz, S., Kühn, P., Li, Y., Niklaus, P. A., von Oheimb, G., and Scholten, T. (2015). Throughfall kinetic energy in young subtropical forests: Investigation on tree species richness effects and spatial variability. *Agricultural and Forest Meteorology*, 213:148–159.
- Govers, G. (1985). Selectivity and transport capacity of thin flows in relation to rill erosion. *CATENA*, 12(1):35–49.
- Grote, E. E., Belnap, J., Housman, D. C., and Sparks, J. P. (2010). Carbon exchange in biological soil crust communities under differential temperatures and soil water contents: implications for global change. *Global Change Biology*, 16(10):2763–2774.
- Harrell Jr, F. E. and Harrell Jr, M. F. E. (2019). Hmisc: Harrell miscellaneous. *R package version*, 2019:235–236.
- Hatch, T. and Choate, S. P. (1929). Statistical description of the size properties of non uniform particulate substances. *Journal of the Franklin Institute*, 207(3):369–387.
- He, S. (1998). A checklist of the mosses of Chile. *The Journal of the Hattori Botanical Laboratory*, 85:103–189.
- Hinsinger, P., Bengough, A. G., Vetterlein, D., and Young, I. M. (2009). Rhizosphere: biophysics, biogeochemistry and ecological relevance. *Plant and Soil*.
- Hooper, D. U. and Johnson, L. (1999). Nitrogen limitation in dryland ecosystems: Responses to geographical and temporal variation in precipitation. *Biogeochemistry*, 46(1):247–293.

- Horn, K. H. H. R. (2009). *Die physikalische Untersuchung von Böden*. Schweizerbart Science Publishers, Stuttgart, Germany.
- Hothorn, T., Bretz, F., and Westfall, P. (2008). Simultaneous inference in general parametric models. *Biom J*, 50(3):346–63.
- Hulton, N. R. J., Purves, R. S., McCulloch, R. D., Sugden, D. E., and Bentley, M. J. (2002). The Last Glacial Maximum and deglaciation in southern South America. *Quaternary Science Reviews*, 21(1-3):233–241.
- Iserloh, T., Ries, J., Arnáez, J., Boix-Fayos, C., Butzen, V., Cerdà, A., Echeverría, M., Fernández-Gálvez, J., Fister, W., and Geißler, C. (2013). European small portable rainfall simulators: A comparison of rainfall characteristics. *Catena*, 110:100–112.
- Issa, O. M., Trichet, J., Défarge, C., Couté, A., and Valentin, C. (1999). Morphology and microstructure of microbiotic soil crusts on a tiger bush sequence (niger, sahel). *Catena*, 37(1-2):175–196.
- Jahn, R., Blume, H., Asio, V., Spaargaren, O., and Schad, P. (2006). *Guidelines for soil description*. Fao.
- Jenny, H. (1941). *Factors of soil formation: a system of quantitative pedology*. Courier Corporation.
- Jung, P., Baumann, K., Emrich, D., Springer, A., Felde, V. J. M. N. L., Dultz, S., Baum, C., Frank, M., Büdel, B., and Leinweber, P. (2020a). Lichens bite the dust x2013; a bioweathering scenario in the atacama desert. *iScience*, 23(11). doi: 10.1016/j.isci.2020.101647.
- Jung, P., Baumann, K., Lehnert, L. W., Samolov, E., Achilles, S., Schermer, M., Wraase, L. M., Eckhardt, K.-U., Bader, M. Y., Leinweber, P., Karsten, U., Bendix, J., and Büdel, B. (2020b). Desert breath—how fog promotes a novel type of soil biocenosis, forming the coastal atacama desert’s living skin. *Geobiology*, 18(1):113–124.
- Jung, P., Emrich, D., Briegel-Williams, L., Schermer, M., Weber, L., Baumann, K., Colesie, C., Clerc, P., Lehnert, L. W., Achilles, S., Bendix, J., and Büdel, B. (2019). Ecophysiology and phylogeny of new terricolous and epiphytic chlorolichens in a fog oasis of the atacama desert. *MicrobiologyOpen*, 8(10):e894.
- Kemper, W. D. and Rosenau, R. C. (1986). *Aggregate stability and size distribution*, volume 5 of *Methods of soil analysis: Part 1 Physical and mineralogical methods*.
- Kidron, G. J., Lichner, L., Fischer, T., Starinsky, A., and Or, D. (2022). Mechanisms for biocrust-modulated runoff generation – a review. *Earth-Science Reviews*, 231:104100.

Bibliography

- Kidron, G. J., Veste, M., and Lichner, (2021). Biological factors impacting hydrological processes: Peculiarities of plants and biological soil crusts. *Journal of Hydrology and Hydromechanics*, 69(4):357–359.
- Kleber, M., Sollins, P., and Sutton, R. (2007). A conceptual model of organo-mineral interactions in soils: self-assembly of organic molecular fragments into zonal structures on mineral surfaces. *Biogeochemistry*, 85(1):9–24.
- Köhn, M. (1929). Bemerkungen zur mechanischen bodenanalyse iv. *Zeitschrift für Pflanzenernährung, Düngung, Bodenkunde*, 14(3):268–280.
- Lange, O. L. and Belnap, J. (2016). *How Biological Soil Crusts Became Recognized as a Functional Unit: A Selective History*, book section Chapter 2, pages 15–33. Ecological Studies. Springer International Publishing, Cham.
- Langfelder, P. and Horvath, S. (2008). Wgcna: an r package for weighted correlation network analysis. *BMC Bioinformatics*, 9:559.
- Lewin, R. A. (1956). Extracellular polysaccharides of green algae. *Canadian Journal of Microbiology*, 2(7):665–672.
- Li, J., Okin, G. S., Alvarez, L., and Epstein, H. (2008). Effects of wind erosion on the spatial heterogeneity of soil nutrients in two desert grassland communities. *Biogeochemistry*, 88(1):73–88.
- Liang, T., Shi, X., Guo, T., and Peng, S. (2015). Arbuscular mycorrhizal fungus mediate changes in mycorrhizosphere soil aggregates. *Agricultural Sciences*, 6(12):1455.
- Lichner, , Holko, L., Zhukova, N., Schacht, K., Rajkai, K., Fodor, N., and Sándor, R. (2012). Plants and biological soil crust influence the hydrophysical parameters and water flow in an aeolian sandy soil / vplyv rastlín a biologického pôdneho pokryvu na hydrofyzikálne parametre a prúdenie vody v piesočnej pôde. *Journal of Hydrology and Hydromechanics*, 60(4):309–318.
- Lightowers, P. (2013). Taxonomic notes on new zealand species of tortula. *Journal of bryology*, 13(3):369–375.
- Lightowers, P. J. (1985). A synoptic flora of south georgian mosses: Tortula. *British Antarctic Survey Bulletin*, 67:41–77.
- Liu, M.-Y., Chang, Q.-R., Qi, Y.-B., Liu, J., and Chen, T. (2014). Aggregation and soil organic carbon fractions under different land uses on the tableland of the loess plateau of china. *Catena*, 115:19–28.

- Loaiza Puerta, V., Pujol Pereira, E. I., Wittwer, R., van der Heijden, M., and Six, J. (2018). Improvement of soil structure through organic crop management, conservation tillage and grass-clover ley. *Soil and Tillage Research*, 180:1–9.
- Martens, D. and Frankenberger, W. (1992). Decomposition of bacterial polymers in soil and their influence on soil structure. *Biology and fertility of soils*, 13:65–73.
- Martinez Arbizu, P. (2020). pairwiseadonis: Pairwise multilevel comparison using adonis. *R package version 0.4*, 1.
- Mavris, C., Egli, M., Plötze, M., Blum, J. D., Mirabella, A., Giaccai, D., and Haeberli, W. (2010). Initial stages of weathering and soil formation in the Morteratsch proglacial area (Upper Engadine, Switzerland). *Geoderma*, 155(3-4):359–371.
- Mazurak, A. P. (1950). Effect of gaseous phase on water-stable synthetic aggregates. *Soil science*, 69(2):135–148.
- Mutz, S. G., Ehlers, T. A., Werner, M., Lohmann, G., Stepanek, C., and Li, J. (2018). Estimates of late Cenozoic climate change relevant to Earth surface processes in tectonically active orogens. *Earth Surface Dynamics*, 6(2):271–301.
- Mägdefrau, K. and Wutz, A. (1951). Die Wasserkapazität der Moos- und Flechtendecke des Waldes. *Forstwissenschaftliches Centralblatt*, 70(2):103–117.
- Nelson, P. N. and Baldock, J. A. (2005). Estimating the molecular composition of a diverse range of natural organic materials from solid-state ^{13}C NMR and elemental analyses. *Biogeochemistry*, 72:1–34.
- Nemergut, D. R., Costello, E. K., Meyer, A. F., Pescador, M. Y., Weintraub, M. N., and Schmidt, S. K. (2005). Structure and function of alpine and arctic soil microbial communities. *Res Microbiol*, 156(7):775–84.
- Newsham, K. K., Hopkins, D. W., Carvalhais, L. C., Fretwell, P. T., Rushton, S. P., O'Donnell, A. G., and Dennis, P. G. (2016). Relationship between soil fungal diversity and temperature in the maritime Antarctic. *Nature Climate Change*, 6(2):182–186.
- Nunan, N., Ritz, K., Crabb, D., Harris, K., Wu, K., Crawford, J. W., and Young, I. M. (2001). Quantification of the in situ distribution of soil bacteria by large-scale imaging of thin sections of undisturbed soil. *FEMS Microbiology Ecology*, 37(1):67–77.
- Oades, J. M. (1993). The role of biology in the formation, stabilization and degradation of soil structure. *Geoderma*, 56(1-4):377–400.

Bibliography

- Oades, J. M. and Waters, A. G. (1991). Aggregate hierarchy in soils. *Soil Research*, 29(6):815–828.
- Ochyra, R. and Matteri, C. M. (2001). Bryophyta, musci: Amblystegiaceae. In Guarnera, S. A., Gamundi de Amos, I., and Matteri, C., editors, *Flora Criptogámica de Tierra del Fuego*, volume 14, pages 1–96. Consejo Nacional de Investigaciones Científicas y Técnicas de la República Argentina, Buenos Aires.
- Oeser, R. A., Stroncik, N., Moskwa, L.-M., Bernhard, N., Schaller, M., Canessa, R., van den Brink, L., Köster, M., Brucker, E., Stock, S., Fuentes, J. P., Godoy, R., Matus, F. J., Oses Pedraza, R., Osses McIntyre, P., Paulino, L., Seguel, O., Bader, M. Y., Boy, J., Dippold, M. A., Ehlers, T. A., Kühn, P., Kuzyakov, Y., Leinweber, P., Scholten, T., Spielvogel, S., Spohn, M., Übernickel, K., Tielbörger, K., Wagner, D., and von Blanckenburg, F. (2018). Chemistry and microbiology of the critical zone along a steep climate and vegetation gradient in the chilean coastal cordillera. *CATENA*, 170:183–203.
- Oksanen, J., Blanchet, F. G., Kindt, R., Legendre, P., Minchin, P. R., O'hara, R., Simpson, G. L., Solymos, P., Stevens, M. H. H., and Wagner, H. (2013). vegan: Community ecology package. *R package version*, 2(0):321–326.
- Oliver, M. J., Velten, J., and Mishler, B. D. (2005). Desiccation tolerance in bryophytes: a reflection of the primitive strategy for plant survival in dehydrating habitats? *Integr Comp Biol*, 45(5):788–99.
- Orchard, V. A. and Cook, F. (1983). Relationship between soil respiration and soil moisture. *Soil Biology and Biochemistry*, 15(4):447–453.
- Pearce, D. A., Newsham, K. K., Thorne, M. A., Calvo-Bado, L., Krsek, M., Laskaris, P., Hodson, A., and Wellington, E. M. (2012). Metagenomic analysis of a southern maritime antarctic soil. *Front Microbiol*, 3:403.
- Peterson, R. A. (2021). Finding optimal normalizing transformations via best normalize. *R Journal*, 13(1).
- Pizarro-Tapia, R., González-Leiva, F., Valdés-Pineda, R., Ingram, B., Sangüesa, C., and Vallejos, C. (2020). A rainfall intensity data rescue initiative for Central Chile utilizing a pluviograph strip charts reader (PSCR). *Water*, 12(7):1887.
- Porada, P., Weber, B., Elbert, W., Pöschl, U., and Kleidon, A. (2014). Estimating impacts of lichens and bryophytes on global biogeochemical cycles. *Global Biogeochemical Cycles*, 28(2):71–85.

- Prater, I., Zubrzycki, S., Buegger, F., Zoor-Füllgraff, L. C., Angst, G., Dannenmann, M., and Mueller, C. W. (2020). From fibrous plant residues to mineral-associated organic carbon—the fate of organic matter in arctic permafrost soils. *Biogeosciences*, 17(13):3367–3383.
- Proctor, M. C. F., Oliver, M. J., Wood, A. J., Alpert, P., Stark, L. R., Cleavitt, N. L., and Mishler, B. D. (2007). Desiccation-tolerance in bryophytes: a review. *The Bryologist*, 110(4):595–621, 27.
- Rasse, D. P., Rumpel, C., and Dignac, M.-F. (2005). Is soil carbon mostly root carbon? mechanisms for a specific stabilisation. *Plant and soil*, 269(1):341–356.
- Rillig, M. C. (2004). Arbuscular mycorrhizae, glomalin, and soil aggregation. *Canadian Journal of Soil Science*, 84(4):355–363.
- Roberts, D. W. and Roberts, M. D. W. (2016). labdsv: Ordination and multivariate analysis for ecology. *R package version*, 775:1–68.
- Rodríguez-Caballero, E., Chamizo, S., Roncero-Ramos, B., Román, R., and Cantón, Y. (2018). Runoff from biocrust: A vital resource for vegetation performance on mediterranean steppes. *Ecohydrology*, 11(6):e1977.
- Rosenbaum, P. R. (2005). *Sensitivity Analysis in Observational Studies*. John Wiley Sons, Ltd.
- Rosentreter, R., Eldridge, D. J., Westberg, M., Williams, L., and Grube, M. (2016). *Structure, Composition, and Function of Biocrust Lichen Communities*, pages 121–138. Springer International Publishing, Cham.
- Rundel, P. W. and Weisser, P. J. (1975). La campana, a new national park in central chile. *Biological Conservation*, 8(1):35–46.
- Samolov, E., Baumann, K., Budel, B., Jung, P., Leinweber, P., Mikhailyuk, T., Karsten, U., and Glaser, K. (2020). Biodiversity of algae and cyanobacteria in biological soil crusts collected along a climatic gradient in Chile using an integrative approach. *Microorganisms*, 8(7):1047.
- Santibáñez Quezada, F. (2017). *Atlas agroclimático de Chile. Estado actual y tendencias del clima. Tomo II: Regiones de Atacama y Coquimbo*. Universidad de Chile. Facultad de Ciencias Agronómicas : FIA, Santiago, Chile.
- Schimel, J. P. and Schaeffer, S. M. (2012). Microbial control over carbon cycling in soil. *Front Microbiol*, 3:348.

Bibliography

- Schlecht-Pietsch, S., Wagner, U., and Anderson, T.-H. (1994). Changes in composition of soil polysaccharides and aggregate stability after carbon amendments to different textured soils. *Applied Soil Ecology*, 1(2):145–154.
- Scholten, T., Goebes, P., Kühn, P., Seitz, S., Assmann, T., Bauhus, J., Bruelheide, H., Buscot, F., Erfmeier, A., Fischer, M., Härdtle, W., He, J.-S., Ma, K., Niklaus, P. A., Scherer-Lorenzen, M., Schmid, B., Shi, X., Song, Z., von Oheimb, G., Wirth, C., Wubet, T., and Schmidt, K. (2017). On the combined effect of soil fertility and topography on tree growth in subtropical forest ecosystems—a study from SE China. *Journal of Plant Ecology*, 10(1):111–127.
- Scholten, T. and Seitz, S. (2019). Soil erosion and land degradation. *Soil Systems*, 3(4):68.
- Schweizer, S., Hoeschen, C., Schlüter, S., Kögel-Knabner, I., and Mueller, C. (2018). Rapid soil structure formation after glacial retreat driven by organic matter accrual at the microscale. *Global Change Biology*, 24:1637–1650.
- Seitz, S. (2015). *Mechanisms of soil erosion in subtropical Chinese forests-effects of species diversity, species identity, functional traits and soil fauna on sediment discharge*. Thesis.
- Seitz, S., Goebes, P., Song, Z., Bruelheide, H., Härdtle, W., Kühn, P., Li, Y., and Scholten, T. (2016). Tree species and functional traits but not species richness affect interrill erosion processes in young subtropical forests. *SOIL*, 2(1):49–61.
- Seitz, S., Nebel, M., Goebes, P., Käppeler, K., Schmidt, K., Shi, X., Song, Z., Webber, C. L., Weber, B., and Scholten, T. (2017). Bryophyte-dominated biological soil crusts mitigate soil erosion in an early successional Chinese subtropical forest. *Bio-geosciences*, 14(24):5775–5788.
- Six, J., Bossuyt, H., Degryze, S., and Denef, K. (2004). A history of research on the link between (micro)aggregates, soil biota, and soil organic matter dynamics. *Soil and Tillage Research*, 79(1):7–31.
- Six, J., Elliott, E. T., and Paustian, K. (2000). Soil macroaggregate turnover and microaggregate formation: a mechanism for C sequestration under no-tillage agriculture. *Soil Biology and Biochemistry*, 32(14):2099–2103.
- Slessarev, E. W., Lin, Y., Bingham, N. L., Johnson, J. E., Dai, Y., Schimel, J. P., and Chadwick, O. A. (2016). Water balance creates a threshold in soil pH at the global scale. *Nature*, 540(7634):567–569.

- Steven, B., Gallegos-Graves, L. V., Belnap, J., and Kuske, C. R. (2013). Dryland soil microbial communities display spatial biogeographic patterns associated with soil depth and soil parent material. *FEMS Microbiology Ecology*, 86(1):101–113.
- Stradling, D. A., Thygerson, T., Walker, J. A., Smith, B. N., Hansen, L. D., Criddle, R. S., and Pendleton, R. L. (2002). Cryptogamic crust metabolism in response to temperature, water vapor, and liquid water. *Thermochimica Acta*, 394(1-2):219–225.
- Team, R. C. (2018). R: A language and environment for statistical computing.
- Thielen, S. M., Gall, C., Ebner, M., Nebel, M., Scholten, T., and Seitz, S. (2021). Water's path from moss to soil: A multi-methodological study on water absorption and evaporation of soil-moss combinations. *Journal of Hydrology and Hydromechanics*, 69(4):421–435.
- Totsche, K. U., Amelung, W., Gerzabek, M. H., Guggenberger, G., Klumpp, E., Knief, C., Lehndorff, E., Mikutta, R., Peth, S., Prechtel, A., Ray, N., and Kögel-Knabner, I. (2018). Microaggregates in soils. *Journal of Plant Nutrition and Soil Science*, 181(1):104–136.
- Vidal, A., Hirte, J., Bender, S. F., Mayer, J., Gattinger, A., Höschen, C., Schädler, S., Iqbal, T. M., and Mueller, C. W. (2018). Linking 3D soil structure and plant-microbe-soil carbon transfer in the rhizosphere. *Frontiers in Environmental Science*, 6:9.
- Wagner, S., Cattle, S. R., and Scholten, T. (2007). Soil-aggregate formation as influenced by clay content and organic-matter amendment. *Journal of Plant Nutrition and Soil Science*, 170(1):173–180.
- Wang, Y., Chen, B., Wieder, W. R., Leite, M., Medlyn, B. E., Rasmussen, M., Smith, M. J., Agusto, F. B., Hoffman, F., and Luo, Y. (2014). Oscillatory behavior of two nonlinear microbial models of soil carbon decomposition. *Biogeosciences*, 11(7):1817–1831.
- Weber, B., Belnap, J., Büdel, B., Antoninka, A. J., Barger, N. N., Chaudhary, V. B., Darrouzet-Nardi, A., Eldridge, D. J., Faist, A. M., Ferrenberg, S., Havrilla, C. A., Huber-Sannwald, E., Malam Issa, O., Maestre, F. T., Reed, S. C., Rodriguez-Caballero, E., Tucker, C., Young, K. E., Zhang, Y., Zhao, Y., Zhou, X., and Bowker, M. A. (2022). What is a biocrust? a refined, contemporary definition for a broadening research community. *Biological Reviews*, 97(5):1768–1785.
- Whitney, K. M., Vivoni, E. R., Duniway, M. C., Bradford, J. B., Reed, S. C., and Belnap, J. (2017). Ecohydrological role of biological soil crusts across a gradient in levels of development. *Ecohydrology*, 10(7):e1875.

Bibliography

- Wickam, H. (2016). *ggplot2: elegant graphics for data analysis*, volume 16 of Springer-Verlag. Accessed March. 2 edition.
- Xiao, B., Bowker, M. A., Zhao, Y., Chamizo, S., and Issa, O. M. (2022). Biocrusts: Engineers and architects of surface soil properties, functions, and processes in dryland ecosystems. *Geoderma*, 424:116015.
- Young, K. E., Ferrenberg, S., Reibold, R., Reed, S. C., Swenson, T., Northen, T., and Darrouzet-Nardi, A. (2022). Vertical movement of soluble carbon and nutrients from biocrusts to subsurface mineral soils. *Geoderma*, 405:115495.
- Zhang, Z.-S., Song, X.-L., Lu, X.-G., and Xue, Z.-S. (2013). Ecological stoichiometry of carbon, nitrogen, and phosphorus in estuarine wetland soils: influences of vegetation coverage, plant communities, geomorphology, and seawalls. *Journal of Soils and Sediments*, 13(6):1043–1051.
- Štyriaková, I., Mockovčiaková, A., Štyriak, I., Kraus, I., Uhlík, P., Madejová, J., and Orolínová, Z. (2012). Bioleaching of clays and iron oxide coatings from quartz sands. *Applied Clay Science*, 61:1–7.

Appendix

Manuscript 1

pp. 59 - 72

GALL, C.; OHAN, J.; GLASER, K.; KARSTEN, U.; SCHLÖTER, M.; SCHOLTEN, T.; SCHULZ, S.; SEITZ, S. & KURTH, J. K. (2022):

Biocrusts: Overlooked hotspots of managed soils in mesic environments.

Journal of Plant Nutrition and Soil Science, 185 (6), 745-751. DOI: 10.1002/jpln.202200252.

Manuscript 2

pp. 73 - 111

GALL, C.; NEBEL, M.; QUANDT, D.; SCHOLTEN, T. & SEITZ, S. (2022):

Pioneer biocrust communities prevent soil erosion in temperate forests after disturbances.

Biogeosciences, 19, 3225–3245. DOI: 10.5194/bg-19-3225-2022.

Manuscript 3

pp. 112 - 126

GALL, C.; NEBEL, M.; SCHOLTEN, T.; THIELEN, S. M. & SEITZ, S. (in preparation):

On the impact of soil-moss combinations on surface runoff, percolation, soil erosion, and temporal dynamics of soil water content.

Manuscript 4

pp. 127 - 159

THIELEN, S. M.; GALL, C.; EBNER, M.; NEBEL, M.; SCHOLTEN, T. & SEITZ, S. (2021):

Water's path from moss to soil: A multi-methodological study on water absorption and evaporation of soil moss combinations.

Journal of Hydrology and Hydromechanics, 69 (4), 421-435. DOI: 10.2478/johh-2021-0021.

subcaption

Appendix A

Biocrust-linked changes in soil aggregate stability along a climatic gradient in the Chilean Coastal Range

Abstract

Biological soil crusts (biocrusts) composed of cyanobacteria, bacteria, algae, fungi, lichens, and bryophytes stabilize the soil surface. This effect has mainly been studied in arid climates, where biocrusts constitute the main biological agent to stabilize and connect soil aggregates. Besides, biocrusts are an integral part of the soil surface under mediterranean and humid climate conditions, mainly covering open spaces in forests and on denuded lands. They often develop after vegetation disturbances, when their ability to compete with vascular plants increases, acting as pioneer communities and affecting the stability of soil aggregates. To better understand how biocrusts mediate changes in soil aggregate stability under different climate conditions, we analyzed soil aggregate samples collected under biocrust communities from four national parks in Chile along a large climatic gradient ranging from (north to south) arid (Pan de Azúcar), semi-arid (Santa Gracia), mediterranean (La Campana) to humid (Nahuelbuta). Biocrust communities showed a stabilizing effect on the soil aggregates in dry fractions for the three northern and the wet aggregates for the southernmost sites. Here, permanent vascular plants and higher contents of organic carbon and nitrogen in the soil control aggregate stability more than biocrusts, which are in intense competition with higher plant communities. Moreover, we found an increase in stability for aggregate size classes <2.0 mm and 9.5–30.0 mm. The geometric mean diameter of the soil aggregates showed a clear effect due to the climatic gradient, indicating that the aggregate stability presents a log-normal instead of a normal distribution, with a trend of low change between aggregate size fractions. Based on our results, we assume that biocrusts affect the soil structure in all climates. Their role in aggregate stability is masked under humid conditions by higher vegetation and organic matter contents in the topsoil.

A.1 Introduction

In recent years, biological soil crusts (biocrusts) have gained particular interest as stabilizers of soil aggregates. Such biocrusts are highly variable communities of microscopic (cyanobacteria, algae, fungi, and bacteria) and macroscopic (lichens, bryophytes) organisms found on the surface and in the upper centimeters of the soil (Gao et al., 2017). They stabilize the soil surface (Garcia-Pichel et al., 2016), especially in arid climates, where biocrusts are the main biological agents for consolidating and connecting soil aggregates (Belnap and Büdel, 2016). However, biocrusts are also present in more mesic regions (e.g., pine barrens, serpentine soils, temperate steppe) (Belnap et al., 2016), but due to their limited ability to compete for light, they are mainly relegated to open spaces or interspaces between vascular plants where sunlight reaches the soil surface (Issa et al., 1999).

Because of their simple structure, biocrusts are present in a wide variety of climatic conditions. Biocrust organisms lack specialized desiccation control structures, such as stomata or impermeable cuticles, so their water content depends on the humidity in the surrounding environment (Thielen et al., 2021). However, low water demand, high drought tolerance (Chen et al., 2020), the ability to grow actively only when water is available, and to recover without physiological damage even after completely drying out for an extended period (Oliver et al., 2005) compensate the lack of dedicated structures. For this reason, biocrusts form an almost continuous layer in arid regions where water availability limits vascular plant cover (Grote et al., 2010)(Colesie et al., 2014). By slightly increasing the water availability, areas covered by plants and biocrusts increase in self-organized patterns where both coexist. However, when water demand is no longer restrained, vascular plants have an advantage in using light due to their canopy development, which leads to a decline of biocrusts (Chen et al., 2018).

The cover and composition of biocrusts strongly depend on water availability (Bowker et al., 2016). Under dry conditions, with high potential evapotranspiration, biocrusts are dominated by cyanobacteria, bacteria, and micro-fungi, with few bryophytes or lichens present. However, the occurrence of lichens is not restricted to more humid locations, but lichens were also found in arid regions like Pan de Azucar in northern Chile (Jung et al., 2020a,b). It implies that the external morphology of the biocrusts ranges from smooth to rugose (Chamizo et al., 2016). In terms of soil conditions, the water-holding capacity determines how much water can be stored in the soil. Typical sources of soil water are precipitation in general and, more specifically, at valley bottoms with close connection to the groundwater table, also groundwater. Further, available water for lichen growth can be provided by fog and dew (Jung et al., 2019). Pore space and pore size and following water-holding capacity of a soil largely depends on the parent material and its degree of weathering. Thus, soil formation indirectly controls the distribution and composition of biocrusts at ecoregional and local scales (Bowker et al., 2016). For instance, Steven et al. (2013) showed that the composition of biocrust com-

munities differed at vertical scales of a few centimeters in soils with different parent material origins, while Bowker et al. (2016) concluded that heterogeneous distributions in parent materials result in abrupt transitions in biocrust distribution and cover.

Biocrusts can be understood as an organic-sedimentary system within the topsoil where the inorganic and the organic part play dynamic roles in determining the architecture, evolution, and properties of the system, including structure and aggregate stability. On a small spatial scale, biocrusts interact with the soil system in nitrogen and carbon cycling (Barger et al., 2016). Globally, Elbert et al. (2012) pointed out that cryptogamic covers take up 3.9 Pg C per year. The main processes of nitrogen enrichment are biological fixation and dust capture, while nitrogen losses typically appear via dissolution, volatilization, and erosional loss (Barger et al., 2016). Photosynthesis is the most crucial carbon fixation process (Elbert et al., 2012; Porada et al., 2014), and soil erosion and biological decomposition are the primary loss source of carbon and other nutrients (Li et al., 2008).

Biocrusts affect soil erosion by acting as a physical barrier that shields the soil from direct exposition to water and wind (Seitz et al., 2016), protecting it from the effect of raindrops and, thus, splash erosion (Seitz et al., 2017; Goebes et al., 2015) and modulating the abrasive effect of wind and surface runoff (Belnap and Büdel, 2016). At the same time, biocrusts control water flow across the landscape and through the soil matrix (Thielen et al., 2021; Eldridge et al., 2020). Eldridge et al. (2020) described a decrease in surface runoff and an increase in water infiltration in the presence of biocrusts under semi-arid conditions, related to a reduction in sediment discharge. The influence of biocrusts on the composition of the soil porosity is variable and depends on its stage of development and composition. In some cases, this structuration generates discontinuities that hinder the flow of water in the soil, while in others, it generates a decrease in the tortuosity that is reflected in rapid infiltration (Fischer et al., 2013). Water infiltration usually is inversely related to surface runoff (Lichner et al., 2012). The successional stage of biocrusts affects water repellency compared to bare soil (Drahorad et al., 2013). It has been observed that with the development of biocrusts, the water repellency increased, and the sorptivity and conductivity decreased (Fischer et al., 2012; Lichner et al., 2012). Therefore, biocrusts affect soil erosion and hydrology through a wide variety of processes (Belnap and Büdel, 2016).

In regards to the stability of the soil surface, biocrusts further have a binding effect on aggregates and can form coherent structures (Belnap and Büdel, 2016). Typically, the organic carbon in the form of exo-polysaccharides or structural filaments of the different organisms present within biocrust communities causes soil stabilization (Garcia-Pichel et al., 2016). Other structure-forming processes due to biocrusts, although to a lesser extent, are the compressive and drying action on the soil matrix and the pH-dependent dissolution of cementing salts (Bowker et al., 2016). The biocrusts-induced soil aggradation results in the formation of a defined layer, increasing the soil resistance and

resilience to wind and water (Rosentreter et al., 2016).

Biocrusts stabilize individual aggregate units through different mechanisms depending on their species composition (Garcia-Pichel et al., 2016). For instance, bacteria, cyanobacteria, and also green-algae play a crucial role in forming and stabilizing aggregates by extracellular polymeric substances that glue soil particles together (Six et al., 2004; Lewin, 1956). Vegetal debris serves as aggregation cores where the soil microorganisms use it as an energy source, but rapid decomposition is limited by the interaction with the inorganic matrix (Oades and Waters, 1991). On the other hand, fungi are important in forming soil aggregates due to their hyphal structure, which physically enmeshes microaggregates and soil particles (Totsche et al., 2018). In summary, soil aggregate stabilization processes are dynamic and occur at different temporal and spatial scales, where an aggregate of soil particles is built up of structural units of various sizes held together by various binding agents.

In this study, we investigate how and to what extent biocrusts under different climatic conditions stabilize the soil surface. Therefore, we compare the stability of macroaggregates and varying soil properties in topsoil with or without biocrust cover along a climatic gradient from arid to humid climate conditions along the Chilean Coastal Range. We test the following hypotheses:

- (i) if biocrusts cover the soil surface, soil aggregates show higher stability because the biocrusts protect the soil surface physically, shelter soil organic matter within aggregates, modify the structure of microbial communities, and change water flow into the soil,
- (ii) if the climate is arid, the effect of biocrusts on the soil surface is most pronounced because other sources of organic matter are at minimum, and biocrusts represent the main soil cover, and
- (iii) if the humidity of the climate increases, the stabilizing effects of biocrust are reduced, although without disappearing entirely, because water availability increases and higher vegetation hinder the growth of biocrusts.

A.2 Materials and methods

A.2.1 Study sites and experimental settings

In order to assess the climatic effect on soil and its interactions with biocrusts, four study sites distributed between latitudes from 26°6'S to 37°48'S and over 1300 km were established in the Chilean Coastal Range: Pan de Azúcar National Park (PA), Santa Gracia Natural Reserve (SG), La Campana National Park (LC), and Nahuelbuta National Park (NA), corresponding to arid, semi-arid, mediterranean, and humid climates, respectively (Bernhard et al., 2018).

The study sites are comparable in geology, geomorphology, land use, and glacial and volcanic influence (Bernhard et al., 2018). The parent material in all the study sites is granitoid, keeping this factor of soil formation nearly constant along the studied gradient (Oeser et al., 2018). The dominant topography is generally fluvial valleys, and the sites had no glacial influence during the last glaciation (Hulton et al., 2002). The sites are located within nature protection areas, with limited anthropogenic influence compared to the surrounding areas. Despite this, the occasional entry of cows to LC (Rundel and Weisser, 1975) and goats to SG (Armesto and Arroyo, 2007) has been reported. These conditions allow us to focus on the environmental effect on two other soil-forming factors, i.e., climate and vegetation.

The mean annual temperature (MAT) decreases from north to south (PA: 16.8 °C, SG: 13.7 °C, LC: 14.1 °C, NA: 6.6 °C). The mean annual precipitation (MAP) in the study sites increases from north to south (PA: 12 mm yr⁻¹, SG: 66 mm yr⁻¹, LC: 367 mm yr⁻¹, NA: 1469 mm yr⁻¹), with similar rainfall distribution mostly concentrated in winter months (May to August) (Bernhard et al., 2018). The elevation of the sites increases from north to south (PA: 329 m to 351 m a.s.l., SG: 642 m to 720 m a.s.l., LC: 708 m to 732 m a.s.l., NA: 1200 m to 1270 m a.s.l.). Paleoclimate modeling studies (Mutz et al., 2018) indicate that these climate patterns have been persistent since the late Pliocene; thus, the study sites represent the long-term impact of climate on the soil (Ewing et al., 2006). Bernhard et al. (2018) classified soils in the study sites as Regosols in PA, Cambisols for SG and LC, and Umbrisols in NA. In general, pedogenic processes such as soil depth, clay contents, organic matter accumulation, porosity, and activity ratio are correlated with the humidity of the site.

For each of the four study sites, five plots of 1x1 m were established as replicates. Each plot was located in the top-slope position with south-facing exposition, considering the presence of site-typical biological soil crust communities, similar slope and aspect, lack of anthropogenic disturbance, and a maximum distance of 30 m between each plot. Each plot included patches with at least the size of the samples with 100 % biocrust cover (BSC+), and additionally, a nearby point without biocrust cover (BSC-) was defined as control.

A.2.2 Biocrust sampling and classification

Biocrust patches of approximately 100 cm² were identified according to Lange and Belnap (2016) and collected in the field by carefully detaching the biocrust layer, removing the loose soil, and storing it in paper envelopes after air-drying for every research plot. Samolov et al. (2020) describes the a biocrusts dominance in PA with cover of up to 40%. The other study sites are dominated by higher vegetation that limits the cover of biocrust up to 15% in SG and 5% in LC and NA. Sampled communities showed all typical biocrust classes from cyanobacteria, algae, fungi, lichens, liverworts, and mosses. The species composition further showed a graduating change from lichen-dominating

biocrusts in the northernmost site to bryophyte-dominating biocrusts in the southernmost site. Biocrusts in NA were specifically found in zones of forest soil disturbance. Bryophytes were sampled with rhizoids down to 5 mm depth; all other species were down to 2 mm. Dominant macroscopic biocrust species were determined for each of the four sites to the genus level by morphological characteristics using a stereomicroscope (Leitz TS, Wetzlar, Germany), a transmitted-light microscope (Leitz Laborlux S, Wetzlar, Germany), and ultraviolet light. Species groups were separated into bryophytes (Lightowers, 1985; He, 1998; Ochyra and Matteri, 2001; Cuvertino et al., 2012; Fariña and Ardiles, 2014) and lichens (Galloway and Quilhot, 2009) and assigned to the different regions (Table A.1). Baumann et al. (2018), based on morphological identification of enrichment cultures, reported that the biocrusts of all studied areas were composed of 18 to 15 species of algae and cyanobacteria; where the richness of green algae increased, while the richness of cyanobacteria decreased with increasing humidity and decreasing mean annual temperature. While Samolov et al. (2020), based on morphological and molecular traits, reported 18 species in PA, 26 species in SG, 40 species in LC, and 27 species in NA. A more detailed survey and classification of individual species, including algae and cyanobacteria, will be sought for further studies.

A.2 Materials and methods



Figure A.1: Sampled biological soil crust for PA (a), SG (b), LC (c), and NA (d).

Table A.1: Taxonomical composition of mosses and lichens in the biological soil crust for the study sites along the climatic gradient.

Site / Division	Family	Genus	No. species
PdA			
Lichens	Cladoniaceae	<i>Cladonia</i> sp.	2
	Verrucariaceae	<i>Placidium</i> sp.	2
	Lecanoraceae	<i>Lecidella</i> sp.	1
	Rhizocarpaceae	<i>Rhizocarpon</i> sp.	1
SG			
Mosses	Pottiaceae	<i>Syntrichia</i> sp.	2
	Pottiaceae	<i>Tortella</i> sp.	2
Unidentified lichens			2
LC			
Mosses	Bartramiaceae	<i>Philonotis</i> sp.	1
	Bryaceae	<i>Bryum</i> sp.	1
	Pottiaceae	<i>Syntrichia</i> sp.	2
	Pottiaceae	<i>Tortella</i> sp.	2
Unidentified mosses and lichens			2 + 1
NA			
Mosses	Amblystegiaceae	<i>Acrocladium</i> sp.	1
	Amblystegiaceae	<i>Amblystegium</i> sp.	1
	Bartramiaceae	<i>Bartramia</i> sp.	1
	Bryaceae	<i>Bryum</i> sp.	1
	Dicranaceae	<i>Campylopus</i> sp.	2
	Pterigynandraceae	<i>Myurella</i> sp.	1
Unidentified liverworts, lichens, fungi			2 + 2 + 1

A.2.3 Soil sampling and analyses

For soil characterization, bulk topsoil samples (0–5 cm) were taken with metal-core sample augers directly under biocrust patches and in comparative zones without biocrust cover and sieved to 2 mm after air drying. Bulk density (BD) and soil water content were determined gravimetrically. The particle size distribution was determined for seven fractions according to Köhn (1929), combining sieving of fractions >20 µm and pipetting of fractions <20 µm. Soil texture was interpreted according to the WRB soil classification system (Jahn et al., 2006). Soil pH was determined in water by a WTW pH 340 (WTW GmbH, Weilheim, Germany) using a Sentix 81 electrode, and electrical conductivity was measured with a conductivity meter (LE703, Mettler Toledo, USA). Total carbon (C_t) and nitrogen (N_t) of the bulk topsoil samples (0–5 cm) were analyzed using oxidative heat combustion at 1150 °C in a Vario EL III elemental analyzer (Elementar Analysensysteme GmbH, Hanau, Germany). Total organic carbon (TOC) was corrected by the carbonate content of samples with pH >6.7. The carbonate content was deter-

mined from the volumetric titration of the reaction with 10% HCl using a calcimeter (Eijkenkamp, Giesbeek, Netherlands).

The physical stability of soil aggregates was measured to quantify the destructive effect of water and mechanical forces through two-stage sieving: dry and wet (Horn, 2009). Water-stable aggregates were measured by sieving 200 g of undisturbed, air-dried soil samples, homogenized to 30.0 mm, through a stack of sieves of decreasing mesh size (19.0, 14.7, 9.8, 6.8, 4.8, 3.3, 2.0 mm, plus that collected the remainder below 2.0 mm) and then repeating the same process underwater (Six et al., 2000). Finally, coarse fragments (stones) were removed, and the values for each size were calculated relative to the weight of the initial sample. With this aggregate stability data, accumulated frequency curves were calculated, and a set of stability indexes were estimated: difference in mean weight diameter of the aggregates (ΔMWD) (Horn, 2009; Bavel, 1950; Loaiza Puerta et al., 2018), difference in geometric mean diameter (ΔGMD) (Mazurak, 1950; Kemper and Rosenau, 1986), water stability aggregate ratio (WSAR) (Liu et al., 2014) and the proportion of soil macroaggregates of a diameter less than 2 mm ($R < 2$ mm) (Liang et al., 2015) as described below. ΔMWD and ΔGMD indicate how much the average diameter of soil aggregates changes between dry and wet conditions. The main difference between ΔMWD and ΔGMD is that the first considers a linear behavior between the different aggregate size classes, while the ΔGMD considers a logarithmic fitting.

Difference in mean weight diameter (ΔMWD)

$$\Delta MWD = \frac{\sum_{i=1}^n X_i * W_i}{\sum_{i=1}^n W_i}$$

where W_i is the corrected mass proportion of stable aggregate fraction i in the total 2–30 mm aggregate fractions, and X_i is the mean diameter of stable aggregate fraction i , and n is the number of particle fractions.

Difference in geometric mean diameter (ΔGMD)

$$\Delta GMD = \exp \left[\frac{\sum_{i=1}^n X_i \lg W_i}{\sum_{i=1}^n W_i} \right]$$

where X_i is the sieve opening size (mm), W_i is the proportion of the total sample mass occurring in the i -size fraction, and n is the number of particle fractions.

Water stability aggregate ratio (WSAR)

$$WSAR = \frac{WSA}{A} * 100$$

where WSA is the >2 mm water-stable aggregate content, and A is the >2 mm dry aggregate content.

Proportion of soil macroaggregate of a diameter less than 2 mm ($R_{<2mm}$)

$$R_{<2mm} = \frac{W_{r>2}}{W_T} * 100 = \left(1 - \frac{W_{r<2}}{W_T} \right)$$

where $W_{r>2}$ is the weight of macroaggregates with a diameter less than 2 mm, W_T is the total sample weight, $W_{r<2}$ is the weight of microaggregates with a diameter less than 2 mm.

A.2.4 Statistical analyses

The influence of the climatic gradient (study site) and biocrust presence on physico-chemical soil parameters and aggregate stability in 40 plots (4 study sites, 2 biocrust treatments, 5 replicates) were assessed by factorial generalized linear models (GLM) because of the lack of normal distribution for most of the variables according to the Shapiro-Wilk test. The link functions used for each model were selected based on the lowest Akaike information criterion (AIC) selection and characteristics of the data (skewness, counts, continuous variables, proportions) between Gaussian, Gamma, inverse Gaussian, and Tweedie distributions. Differences in treatments were tested using Tukey post-hoc-test with $p < 0.05$ as significance criteria. The analyses were conducted in R 4.2.0 (Team, 2018), and the GLM distributions were extended from the base R core with the Tweedie 2.3.3 package (Dunn, 2017). All visualizations were made with the package ggplot2 3.3.3 (Wickam, 2016).

A.3 Results

A.3.1 Soil properties

Soil pH was significantly affected by the climatic gradient (Figure A.2), with mean values of 7.7 in PA, 6.2 in SG, 5.9 in LC, and 4.4 in NA, with acidification levels of 6.2 in BSC- to 5.9 in BSC+. In terms of electrical conductivity (EC), a remarkably higher value of $2646.1 \mu\text{S cm}^{-1}$ in PA is outstanding in comparison with the low and homogeneous values of $109.3 \mu\text{S cm}^{-1}$ for SG, $153.8 \mu\text{S cm}^{-1}$ for LC, and $102.3 \mu\text{S cm}^{-1}$ for NA. EC did not differ for the biocrust treatment. Nevertheless, when looking at the site and biocrust in combination, the BSC+ results in a reduction of the EC in PA; meanwhile, in SG, LC, and NA there was no noticeable change.

Bulk density (BD) showed a significant difference between the study sites, with higher values in the two dryer sites, with 1.5 g cm^{-3} in PA, and 1.6 g cm^{-3} in SG, and a

A.3 Results

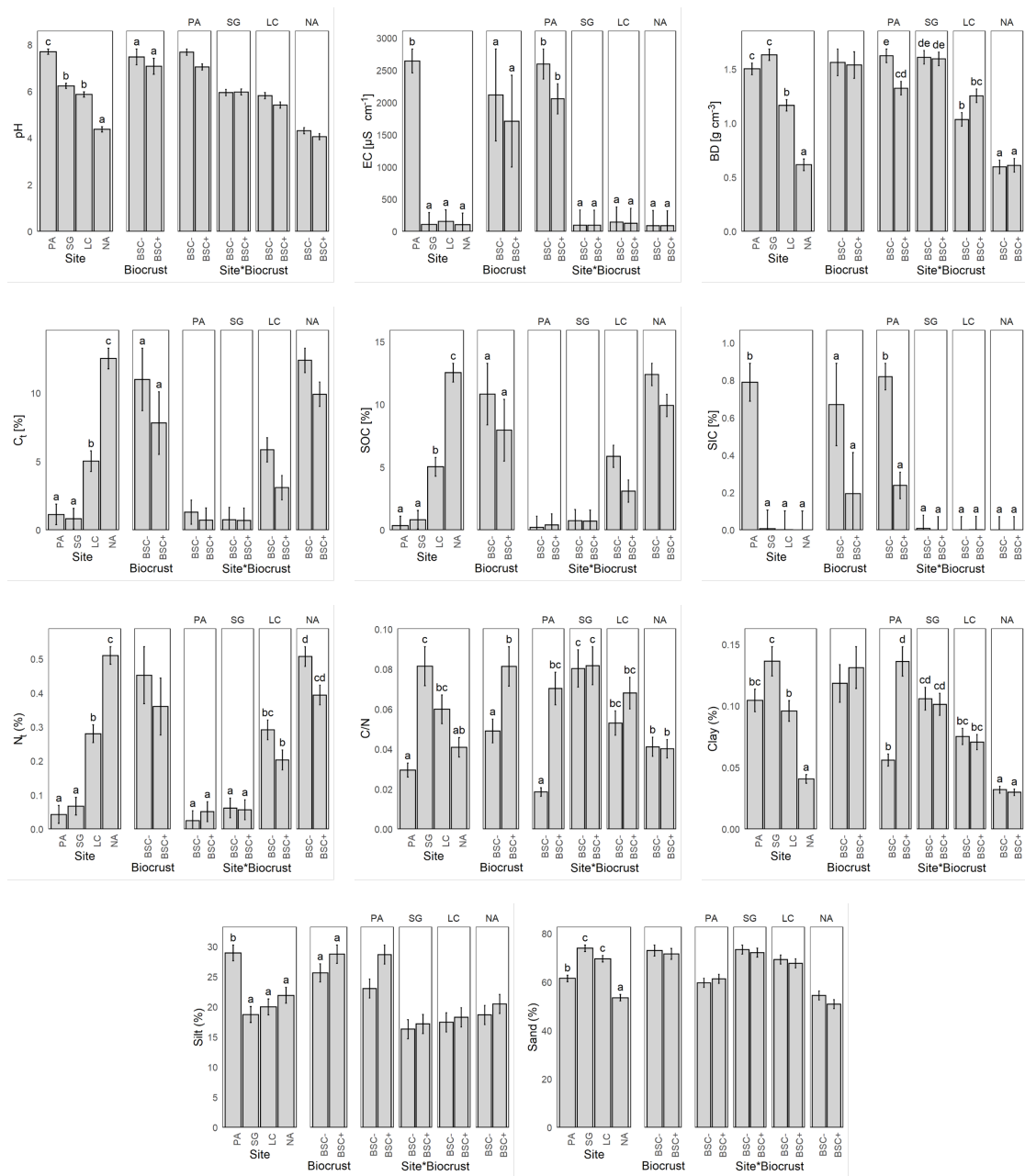


Figure A.2: Mean and standard error of soil properties for Pan de Azúcar (PA), Santa Gracia (SG), La Campana (LC) and Nahuelbuta (NA), without (BSC-) and with biocrust cover (BSC+), and the interaction of both factors. (EC = electrical conductivity, BD = bulk density, C_t = total carbon, SOC = soil organic carbon, SIC = soil inorganic carbon, N_t = total nitrogen, C/N = carbon to nitrogen ratio). Significant factors include Tukey's Post-hoc-Test indicated by letters on the top of the bars. Different letters represent significant differences at $p < 0.05$.

decrease in the more humid sites, with 1.2 g cm^{-3} in LC and 0.6 g cm^{-3} in NA. Biocrust showed no changes for BD in SG and NA, but in PA BSC+ resulted in a reduction of the BD of 18.2%, while in LC BSC+ showed an increase in BD of 21.9% (Figure ??).

Total carbon (C_t) content was directly proportional to the humidity along the climatic gradient (Figure ??), with values of 1.1% in PA, 0.8% in SG, 5.0% in LC, and 12.5% in NA, but with a significant decrease when the BSC+ is present, from 5.6% to 4.2% in average. Soil inorganic carbon (SIC) was significantly higher in PA, with an average of 0.8% of the mass of the soil, while in SG, LC, and NA, it was not found. When looking at the SIC along the different sites and under biocrust in combination, the BSC+ results in a reduction of 70.1% in the SIC for PA, while in SG, LC and NA was no change. Soil organic carbon (SOC) showed a similar pattern as C_t , with a reduction in PA to 0.3% and the same 0.8% in SG, 5.0% in LC, and 12.5%. Total nitrogen (N_t) content was directly proportional to the humidity along the climatic gradient, with values of 0.04% for PA, 0.07% for SG, 0.28% for LC and 0.51% for (Figure ??). BSC+ showed a reduction of 30.3% in LC and 22.3% in NA, while the N_t content remained stable in PA and SG under the influence of BSC. The relation between C_t and N_t , expressed as C/N, showed significantly different values of 33.9 in PA, 12.3 in SG, 16.7 in LC, and 24.5 in NA on average; and with a significant decrease from 27.0 in BSC- to 16.7 in BSC+ (Figure ??). It is important to note that although PA and NA present the highest values, the condition changes diametrically when observed together with the BSC+ treatment, with a large dispersion in PA and stable values in NA.

The distribution of the soil particle size classes did not show clear patterns along the climatic gradient, with PA deviating from it in all cases. Despite this, the observed values were significant, with clay values of 9.6% for PA, 7.3% in SG, 10.4% in LC, and 24.6% in NA, while when looking at the interaction between site and biocrust, there is an increase of 143.4% in clay content for the BSC+ condition, while for SG, LC and NA was no difference; silt with 28.9% in PA, 18.7% in SG, 20.0% in LC and 21.9% in NA; and sand with 61.5% in PA, 73.9% in SG, 69.6% in LC and 53.5% in NA. When biocrusts were present, a significant decrease from 13.6% to 12.6% in clays and an increase from 21.2% to 23.6% in silt was observed, with higher dispersion for the arid site (PA) (Figure ??).

A.3.2 Soil aggregate stability

Dry sieving showed a significant difference between study sites but not for the biocrust treatment (Figure A.3). Dry aggregates in the 19.5–30.0 mm range showed significantly different values of 4.4% in PA, 1.2% in SG, 5.5% in LC, and 36.2% in NA. The fraction 9.5–19.0 mm revealed differences in the interaction between study sites and biocrusts, increasing the proportion of aggregates from 13.2% in PA to 19.3% SG and 29.3% in LC, not in NA with only 2.9% in the presence of biocrusts. The aggregates between 6.7–9.5 mm showed a significant decrease from 13.3% in PA, 5.2% in SG, 6.5% in LC,

and 4.1% in NA. In interaction with biocrusts, it showed a significant increase in the proportion when it was present. The fraction from 4.7–6.7 mm showed significantly different values of 13.6% in PA, 3.4% in SG, 5.0% in LC, and 5.6% in NA, while the interaction with biocrusts showed a significant increase when is present (BSC+). Aggregates from 3.4–4.7 mm size showed significance among study sites, with 9.8% in PA, 3.6% in SG, 4.4% in LC, and 7.9% in NA. Aggregates between 2.0–3.4 mm showed a slightly similar amount of 9.9% in PA, 5.9% in LC, and 14.3% in NA, but with a minor proportion of 4.9% in LC, while when biocrust is present in LC, it showed a slight decrease. Finally, for the dry sieved aggregates under 2 mm, there was a significant reduction for the study sites, with values of 69.1% in SG and 47.3% in LC relative to 30.1% in PA, but not in NA with 28.9%; while the biocrust effect in interaction with the site is significant with 60.6% in SG and 40.8% in LC, indicating the same proportion of aggregates in this site for SG with 30.0% and NA with 39.8%.

In a second stage, aggregate stability under wet conditions was characterized, with a clear difference between sites, while biocrusts had a significant effect only on the aggregate size classes <2.0 mm and 19.0–30.0 mm (Figure A.3). At the same time, the fraction 19.0–30.0 mm showed an increasing significant pattern in the amount of aggregates, with 2.8% in NA, 0.8% in SG, 8.9% in LC, and 29.9% in NA, while biocrusts significantly increased the proportion of aggregates by 35.6%, from 9.0% for BSC- to 12.2% for BSC+. For the fraction 9.5–19.0 mm, there were significant differences between the study sites, the biocrust effect, and its interactions, with an increase from 5.4% to 11.7% on average when biocrusts were present. The wet sieved aggregates in the range of 6.7–9.5 mm showed significant differences only between the study sites, with 10.6% in PA, 2.5% in SG, 4.2% in LC and 4.3% in NA. Wet aggregates in the range of 4.7–6.7 mm showed significant differences between the study sites with 10.6% in PA, 2.3% in SG, 3.7% in LC and 5.8 in NA. The fraction between 3.4–4.7 mm showed only significant differences between the study sites, with 6.9% in PA, 2.2% in SG, 3.0% in LC, and 6.1% in NA. Aggregates ranging from 2.0–3.4 mm showed differences between the study sites, with 5.8% in PA, 3.2% in SG, 4.2% in LC, and 6.8% in NA. The fractions under 2.0 mm were significantly different for the study sites, with 58.3% in PA, 79.6% in SG, 62.4% in LC, and 41.3% in NA; and for biocrusts from 63.9% for BSC+ treatment to 56.9% for BSC- treatment.

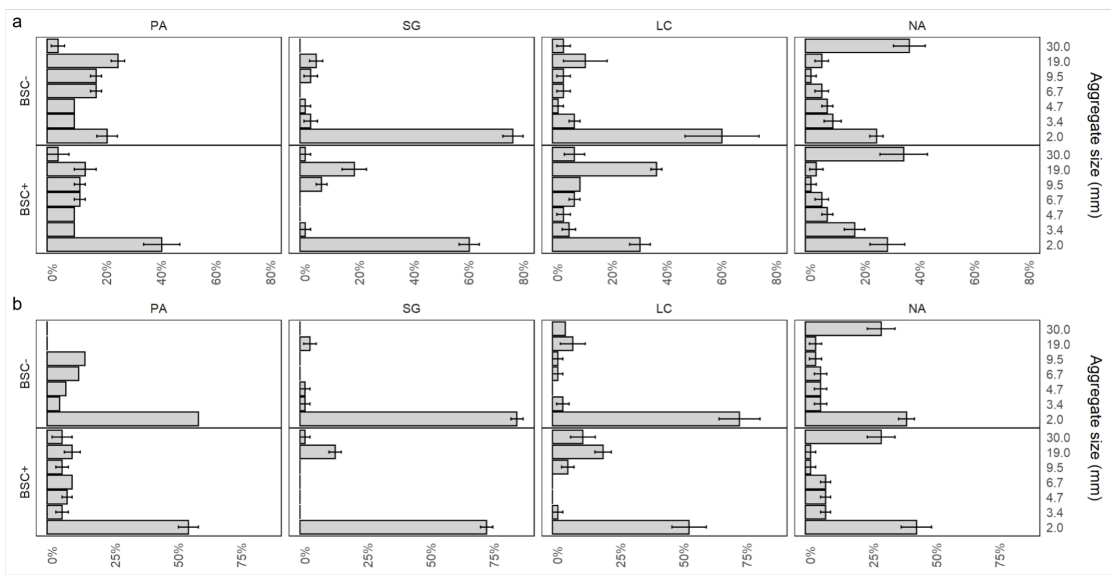


Figure A.3: Mean value and standard error of aggregate proportion for dry (a) and wet (b) sieved fractions for Pan de Azúcar (PA), Santa Gracia (SG), La Campana (LC), and Nahuelbuta (NA) for biocrust (BSC+) and non-biocrust (BSC-) treatments. Significant factors and corresponding models for response variables are included in Appendix A.2.

When comparing the changes of the aggregate distributions between wet and dry conditions (Figure A.4), an irregular pattern was observed, with a general decrease in most of the analyzed fractions, except for an increase in the amount of aggregates of 19.0 mm for NA. This was even higher than for the BSC+ treatment. It is important to mention that NA also showed a slight increase in the proportion of 9.5 mm and 6.7 mm aggregates.

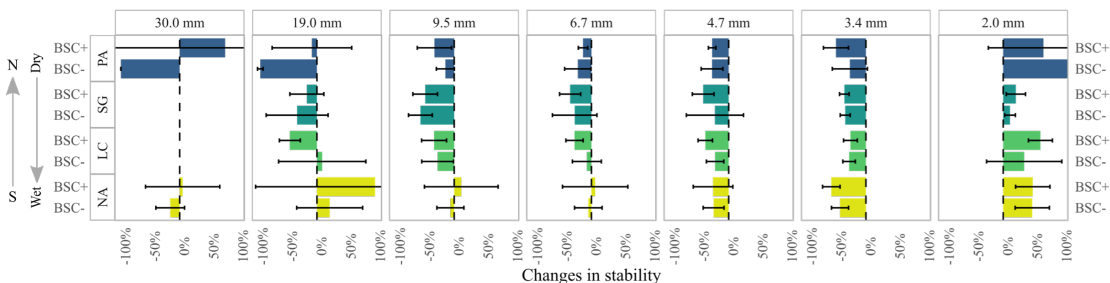


Figure A.4: Mean and standard deviation of aggregate size distribution changes between dry and wet sieving for the sites Pan de Azúcar (PA), Santa Gracia (SG), La Campana (LC), and Nahuelbuta (NA) for biocrust (BSC+) and non-biocrust (BSC-) treatments. Error bars were, in some cases, truncated for better visualization.

Soil aggregate stability was evaluated through different indexes to integrate the different sizes and sieving conditions in a summary value. The difference in mean weight

diameter of the aggregates (ΔMWD) showed no significance in any of the conditions (Figure A.5). However, there was a significant difference in the difference of the geometric mean diameter of the aggregates (ΔGMD) for the study sites, with values of 1.86 mm for PA, 1.2 mm for SG, 1.4 mm for LC, in comparison with the more stable condition of 0.83 mm for NA. The water-stable aggregates ratio was significant for the study sites, showing differences between NA with 81.1% and the other study sites (57.7% PA, 66.2% SG, and 73.4% LC). The ratio of soil macroaggregates of a diameter less than 2.0 mm ($R_{<2\text{ mm}}$) presents differences in the study sites and for biocrust treatments. SG showed a value of $R_{<2\text{ mm}}$ of 79.6% and NA of 41.9%, which was different from PA and LC, with 58.6% and 62.4%, respectively. For biocrust treatments, $R_{<1.4\text{ mm}}$ changed from 63.7% to 57.5% with biocrusts, indicating a biocrust-induced decrease in the proportion for this fraction. Finally, according to the analyzed indexes, NA showed the most stable conditions, and alternating PA and SG showed the most unstable conditions.

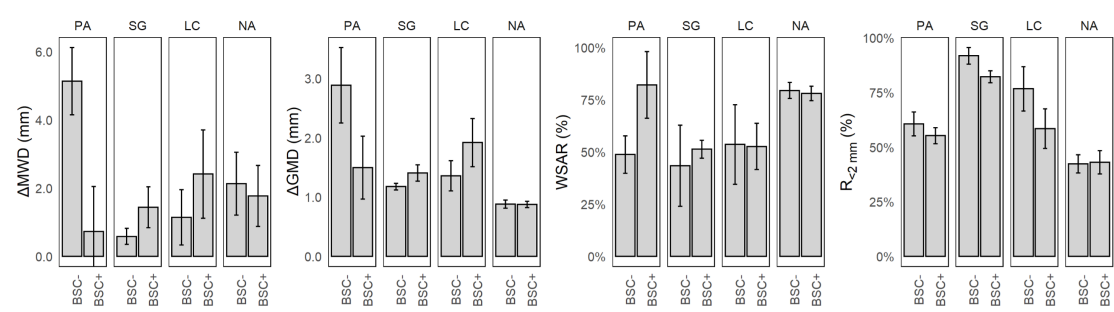


Figure A.5: Mean and standard error of aggregate stability indexes for Pan de Azúcar (PA), Santa Gracia (SG), La Campana (LC), and Nahuelbuta (NA) for biocrust (BSC+) and non-biocrust (BSC-) treatments. ΔMWD =difference in mean weight diameter, ΔGMD =difference in geometric mean diameter, WSAR=water stability aggregate ratio, $R_{<2\text{ mm}}$ =ratio of aggregates less than 2 mm. Significant factors and corresponding models for response variables are included in Appendix A.2.

As shown in Figure A.2, the climatic gradient (site) had significant pH, electrical conductivity (EC), bulk density (BD), total carbon (C_t), soil organic carbon (SOC), soil inorganic carbon (SIC), total nitrogen (N_t), C/N, clay, silt, sand, dry and wet aggregates under 30 mm, ΔGMD , WSAR, $R_{<2\text{ mm}}$. Biocrust treatments were significant for clay, silt, pH, EC, C_t , SOC, SIC, N_t , C/N, and wet aggregates from 9.5 mm to 30.0 mm and >2 mm, and $R_{<2\text{ mm}}$. Finally, the interaction of the site and biocrusts was significant for clay, bulk density (BD), total nitrogen (N_t), dry aggregates from 4.7 mm to 19.0 mm and 0 mm to 3.4 mm, wet aggregates from 9.5 mm to 30.0 mm, and ΔMWD .

A.4 Discussion

A.4.1 Aggregate stability and soil properties along the climatic gradient

The climatic gradient has a significant effect on the stability of soil aggregates. Using the geometric mean diameter (ΔGMD), an index that replaces the linear fitting of ΔMWD with a logarithmic one, significant differences for the study sites along the climatic gradient can be observed ($p - \text{value} : < 0.001$). When soil aggregate stability was evaluated with the difference in mean weight diameter (ΔMWD), it did not show significant changes along the climatic gradient. WSAR, an index that shows the ratio of aggregates that persist stably after disruption by water, showed a similar behavior as ΔMWD . The main difference between ΔMWD and ΔGMD is that ΔGMD performs better in non-uniform particulate substances (Hatch and Choate, 1929; Gardner, 1956), which corresponds to soils equilibrated in the content of sand, silt, and clay (Mazurak, 1950) and pointing soil texture indirectly as a critical factor in aggregate stability along the climatic gradient. Further, considering the ΔGMD data, an increase in stability was observed as moving along the climatic gradient to higher water availability conditions except for SG. The lower value of ΔGMD for SG indicates comparably higher aggregate stability as it would be expected when we assume a steady trend from arid to humid climate. In PA, in the drier north, the condition proved to be less stable than NA, despite the high content of inorganic carbon. SG presented the highest ratio of unstable aggregates under the studied range of sizes (highest $R_{<2\text{ mm}}$) and NA the lowest, with close to half of it, indicating augmented aggregate stability in the complementary range of sizes.

The effect of the climatic gradient is not only expressed in the stability of soil aggregates, but it is also present with different intensities in a variety of soil properties. The pH decreases continuously from the northern arid to the southern humid study site in accordance with Bernhard et al. (2018). The high pH in PA can be attributed to the constant input of atmospheric aerosols, e.g., salts, gypsum, and calcium carbonates (Ewing et al., 2006) in combination with the arid climate that allows salts to accumulate in the topsoil (Slessarev et al., 2016). Whereas in the southern sites, the forwarding increase of precipitations results in a reduction in the pH due to leaching of soluble salts (Slessarev et al., 2016) and an increase in soil respiration (Orchard and Cook, 1983). The accumulation of soluble salts is well established for the arid site PA, as saline conditions (Allison and Richards, 1954) are indicated by the high electrical conductivity value. These higher amounts of salts have a strong effect in structure degradation dynamics, linked to the destabilizing effect of sodium and stabilizing of carbonates (Corwin, 2021). Although C_t and N_t follow the climatic gradient, when comparing the C/N, PA and NA have higher values. High values of the C/N indicate a nitrogen limitation of plants and other organisms (Brust, 2019), pointing out that this occurs at the two opposite sites along the climatic gradient. This could be explained by the biological activity (Zhang

et al., 2013), which may be close to a physiological limitation in the case of NA, while for PA, it may indeed be due to low nitrogen availability (Hooper and Johnson, 1999). However, there was also a high amount of carbonates in PA, which makes PA hardly comparable in terms of C_t . Despite the properties following the climatic gradient, SG deviates from the other sites in terms of higher bulk density (BD), lower clay, and higher sand content. This can indicate a degraded condition for the semi-arid site caused by the current land use, including grazing (Armesto and Arroyo, 2007), compacting the surface and thus activating erosive processes (Scholten and Seitz, 2019), in favor of the accumulation of sand particles (Govers, 1985). The aggregate distribution stresses this finding, where SG has a lower proportion of water-stable aggregates >2 mm and a higher water-destabilization of aggregates between 9.5 mm to 4.7 mm, indicating that the nature of the structuring agent in that zone is water-soluble.

A.4.2 Biocrusts altering soil properties along the climatic gradientt

Despite these factors beyond the climatic gradient, biocrusts showed effects on clay, silt, pH, C_t , N_t , C/N, and wet aggregates from 9.5 mm to 30.0 mm and >2 mm. However, as this was an observational study, it only allows establishing associations between factors and not cause-effect relationships (Cox, 1992; Rosenbaum, 2005). It is thus possible that changes in soil characteristics promote the biocrust establishment, as well as that biocrust establishment triggers changes in these properties (Belnap, 2003).

The biocrust treatments showed a significant decrease in pH ($p - value : 0.002404$), reflecting the biological activity of its constituent organisms, which acidifies the soil due to the carbon dioxide released by cellular respiration (Bachar et al., 2010). The pH values reported by Bernhard et al. (2018) are in the same range as ours but without differentiating between BSC+ and BSC-, as this factor was not part of their study. The content of C_t and N_t were significantly different when biocrusts were present, but it did not affect any aggregate sizes or stability indexes. In this sense, biocrusts play a role in the carbon and nitrogen cycles (Chen et al., 2000), as they are formed mainly by photosynthetic and nitrogen-fixing organisms (Maestre et al., 2013), but it has not had an immediate impact on the soil aggregate stability and points out that the primary stabilizing agent is of organic origin (Wagner et al., 2007; Six et al., 2004).

Considering the stabilizing effect of biocrusts on wet sieved aggregates between 9.5 and 30 mm, we could show that it occurs prominently at the three northern sites, whereas in NA there was no difference with and without biocrusts. This points to a threshold in the biocrust-induced stabilization of the soil aggregates between LC and NA and partially confirms our initial assumption that biocrusts have the greatest effect in arid conditions. However, the effect on aggregate stability for the wet condition varies according to the variable used, being specific for limited aggregate sizes in terms of mechanical disturbances (dry sieving) but without a substantial improvement concerning water stability (wet sieving). This lack of difference in wet sieved aggregate point to a non-

soluble nature of the stabilizing agents, which can be attributed to stabilization due to organic structures and exudates (Rillig, 2004), and stress the idea that NA differs to the other sites in the mechanisms of aggregate stabilization as a local adaptation, where due to the higher proportion of precipitation, is conducted by water stable mechanisms.

Soil aggregate stability showed clear differences along the climatic gradient. However, when considering the effect of biocrusts, differences were limited to the smallest aggregate size class (R).

The results indicate that soil aggregate stabilization mechanisms are different in PA than at the other sites. With that in mind, it was found that in PA, biocrusts grow in areas with a lower content of clay and higher content of silt, which implies increased nutrient availability and water-holding capacity (Chen et al., 2020), while the sand fraction was not related. However, the method used can amplify that difference since the determination of particle size distribution does not consider coarse fragments (Köhn, 1929), which were abundant at PA. In addition, the soil covered with biocrusts showed a lower value for bulk density (BD) only for PA, while in the other sites, this property was not affected. This can be interpreted as a biocrust-induced decrease in soil density due to increased intra- and extra-aggregate porosity and organic matter (Whitney et al., 2017) or that biocrusts grow under the least limiting condition (Bowker et al., 2014). Soils with biocrust cover showed a trend of lower electrical conductivity, which can be explained by the inhibition of biocrusts by toxicity due to the accumulation of salts in the soil, or to the consumption of salts as a source of nutrients by the organisms in the biocrusts (Abed et al., 2019).

Biocrust plays a role along the climatic gradient affecting different properties, i.e., clay, silt, pH, C_t, N_t, C/N, and wet aggregates from 9.5 to 30.0 mm and >2 mm. Nevertheless, the way that each property change responds to local conditions: In the arid northernmost site, there is a strong influence of the salts in terms of stabilization and establishment of biocrusts, while at the southernmost site, there is no stabilization of the aggregates, but a contribution to the carbon and nitrogen contents. The most consistent property along the climatic gradient was pH, an indicator of biological activity. However, at the scale of the climatic gradient it is not possible to distinguish the origin of biological activity between plants, microorganisms, fungi, bacteria, etc. Finally, considering the largest size of the persistent wet aggregates match the characteristics attributed to fungi and bryophytes, capable of retaining micro-aggregates and soil particles between their hyphae and rhizoids, respectively (Kleber et al., 2007; Six et al., 2004; Totsche et al., 2018) and points to this as the most significant mechanism of soil aggregate stabilization of biocrusts.

A.5 Conclusions

This study aimed to investigate how and to what extent biocrusts stabilize soil aggregates along an arid to humid climatic gradient in Chile. We show that biocrusts play a role in soil aggregate stability along the climatic gradient by increasing the stability for wet aggregates from 9.5 to 30.0 mm and >2 mm. Biocrusts also modify other soil properties such as C_t, N_t, C/N, clay, and sand, indicating an initial accumulation of organic matter that then give place to aggregation processes. The biocrusts effect on aggregates stability was lower under humid climate conditions, which indicates a transition in the main biotic agents driving the aggregation of the soil surface, moving from biocrust communities in arid regions to vascular plants in humid conditions. Finally, we conclude that the biocrusts in our study area showed to be a valuable agent in stabilizing the upper topsoil layer, but for a narrow spectrum of conditions and mostly under arid conditions. Therefore, the effect could be considered a transition in ecological succession toward a stable ecosystem. In this process, biocrusts improve conditions for other more demanding species, such as vascular plants, initially improving the availability of carbon and nitrogen in the soil.

Appendices

Table A.2: Appendix A. Significant factors for response variables based on generalized linear models. Models with significant interaction also include the predictors as simple parameters based on marginality principle.
 $(p\text{-value} \leq 0: "****"; p\text{-value} \leq 0.001: "**"; p\text{-value} \leq 0.01: "*")$

Dependent variable	Distribution (link-function for GLM)	Significance for independent variable		
		Site	Biocrust	Site \times Biocrust
Clay	Gaussian	***	*	
Silt	Inverse Gaussian	***	*	
Sand	Gaussian	***		
Fine Silt	Tweedie	***		*
Medium silt	Tweedie	***	***	*
Coarse silt	Tweedie	***		
Very fine sand	Gaussian	***		
Fine sand	Tweedie	***		
Medium sand	Gaussian	***		
Coarse sand	Tweedie	***		
pH	Gaussian	***	**	
EC	Tweedie	***		
BD	Gaussian	***		**
N _t	Gamma	***		**
C _t	Tweedie	***	**	
C/N	Tweedie	***	**	
19.0-30.0 mm Dry	Tweedie	***		
9.5-19.0 mm Dry	Tweedie	***		**
6.7-9.5 mm Dry	Tweedie	***		**
4.7-6.7 mm Dry	Tweedie	***		*
3.4-4.7 mm Dry	Tweedie	***		
2.0-3.4 mm Dry	Tweedie	***		*
<2.0 mm Dry	Tweedie	***		***
19.0-30.0 mm Wet	Tweedie	***	*	**
9.5-19.0 mm Wet	Tweedie	*	**	*
6.7-9.5 mm Wet	Tweedie	***		
4.7-6.7 mm Wet	Tweedie	***		
3.4-4.7 mm Wet	Tweedie	***		
2.0-3.4 mm Wet	Tweedie	***		
<2.0 mm Wet	Tweedie	***	*	
Δ MWD	Gaussian			
Δ GMD	Tweedie		***	
WSAR	Gaussian			
R<2 mm	Gaussian	***	*	

Data availability

The data that support the findings of this study are available from the corresponding author upon request.

Code availability

The code that supports the findings of this study are available from the corresponding author upon request.

Author contribution

TS, DW, CWM, OS, and StS conceptualized the study. OS, KW, and NRM collected the soil samples. StS collected and analyzed the biocrust samples, and NRM analyzed the soil samples. NRM performed the analyses and prepared the manuscript.

Competing interests

The authors declare that they have no conflict of interest.

Acknowledgments

We are deeply grateful to the students, technical assistants, and colleagues who helped in the field and laboratory phases. A special thanks to Martin Nebel and Sonja Thielen for their help in classifying bryophytes and lichens. Oliver Burkhardt (GFZ German Research Centre for Geosciences) and Franziska Steiner (Technical University of Munich) for their support in the field. Hugo Pérez for his help and experience in the soil physics laboratory of the Universidad de Chile. We are grateful to the Chilean National Forest Corporation (CONAF) and Sucesión Gálvez Muñoz, who provided access to the study sites. The study was funded by the German Science Foundation DFGSPP 1803 (EarthShape; www.earthshape.net). We acknowledge support by Open Access Publishing Fund of University of Tübingen.

Appendix B

Biocrusts as climate-dependent regulators of erosion, water and nutrient cycling

Abstract

Biocrusts, complex communities of organisms, significantly alter surface and sub-surface processes, including water infiltration, and the cycling of carbon (C) and nitrogen (N). While their importance is recognized, studies across broad climatic gradients are scarce. We conducted rainfall simulation experiments at four sites along a 910 km Chilean Coastal Range transect, representing coastal and inland semi-arid, mediterranean, and humid climates. We quantified overland flow, sediment discharge, and fluxes of C and N in percolating water, comparing paired biocrust-covered and bare soil surfaces. Our findings reveal that biocrusts, compared to bare soil, significantly increased cumulative infiltration rates across all climates, indicating enhanced saturated hydraulic conductivity. Biocrust presence reduced runoff by 73% in humid climates and sediment flux by 80% in inland semi-arid climates. On average, soil erosion was reduced by up to 69%. Additionally, biocrusts significantly reduced C loss via erosion. Dissolved organic carbon and nitrogen fluxes were also strongly influenced by the presence of biocrusts. Overall, our study demonstrates that, though the presence of biocrust significantly reduced erosion, water and nutrient dynamic are strongly influence by its presence and the climates, showing that biocrusts act as climate-dependent regulators of crucial surface and sub-surface transport processes.

Keywords

Biocrusts, Erosion, Infiltration, Climate gradient, Carbon, Nitrogen, Runoff

B.1 Introduction

Biological soil crusts (BSC) are formed by a close association between soil particles and various proportions of photoautotrophic organisms, such as cyanobacteria, algae, lichens, and bryophytes, along with heterotrophic organisms like bacteria, fungi, and archaea that live within or immediately above the top millimeters of the soil (Weber et al., 2022). They are a primary soil cover in arid environments, where the scarce availability of water limits the establishment of higher plants (Ding and Eldridge, 2020; Weber et al., 2022). However, biocrusts are also present in mesic environments without water limitation, where vascular plants and litter reduce their ability to compete (Corbin and Thiet, 2020; Gall et al., 2022b). Nevertheless, biocrusts can be abundant in such areas when disturbance and the subsequent ecological succession provide favorable conditions for their establishment (Büdel and Colesie, 2014; Gall et al., 2022a).

Biocrust composition, growth, and survival depend on climatic factors such as temperature, moisture availability, and rainfall characteristics (Belnap, 2003). Moreover, climatic diversity shapes the morphological, chemical and physiological characteristics of the different biocrusts (Concostrina-Zubiri et al., 2014). In arid environments, biocrusts typically dominated by algae, cyanobacteria, and lichens, form smooth and flat surfaces that concentrate a large amount of microbial biomass and serve as nutrient sources within these ecosystems (Weber et al., 2022). In these settings, cyanobacteria can fix large amounts of nitrogen and produce reserve exopolysaccharides (EPS) that support other organisms (Rodríguez-Caballero et al., 2018; Samolov et al., 2020).

In addition, under humid conditions, biocrusts have a higher proportion of fungi and bryophytes, resulting in rough surfaces with a remarkable capacity to store capillary water, increased pore space in their structure and enhanced carbon fixation (Riveras-Muñoz et al., 2022; Weber et al., 2022). These changes in surface roughness affect the surface hydrology of the soil by modifying the residence time of water on the surface (Kidron et al., 2022). Changes in water residence time, in turn, affect the distribution of infiltration and runoff, alter surface redox conditions, modify soil erodibility, and regulate the release of solutes into water (Kalnejais et al., 2010). This emphasizes the ability of biocrusts to modify water and sediment fluxes. In particular, lichen-dominated dryland biocrusts can enhance surface runoff and reduce sediment yield by surface clogging and subsequently surface saturation, and runoff initiation (Kidron et al., 2021). They can also dramatically alter albedo, soil temperature dynamics and thus consequently the potential evapotranspiration (Liu and She, 2020; Rutherford et al., 2017; Whitney et al., 2017; Xiao et al., 2019). Moss-dominated biocrusts with a rough morphology have a high water-holding potential and can decrease both runoff and sediment yield (Juan et al., 2023; Seitz et al., 2017; Silva et al., 2019; Zeng et al., 2025). Other effects of biocrusts that also include near-surface infiltration within the biocrust cover and its effect on percolation report enhanced infiltration and percolation in semi-arid ecosystems (Chamizo et al., 2016) and reclaimed soils (Gypser et al., 2016), alteration rainwater

flow in drylands (Li et al., 2022), and reduced infiltration while increasing erosion resistance in disturbed forests (Szyja et al., 2023). Moreover, comparative experimental studies focusing on soil water movement through different types of biocrust remain limited.

Along with their ability to modify water and sediment fluxes, biocrust communities significantly shape carbon (C) and nitrogen (N) cycles. Many researchers point biocrusts as one of the most important factors that initially influence soil organic carbon (SOC) in the uppermost soil horizon before higher plants appear (Belnap et al., 2007). Furthermore, Young et al. (2022) demonstrated that biocrusts facilitate the vertical movement of soluble carbon and nutrients from the surface to subsurface mineral soils, thereby enhancing overall carbon sequestration. The significance of biocrusts in the carbon cycle extends beyond their local role in building SOC (Witzgall et al., 2024), with these communities estimated to account for 7% of total net carbon uptake and 50% of terrestrial nitrogen fixation (Elbert et al., 2012). They further enhance C fixation through photosynthetic sequestration (Belnap et al., 2016; Grote et al., 2010). An increase in soil aggregate stability hinders C discharge by erosion (Riveras-Muñoz et al., 2022; Xiao et al., 2022), enhances soil fertility (Kheirfam et al., 2017), and fosters the establishment of other vascular and non-vascular organisms, further increasing C storage potential (Molina-Montenegro et al., 2016). In disturbed temperate forests, Gall et al. (2024) found that mosses significantly influence the relocation of SOC and total N via soil erosion and percolation, further highlighting biocrusts' impact on nutrient redistribution. Additionally, biocrusts play an active role in the N cycle as they are responsible for approximately 40 to 85% of N fixation worldwide, mainly through the activity of cyanobacteria , enhances soil fertility (Kheirfam et al., 2017), and foster the establishment of other vascular and non-vascular organisms, further increasing C storage potential (Molina-Montenegro et al., 2016). Additionally, biocrusts play an active role in the N cycle as they are responsible for approximately 40 to 85% of N fixation worldwide, mainly through the activity of cyanobacteria (Rodríguez-Caballero et al., 2018; Samolov et al., 2020). As for C, biocrusts immobilize N by incorporating it into their biomass, thereby reducing losses by leaching or volatilization (Nevins et al., 2020; Pan et al., 2021). Furthermore, biocrusts can mineralize N from SOC, making it available to other organisms in the soil ecosystem (Weber et al., 2015).

All these properties of biocrusts impact soil erosion, a central process that shapes the Earth's surface (Luetzenburg et al., 2020; Scholten and Seitz, 2019). Water-induced erosion occurs in humid and semi-humid regions (Gholzom and Gholami, 2012; Khaleghi and Varvani, 2018) but also occurs in arid environments due to rare extreme rainfall events (Hu et al., 2022). Biocrusts not only influence infiltration and overland flow, but also form a physical barrier against erosive agents, partially absorbing the kinetic energy of running water and falling raindrops. A reduction of runoff by 25.6% and sediment discharge by 75.5% was observed when comparing runoff plots with biocrust

cover below 10% and above 50% in early successional subtropical forests (Seitz et al., 2017). Similar effects of biocrusts on soil erosion have been reported in arid (Bowker et al., 2018; Eldridge et al., 2021), temperate (Gall et al., 2022a) and humid environments (Guo et al., 2022; Zhao et al., 2014). Another process of land surface stabilisation by biocrusts is the formation of aggregates from organic and mineral particles through the secretion of bacterial metabolites such as exo- and lipopolysaccharides (Costa et al., 2018; Tourney and Ngwenya, 2014; Xiao et al., 2022). Further, the trapping of soil particles within the structures of biocrusts helps prevent soil erosion (Riveras-Muñoz et al., 2022; Rodriguez et al., 2024; Xiao et al., 2022).

Biocrusts are increasingly observed and described outside their classical dryland habitats—hyper-arid, arid, semi-arid, and dry sub-humid habitats (Gall et al., 2022b; Weber et al., 2022). Furthermore, investigations into climate variability have covered multiple scales. For example, Munoz-Martin et al. (2019) studied cyanobacterial biocrust diversity along an aridity gradient in Mediterranean semi-arid soils and found that temperature and precipitation determine biocrust composition, with a greater prevalence of extremotolerant in harsher climates. Regarding topography, Castillo-Monroy et al. (2016) reported that species composition and richness of biocrusts increase with elevation in tropical shrublands. Additionally, Ding and Eldridge (2020) observed that, on smaller spatial scales in Australia, microsite differences correlate with an increase in biocrust cover as aridity rises, while Riveras-Muñoz et al. (2022) demonstrated that soil aggregate stabilization by biocrust improved from arid to humid climates in Chile. Both studies reveal that the dominant structuring mechanisms of biocrusts shift with climate: under dry conditions, biocrusts stabilize the soil surface through exopolysaccharide production that promotes aggregate formation and structural stability, evidenced by the development of water-stable aggregates; whereas under humid conditions, biocrust structures further entangle and stabilize the soil surface, resulting in a more defined crust (Riveras-Muñoz et al., 2022). Although studies investigating the role of biocrusts in regulating water, sediment, and C and N fluxes in different climates are limited, the interactions and feedback mechanisms between the underlying processes are not yet fully understood.

To enhance our understanding of the interrelation between climate and the multi-functional roles of biocrusts in regulating water, sediment, and matter fluxes at the soil surface and within the topsoil, we conducted a field experiment comparing land surfaces with and without biocrusts. We quantified changes in C and N fluxes, both in particulate and water-dissolved forms influenced by the presence of biocrusts. Additionally, we examined how biocrusts modulated the interactions between water, sediment, and nutrient fluxes along a gradient ranging from arid to humid climates. We introduced a new measuring device capable of simultaneously sampling runoff, sediment and seepage flow in an undisturbed soil monolith during simulated rainfall events. This study focused on four sites within the Coastal Mountain Range of Chile, representing a climate gradient

that includes coastal and inland semi-arid, Mediterranean and humid climates. All study sites (Figure 1) have a comparable topography and almost the same parent materials. Our experimental approach utilizing undisturbed soil monoliths subjected to standardized rainfall simulations allows us to assess biocrusts' effects on various fluxes. Our main hypotheses are that (i) biocrusts modify runoff, sediment discharge and percolation flow, including liquid and solid C and N fluxes and reduce soil erosion irrespective of climatic conditions, but (ii) feedbacks between overland flow, percolation flow, sediment and liquid and solid C and N fluxes are climate specific

B.2 Materials and methods

B.2.1 Study sites

B.2.2 Rainfall simulation experiment

At the research sites, one-square-meter plots were established for the actual rainfall simulation experiments. Each plot was located at top slope with a south-facing orientation. The setups considered the presence of site-typical biocrust communities, similar slope and aspect, and a lack of anthropogenic disturbance and ensured that the distance between each plot did not exceed 30 meters. Rainfall simulation was designed as a factorial, completely randomized experiment with eight treatments (four sites, each with and without biocrust). Five field replicates and three soil samples as technical replicates were taken, resulting in a sample size of $n = 120$ rainfall simulations.

Infiltration boxes (Figure 3) were developed as part of a rainfall simulation experiment to measure runoff and percolation flow, including their matter content. Undisturbed soil samples were collected using cutting frames ($20\text{ cm} \times 30\text{ cm} \times 7\text{ cm}$, Figure 3a), carefully installed with minimal surface and subsurface disturbances (Figure 3c, Seitz (2015)). Cutting frames are made from 1 mm metal plates, sharpened in the bottom sides, and include an upper border to transfer the strength to them without direct contact with the soil and a lower one to stop the frame from burying beyond the desired height of the sample (Figure 3a). Subsequently, the cutting frames were excavated around, and a metal plate was inserted underneath it (Figure 3d). The cutting frames with the soil samples were covered with metal plates, wrapped in plastic foil, and carefully transported to a flat area with water available. Then, the wrappings were removed, and the frames with the soil samples were stacked on a permeable metal plate and placed inside the soil erosion flux box (Figure 3a) designed as steel containers with a triangular surface runoff gutter and an outlet at the bottom to capture the percolation flow (Figure 3a). Soil depth within the boxes is 7 cm. In the case of the presence of small plants, they were cut flush with the surface using a scissor and paying attention to not pull them and avoid surface disturbances. The water content of each sample was measured by

a TDR probe (Delta-T Devices Ltd. Cambridge, UK) when sampling, using the average of 3 measurements directly next to the sampling area. Perpendicular photographs were taken on each sample with a digital camera (Sony ILCE-6000 equipped with a lens SELP1650, Tokyo, Japan) and processed with the grid quadrat method overlying a digital grid of 100 subdivisions and separating biocrusts by visual inspection (Belnap et al., 2001) to assess the biocrust ground cover.

Rainfall simulations were conducted near the sampling site with the Tübingen rainfall simulator (Iserloh et al., 2013; Seitz, 2015), equipped with a Lechler 460.788.30 nozzle and adjusted to a falling height of 3.5 m. The stack with the sample was placed inside the rainfall simulator and set to a 10° slope (Figure 3e). A rainfall event was simulated using an intensity of 45mmh⁻¹ sustained over a 30-minute period. According to regional intensity-duration-frequency analyses for central Chile (Pizarro-Tapia et al., 2020), such an intensity falls within the extreme rainfall category, well above the heavy precipitation threshold even for relatively wet climates. This extreme intensity was selected to exceed the soil infiltration capacities and reliably generate surface runoff at all study sites. In particular, the four sites represent a pronounced climatic gradient, ensuring that the simulated storm event is sufficiently intense to produce runoff under the diverse hydrological conditions encountered across these regions. The time to start runoff and percolation generation was recorded with a timer. Sediment-water samples were collected in bottles at the runoff gutter and percolation valve. The volume of water was registered with a graduated beaker. The samples were left to sedimentation by gravity, and a water sample was extracted from the supernatant using a siphon and frozen at 4°C. The remaining sample was dried in an oven at 105°C until no water was observed and then for 48 hours. The weight of the sediment was measured using a balance, and the total C and N content of the sediment was subsequently analyzed. The sediment load was calculated by dividing the sediment amount by the water volume. The nutrient load on sediments was measured using an elemental analyzer (Vario EL III, Elementar Analysensysteme GmbH, Hanau, Germany). The water samples were filtered to 0.45 µm and analyzed for DOC and DON using a Multi N/C 2100 S from Analytik Jena (Jena, Germany).

B.2.3 Statistical analysis

The experiment was designed as a factorial combination of site (4 levels) and biocrust (2 levels). Differences in the properties analyzed were proven by ANCOVA, using the soil baseline variables clay, silt, sand, CT, and NT as covariates. When covariates were not significant, analyzes continued using ANOVA. ANCOVA and ANOVA were implemented in R using the package stats 4.2.1 (R Core Team, 2022). In case normality or homoscedasticity were not accomplished, automatic data transformation was applied using the package bestNormalize 1.8.3 (Peterson, 2021; Peterson and Cavanaugh, 2020). We evaluated the normal distribution of the data using Shapiro-Wilk's Normality Test ($p >$

0.05) implemented in R stats 4.2.1 (R Core Team, 2022) and homoscedasticity by Levene's Test ($p<0.05$) implemented in the car 3.1-0 package (Fox and Weisberg, 2018). The individual significance of treatments was assessed by the Dunn–Šidák correction implemented in the package multcomp 1.4-20 (Hothorn et al., 2008).

B.3 Results

B.3.1 Surface runoff, percolating water fluxes, and their interrelation with biocrust cover along different climatic conditions

Our findings reveal that biocrusts play a critical role in modulating associated with erosion, runoff, and percolation across varying climatic conditions (Table 1 and 2). Overall, the time required to start runoff was significantly longer in NA, with the shortest time observed in the coastal arid site, SG. Biocrusts significantly delayed runoff initiation by 97.7%, mainly due to increased surface roughness. This delay was more pronounced in NA, where the combination of enhanced roughness and high infiltration capacity extended the time for runoff initiation by three to four times. However, these effects did not extend to the subsoil, as biocrust had no measurable impact on the time needed for percolation to start.

The total runoff volume was significantly higher in SG compared to the other sites. Biocrust contributed to a significant reduction of the runoff volume, averaging a 28.0% reduction, corresponding to a significant 50.0% reduction in percolation. Regarding site-specific effects, biocrusts significantly reduced the runoff volume by 72.4% in NA. Contrarily, a contrasting trend in LC was observed, with a 36.4% increase in runoff volume associated with the biocrust presence.

The climatic gradient significantly influenced the total sediment transported by runoff, decreasing sediment mobilization as humidity increased. Biocrusts were pivotal in reducing sediment transport via runoff, resulting in an overall decrease of 69.9%. However, this reduction in runoff-associated sediment transport was accompanied by a 28.3% increase in the sediment mobilization via percolation. The interaction between the study site and biocrust presence showed significant sediment reductions across the northern sites, with NA exhibiting a similar trend, albeit without statistical significance.

The sediment load in the runoff, measured as sediment concentration in water, was significantly reduced by an average of 60.9% in the presence of biocrust. In contrast, sediment concentration in percolation increased significantly by 58.3%, highlighting a shift in sediment dynamics influenced by biocrust interactions across the study sites.

Table B.1: Surface runoff fluxes on the study sites (SG: Santa Gracia, QdT: Quebrada de Talca, LC: La Campana, NA: Nahuelbuta) with (+) and without (-) biocrust (BSC) cover. Values correspond to mean \pm standard deviation (SD) of five field replicates. A letter-based display of Šidák correction accompanies surface runoff parameters^a, and the significance of the studied factors is shown as a p-value and list of covariates (C_T , N_T : total carbon and nitrogen content). Different letters indicate statistically significant different values based on our data, ns: non-significant.

Factor	Time to start runoff		Runoff		Sediment in runoff		Sediment load of runoff		
		[s]		[L h ⁻¹]		[g m ⁻² h ⁻¹]		[g L ⁻¹ m ⁻²]	
Mean \pm SD									
Site	SG	65.1 \pm 20.7 (a)	49 \pm 18 (b)	617 \pm 473 (c)	12.1 \pm 7.9 (a)				
	QdT	78.7 \pm 30.4 (a)	40 \pm 16 (a)	398 \pm 459 (b)	9.6 \pm 9.6 (a)				
	LC	83.5 \pm 56.0 (a)	39 \pm 22 (a)	241 \pm 293 (b)	7.3 \pm 8.8 (a)				
	NA	236.7 \pm 273.0 (b)	44 \pm 43 (a)	28 \pm 44 (a)	3.0 \pm 14.0 (a)				
Biocrust	BSC+	154.0 \pm 211.5 (b)	36 \pm 21 (a)	149 \pm 222 (a)	4.5 \pm 10.4 (a)				
	BSC-	77.9 \pm 33.8 (a)	50 \pm 31 (b)	495 \pm 492 (b)	11.5 \pm 10.0 (b)				
Site*Biocrust									
SG	BSC+	62.7 \pm 21.2 (ab)	44 \pm 16 (ab)	340 \pm 340 (bc)	7.5 \pm 5.7 (abc)				
SG	BSC-	67.5 \pm 20.6 (ab)	54 \pm 18 (ab)	873 \pm 456 (d)	16.7 \pm 7.1 (de)				
QdT	BSC+	87.3 \pm 37.5 (ab)	38 \pm 15 (ab)	131 \pm 96 (ab)	3.3 \pm 2.0 (abd)				
QdT	BSC-	70.1 \pm 18.7 (ab)	42 \pm 18 (ab)	665 \pm 524 (cd)	15.8 \pm 10.2 (ce)				
LC	BSC+	85.8 \pm 67.1 (ab)	45 \pm 20 (ab)	87 \pm 94 (a)	2.1 \pm 1.9 (a)				
LC	BSC-	81.2 \pm 44.6 (ab)	33 \pm 23 (ab)	395 \pm 344 (bc)	12.6 \pm 9.9 (bcde)				
NA	BSC+	380.4 \pm 329.5 (b)	19 \pm 23 (a)	16 \pm 49 (a)	5.2 \pm 19.9 (abcde)				
NA	BSC-	93.0 \pm 40.2 (a)	69 \pm 45 (b)	40 \pm 36 (a)	0.9 \pm 1.2 (abcde)				
Significance (p-value)									
Site		1.03×10^{-5}	*	0.0304	*	2.21×10^{-14}	*	1.93×10^{-9}	*
Biocrust		0.01452	*	0.0034	*	4.37×10^{-11}	*	7.57×10^{-10}	*
Site*Biocrust		0.0166	*	1.83×10^{-5}	*	0.00129	*	0.000177	*
Covariates		clay + C_T		silt + sand + N_T		clay + sand + C_T + soil water content			

^aLetters indicate significant differences between means according to post-hoc tests with Šidák correction for multiple comparisons. Levels not sharing any letter are significantly different ($p < 0.05$).

* Statistically significant effect ($p < 0.05$). SD Standard Deviation. C_T Total Carbon content.

N_T Total Nitrogen content.

Table B.2: Percolating water fluxes on the study sites (SG: Santa Gracia, QdT: Quebrada de Talca, LC: La Campana, NA: Nahuelbuta) with (+) and without (-) biocrust (BSC) cover. Values correspond to mean \pm standard deviation (SD) of five field replicates. A letter-based display of Šidák correction accompanies surface runoff parameters^a, and the significance of the studied factor is shown as a p-value and list of covariates (C_T , N_T : total carbon and nitrogen content). Different letters indicate statistically significant different values based on our data, ns: non-significant.

Factor	Time to start percolation flow		Percolation [L h ⁻¹]	Sediments in percolation flow [g m ⁻² h ⁻¹]		Sediment load in percolation [g L ⁻¹ m ⁻²]
		[s]				
Mean \pm SD						
Site	SG	223	± 190	18.0 ± 140 (a)	19 ± 34	4.2 ± 19.7
	QdT	175.0	± 94.5	22.8 ± 150 (a)	7 ± 10	0.2 ± 0.3
	LC	234	± 183	22.4 ± 130 (a)	13 ± 15	0.5 ± 0.5
	NA	145	± 169	65.0 ± 390 (b)	23 ± 25	0.4 ± 0.4
Biocrust	BSC+	171	± 133	42.6 ± 340 (b)	19 ± 22 (b)	0.5 ± 0.5
	BSC-	218	± 190	21.5 ± 210 (a)	12 ± 24 (a)	2.1 ± 13.7
Site*Biocrust						
SG	BSC+	202	± 103	24.8 ± 150 (ab)	19 ± 18	0.7 ± 0.5
SG	BSC-	244	± 251	11.1 ± 100 (a)	18 ± 46	7.5 ± 27.5
QdT	BSC+	148.0	± 63.9	30.5 ± 130 (b)	9 ± 13	0.3 ± 0.3
QdT	BSC-	202	± 113	15.1 ± 130 (ab)	5 ± 6	0.2 ± 0.2
LC	BSC+	226	± 223	23.5 ± 140 (ab)	17 ± 19	0.6 ± 0.5
LC	BSC-	241	± 139	21.3 ± 140 (ab)	9 ± 9	0.4 ± 0.3
NA	BSC+	107.0	± 35.6	91.5 ± 280 (c)	30 ± 32	0.4 ± 0.4
NA	BSC-	183	± 234	38.5 ± 300 (b)	16 ± 15	0.4 ± 0.3
Significance (p-value)						
Site		(ns)		1.78×10^{-12} *	(ns)	(ns)
Biocrust		(ns)		8.11×10^{-8} *	0.00946 *	(ns)
Site*Biocrust		(ns)		0.00164 *	(ns)	(ns)
Covariates		clay		clay + silt + sand + clay + silt + sand		
				$C_T + SOC$	+ $C_T + SOC$	

^a Letters indicate significant differences between means according to post-hoc tests with Šidák correction for multiple comparisons. Levels not sharing any letter are significantly different ($p < 0.05$). * Statistically significant effect ($p < 0.05$). ns Non-significant ($p \geq 0.05$).

SD Standard Deviation. C_T Total Carbon content. N_T Total Nitrogen content.

SOC Soil Organic Carbon.

